THE UNIVERSITY OF MICHIGAN

5548-1-T

THE MINIMIZATION OF THE RADAR CROSS SECTION OF A CYLINDER BY CENTRAL LOADING

by

Kun-Mu Chen and Valdis V. Liepa

April 1964

Scientific Report No.

Contract AF 19(628)-2374
Project 5635
Task 563502

Prepared for

Air Force Cambridge Research Laboratories
Office of Aerospace Research
L. G. Hanscom Field
Bedford, Massachusetts

ensn

UMRI183

Requests for additional copies by agencies of the Department of Defense, their contractors, and other government agencies should be directed to:

DEFENSE DOCUMENTATION CENTER
CAMERON STATION
ALEXANDRIA, VIRGINIA 22314

Department of Defense contractors must be established for DDC services or have their 'need-to-know' certified by the cognizant military agency of their project or contract.

All other persons and organizations should apply to:

U.S. DEPARTMENT OF COMMERCE
OFFICE OF TECHNICAL SERVICES
WASHINGTON 25, D.C.

TABLE OF CONTENTS

Table of Contents (Cont'd)

INTRODUCTION

Many investigations have been made concerning methods of reducing the radar cross section of metallic bodies, especially with regard to applications to radar camouflage techniques. Two methods have been widely used: the first utilizes radar absorbing materials, the second consists in reshaping the body to change the reflection pattern.

A third method, known as the method of reactive loading, is the subject of investigation of this report. Only the case of back scattering is considered, and all references to cross sections are to be understood as such.

The first known use of reactive loading to minimize the back scattering cross section was made by Iams (1950) who applied the technique to metallic posts in a parallel plate pillbox structure. Shortly after this Sletten (1962) employed the method to decrease the radar cross section of objects in space.

Several authors (King, 1956; Hu, 1958; Ås and Schmitt, 1958) have studied the problem of cross sections of a cylinder with and without a central load. Although these investigations indicated that the cross section of a half-wavelength cylinder can be significantly reduced by the use of a high reactive impedance load at its center, the exact way in which the reactive loading behaves, as well as the optimum method (i.e. that loading which minimizes the cross section) of loading are still not well understood.

This report has two purposes: (1) to develop a theory to explain the behavior of the cross section of a cylinder with loading; and (2) to determine the optimum loading.

The problem is studied by considering the currents induced in a body illuminated by an electromagnetic wave. We consider the case of a plane wave which illuminates a perfectly conducting cylinder whose radius is small and whose length is less than two wavelengths. The plane wave induces a current on the cylinder;

this in turn produces a scattered electromagnetic field. If an impedance is added at the center of the cylinder, the induced current is modified, hence so is the scattered field. It should be noted that there are three ways in which an impedance change can reduce the scattered field: (i) by reducing the magnitude of the induced current; (ii) by reversing the phase of the induced current over some part of the cylinder; and (iii) by the combination of (i) and (ii). This third way is the most effective for reducing the back scattering cross section. In fact, we shall show that with central loading it is possible to reduce the broadside cross section to zero.

For a center-loaded cylinder the induced current is first determined as a function of the cylinder dimensions, the midpoint impedance and the incident electric field. Using this solution we obtain an optimum impedance, i.e. an impedance which gives a minimum back scattering. In order to verify this solution experimentally, the induced current on loaded cylinders and the return from a cylinder whose impedance is close to the calculated value are measured. The experimental data for induced current and cross section areas are found to be in excellent agreement with the theoretical values.

Throughout the study a resonant cylinder whose total length is equal to 0.43λ (λ = wavelength) and an antiresonant cylinder of total length 0.85λ are used as typical examples. When a plane wave is obliquely incident on the cylinder the induced current can be divided into a symmetrical and an antisymmetrical component. The symmetrical component is predominant for a resonant cylinder while the antisymmetrical component is predominant for an antiresonant cylinder. Although the midpoint impedance can have a strong effect on the symmetrical component of the induced current it does not affect the antisymmetrical component. For this reason central loading cannot appreciably reduce the large cross section lobes occurring at off-normal aspects for the case of an antiresonant cylinder.

This report is divided into two parts. In Part I we consider the case of a center-loaded cylinder illuminated by a plane wave at normal incidence, and develop the basic theory of central loading. In Part II the case is generalized to cover incidence at any arbitrary aspect angle.

In the interests of simplicity, the analysis in both parts is limited to the case of a thin cylinder. The case of a thicker cylinder and the effect of multiple loadings will be investigated in the future. MKS rationalized units are used in the analysis and the time dependence factor $e^{j\omega t}$ is omitted.

I
THE MINIMIZATION OF THE CROSS SECTION OF A CYLINDER BY CENTRAL LOADING (BROADSIDE ASPECT)

We consider here only the cross section of a center-loaded cylinder for broadside aspects. We first determine the induced current and then investigate the scattered field.

1-1 INDUCED CURRENT ON A CENTER-LOADED CYLINDER

1-1.1 Basic Equation and Solution

The geometry of the problem is as shown in Fig. 1-1. A cylinder of radius a and length 2h is assumed to be perfectly conducting and illuminated by a plane electromagnetic wave at normal incidence with the E field parallel to the axis. At the center of the cylinder is connected a lumped impedance Z_L. The dimensions of interest are

$$\frac{1}{4}\lambda < 2h < 2\lambda$$

$$\beta_o^2 a^2 \ll 1$$

where λ is the wavelength and β_o the wave number. The second condition implies that the cylinder is thin, and allows us to assume that only the axial current is induced.

1-1.1a Integral Equation for the Induced Current on the Cylinder

In order to determine the induced current on the cylinder we apply an integral equation method.

The incident tangential electric field is assumed to be

$$E_z^{in} = E_o \tag{1.1}$$

where E_o is constant along the cylinder. The tangential electric field at the cylinder surface due to the current and charge on the cylinder is

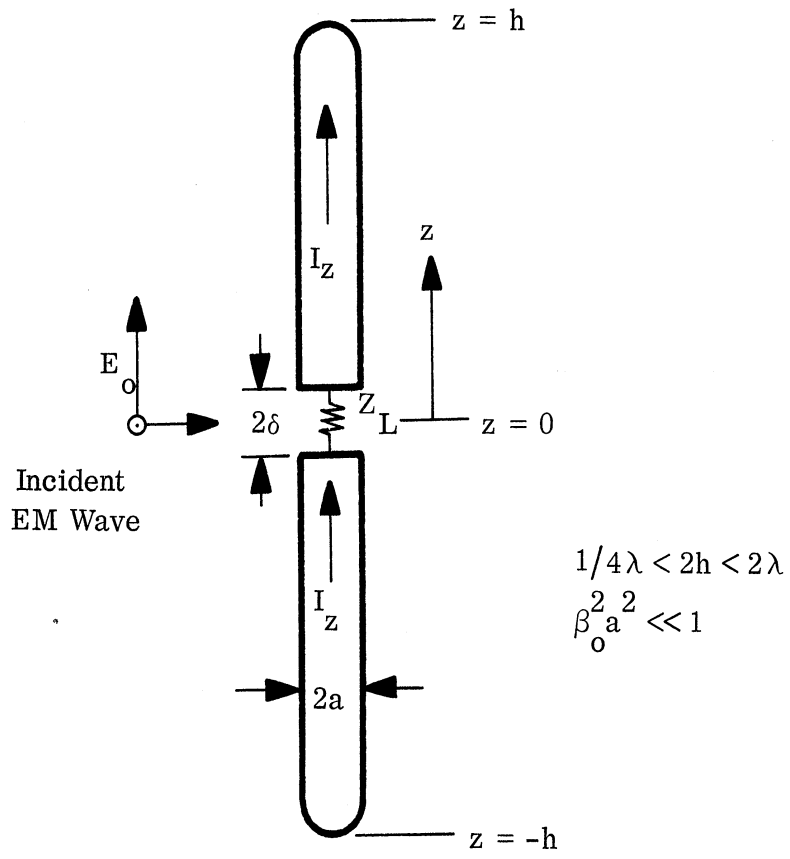

FIG. 1-1: CYLINDER WITH CENTRAL LOADING ILLUMINATED BY AN ELECTROMAGNETIC WAVE

$$E_z^a = -\frac{\partial \phi}{\partial z} - j\omega A_z \tag{1.2}$$

where ϕ is the scalar potential maintained by the charge and A_z is the tangential component of the vector component maintained by the current. By using the Lorentz condition

$$\phi = j \frac{\omega}{\beta_o^2} \nabla \cdot \vec{A} \tag{1.3}$$

(1.2) can be expressed as

$$E_z^a = -j \frac{\omega}{\beta_o^2} \left(\frac{\partial^2}{\partial z^2} + \beta_o^2 \right) A_z \quad . \tag{1.4}$$

The electric field maintained across the gap at the center of the cylinder is related to the voltage drop across the center by the relation

$$\int_{-\delta}^{\delta} E_z^g dz = -V^L = Z_L I_z(z=0) = Z_L I_o \tag{1.5}$$

where V^L is the voltage drop across the center load Z_L and I_o is the induced current at the center of the cylinder. From (1.5) E_z^g can be expressed as

$$E_z^g = Z_L I_o \delta(z) \tag{1.6}$$

where $\delta(z)$ is the usual Dirac delta function.

If the cylinder is perfectly conducting, the tangential electric field at the surface (excluding the gap) of the cylinder vanishes. That is

$$E_z^a + E_z^{in} = 0 \qquad \text{for } \delta \leqslant z \leqslant h \qquad \text{and} \qquad -h \leqslant z \leqslant -\delta. \tag{1.7}$$

At the gap, the electric field is continuous. Hence

$$E_z^a + E_z^{in} = E_z^g = Z_L I_o \delta(z), \qquad \text{for} \quad -\delta \leqslant z \leqslant \delta . \tag{1.8}$$

By combining (1.7) and (1.8) and making use of (1.4) it is possible to obtain a single equation valid for the entire length of the cylinder:

$$\frac{\partial^2}{\partial z^2} A_z + \beta_o^2 A_z = -j \frac{\beta_o^2}{\omega} \left[E_o - Z_L I_o \delta(z) \right] \tag{1.9}$$

$$\text{for } -h \leqslant z \leqslant h.$$

Equation (1.9) is an inhomogeneous differential equation for A_z. Consequently the general solution is expressible as the sum of a complementary function and a particular integral.

$$A_z = \frac{-j}{v_o} \left[C_1 \cos\beta_o z + C_2 \sin\beta_o z + \theta(z) \right] \tag{1.10}$$

where V_o is $1/\sqrt{\mu_o \epsilon_o}$, C_1 and C_2 are arbitrary constants, and $\theta(z)$ is a particular integral which can be written as

$$\theta(z) = \int_o^z \left[E_o(s) - Z_L I_o \delta(s) \right] \sin\beta_o(z-s)\, ds$$

$$= \frac{E_o}{\beta_o} (1 - \cos\beta_o z) - \frac{1}{2} Z_L I_o \sin\beta_o |z| . \tag{1.11}$$

If E_o is assumed to be constant along the cylinder, the symmetry implies that C_2 must be zero. Equation (1.10) then becomes

$$A_z(z) = \frac{-j}{v_o} \left[C_1 \cos\beta_o z + \frac{E_o}{\beta_o} (1 - \cos\beta_o z) - \frac{1}{2} Z_L I_o \sin\beta_o |z| \right] \tag{1.12}$$

$$\text{for } -h \leqslant z \leqslant h .$$

From (1.12), C_1 can be expressed in terms of $A_z(h)$ as

$$C_1 = \sec\beta_o h \left[jv_o A_z(h) - \frac{E_o}{\beta_o}(1-\cos\beta_o h) + \frac{1}{2} Z_L I_o \sin\beta_o h \right] . \tag{1.13}$$

Thus from (1.12) and (1.13) we obtain the following equation:

$$A_z(z) - A_z(h) = \frac{-j}{v_o} \sec\beta_o h \left[(jv_o A_z(h) - \frac{E_o}{\beta_o})(\cos\beta_o z - \cos\beta_o h) + \frac{1}{2} Z_L I_o \sin\beta_o (h - |z|) \right]$$

$$\text{for } -h \leqslant z \leqslant h . \tag{1.14}$$

On the other hand, the left side of (1.14) is also related to the induced current by

$$A_z(z) - A_z(h) = \frac{\mu_o}{4\pi} \int_{-h}^{h} I_z(z') K_d(z, z') dz' \tag{1.15}$$

where

$$K_d(z, z') = K_a(z, z') - K_a(h, z') , \tag{1.16}$$

$$K_a(z, z') = \frac{e^{-j\beta_o \sqrt{(z-z')^2 + a^2}}}{\sqrt{(z-z')^2 + a^2}} \tag{1.17}$$

and $I_z(z')$ is the induced current on the cylinder.

By equating (1.14) and (1.15) we obtain an integral equation for the induced current on the cylinder.

$$\int_{-h}^{h} I_z(z')K_d(z,z')dz' = \frac{-j4\pi}{\zeta_o}\sec\beta_o h\left[(jv_o A_z(h) - \frac{E_o}{\beta_o})(\cos\beta_o z - \cos\beta_o h) + \frac{1}{2} Z_L I_o \sin\beta_o(h-|z|)\right] \quad (1.18)$$

where $\zeta_o = 120\pi$ and (1.18) is valid for $-h \leqslant z \leqslant h$. Both $A_z(h)$ and I_o in the right side of (1.18) are functions of $I_z(z)$ and are still unknown.

1-1.1b Solution for the Induced Current on a Cylinder

The kernel $K_d(z,z')$ in (1.18) has a sharp peak at $z'=z$. Moreover, it can be shown numerically that the left side of (1.18) is nearly proportional to $I_z(z)$ for $-h \leqslant z \leqslant h$. Hence we may assume

$$I_z(z) = C_c(\cos\beta_o z - \cos\beta_o h) + C_s \sin\beta_o(h-|z|) . \quad (1.19)$$

where C_c and C_s are constants to be determined. To obtain approximations to C_c and C_s it is reasonable to divide (1.18) into two parts:

$$C_c\int_{-h}^{h}(\cos\beta_o z' - \cos\beta_o h)K_d(z,z')dz' = \frac{-j4\pi}{\zeta_o}\sec\beta_o h(jv_o A_z(h) - \frac{E_o}{\beta_o})\cdot \cdot(\cos\beta_o z - \cos\beta_o h) \quad (1.20)$$

$$C_s\int_{-h}^{h}\sin\beta_o(h-|z'|)K_d(z,z')dz' = \frac{-j2\pi}{\zeta_o}\sec\beta_o h\, Z_L I_o \sin\beta_o(h-|z|). \quad (1.21)$$

Both (1.20) and (1.21) are valid for $-h \leqslant z \leqslant h$. They also agree at the end points, $z = \pm h$, since both sides of the equations become zero at these points. To find the constants C_c and C_s we can match both sides of (1.20) and (1.21) at the center of the cylinder, $z = 0$.

From (1.20)

$$C_c = \frac{-j4\pi}{\zeta_o T_{cd}} \sec\beta_o h\left(jv_o A_z(h) - \frac{E_o}{\beta_o}\right)(1 - \cos\beta_o h) \tag{1.22}$$

where

$$T_{cd} = \int_{-h}^{h} (\cos\beta_o z' - \cos\beta_o h) K_d(0, z')dz' \tag{1.23}$$

From (1.21)

$$C_s = \frac{-j2\pi}{\zeta_o T_{sd}} \sec\beta_o h Z_L I_o \sin\beta_o h \tag{1.24}$$

where

$$T_{sd} = \int_{-h}^{h} \sin\beta_o(h - |z'|) K_d(0, z')dz' \,. \tag{1.25}$$

It should be noted that if C_c and C_s had been evaluated using a value of z other than $z = 0$ the values for C_c and C_s would be relatively little affected. The substitution of (1.22) and (1.24) in (1.19) gives

$$I_z(z) = \frac{-j4\pi}{\zeta_o}\left[\frac{1}{T_{cd}}\left(jv_o A_z(h) - \frac{E_o}{\beta_o}\right)(\sec\beta_o h - 1)(\cos\beta_o z - \cos\beta_o h) + \frac{1}{2T_{sd}} Z_L I_o \tan\beta_o h \sin\beta_o(h - |z|)\right]. \tag{1.26}$$

In order to obtain the final form of the solution we must still determine $A_z(h)$ and I_o in (1.26). By setting $z = 0$, $I_o = I_z(z = 0)$ and we can express I_o

in terms of $A_z(h)$. A straightforward rearrangement of (1.26) then yields

$$I_z(z) = \frac{-j4\pi}{\zeta_o}\left(jv_o A_z(h) - \frac{E_o}{\beta_o}\right)\left[M'(\cos\beta_o z - \cos\beta_o h) + N'\sin\beta_o(h - |z|)\right] \tag{1.27}$$

where

$$M' = \frac{1}{T_{cd}}(\sec\beta_o h - 1) \tag{1.28}$$

$$N' = \frac{-Z_L\tan\beta_o h(\sec\beta_o h + \cos\beta_o h - 2)}{T_{cd}Z_L\tan\beta_o h\sin\beta_o h - j60T_{cd}T_{sd}} \tag{1.29}$$

In (1.27) the only remaining unknown is $A_z(h)$. To determine it, we use the definition of the vector potential

$$A_z(h) = \frac{\mu_o}{4\pi}\int_{-h}^{h} I_z(z')K_a(h, z')dz' \tag{1.30}$$

where $K_a(h, z')$ is defined in (1.17). Substituting (1.27) in (1.30) gives

$$A_z(h) = \frac{jE_o}{v_o\beta_o}\,\frac{M'T_{ca} + N'T_{sa}}{1 - M'T_{ca} - N'T_{sa}} \tag{1.31}$$

where

$$T_{ca} = \int_{-h}^{h}(\cos\beta_o z' - \cos\beta_o h)K_a(h, z')dz' \tag{1.32}$$

$$T_{sa} = \int_{-h}^{h}\sin\beta_o(h - |z'|)K_a(h, z')dz' \tag{1.33}$$

A final form for the solution of $I_z(z)$ is then obtained by substituting (1.31) into (1.27). After some rearrangement we have

$$I_z(z) = \frac{jE_o}{30\beta_o}\left(\frac{1}{\cos\beta_o h - MT_{ca} - NT_{sa}}\right)\left[M(\cos\beta_o z - \cos\beta_o h) + N\sin\beta_o(h - |z|)\right] \tag{1.34}$$

where

$$M = \frac{1}{T_{cd}}(1 - \cos\beta_o h) \tag{1.35}$$

$$N = \frac{-Z_L \sin\beta_o h(I - \cos\beta_o h)^2}{T_{cd}Z_L\sin^2\beta_o h - j60T_{cd}T_{sd}\cos\beta_o h} \tag{1.36}$$

and T_{cd}, T_{sd}, T_{ca}, T_{sa} are defined in equations (1.23), (1.25), (1.32) and (1.33) respectively.

Equation (1.34) gives a complete expression for the induced current on a cylinder with a central load Z_L when illuminated by a broadside constant electric field E_o. Moreover, (1.34) is both simple in form and accurate. That it agrees well with experimental values will be shown in section 1-2.

For completeness as well as convenience in computations, the integrals T_{cd}, T_{sd}, T_{ca} and T_{sa} are reformulated as

$$T_{cd} = C_a(h, 0) - C_a(h, h) - \cos\beta_o h\left[E_a(h, 0) - E_a(h, h)\right] \tag{1.37}$$

$$T_{sd} = \sin\beta_o h\left[C_a(h, 0) - C_a(h, h)\right] - \cos\beta_o h\left[S_a(h, 0) - S_a(h, h)\right] \tag{1.38}$$

$$T_{ca} = C_a(h, h) - \cos\beta_o h\, E_a(h, h) \tag{1.39}$$

$$T_{sa} = \sin\beta_o h\, C_a(h, h) - \cos\beta_o h S_a(h, h) \tag{1.40}$$

where

$$C_a(h,0) = \int_{-h}^{h} \cos\beta_o z' K_a(0,z')dz' \tag{1.41}$$

$$C_a(h,h) = \int_{-h}^{h} \cos\beta_o z' K_a(h,z')dz' \tag{1.42}$$

$$E_a(h,0) = \int_{-h}^{h} K_a(0,z')dz' \tag{1.43}$$

$$E_a(h,h) = \int_{-h}^{h} K_a(h,z')dz' \tag{1.44}$$

$$S_a(h,0) = \int_{-h}^{h} \sin\beta_o |z'| K_a(0,z')dz' \tag{1.45}$$

$$S_a(h,h) = \int_{-h}^{h} \sin\beta_o |z'| K_a(h,z')dz' \tag{1.46}$$

The integrals of (1.41) through (1.46) can be calculated on a digital computer.

We now consider a number of examples.

1-1.2 Induced Current on a Cylinder without Central Loading

The first and simplest case is that of a cylinder without loading. By setting $Z_L = 0$ the induced current can be found directly from (1.34):

$$I_z(z) = \frac{jE_o}{30\beta_o}\left(\frac{1-\cos\beta_o h}{(T_{cd}+T_{ca})\cos\beta_o h - T_{ca}}\right)(\cos\beta_o z - \cos\beta_o h) .$$

Using (1.37) and (1.39) to express T_{cd} and T_{ca}, $I_z(z)$ can be written

$$I_z(z) = \frac{jE_o}{30\beta_o}\left[\frac{(1-\cos\beta_o h)(\cos\beta_o z - \cos\beta_o h)}{C_a(h,0)\cos\beta_o h - E_a(h,0)\cos^2\beta_o h - C_a(h,h) + E_a(h,h)\cos\beta_o h}\right] \tag{1.47}$$

In this case the distribution of the induced current is that of a shifted cosine curve. The maximum induced current occurs at

$$\left.\begin{aligned} z &= 0 && \text{for } \beta_o h < \frac{3\pi}{2} \\ z &= \lambda/2 && \text{for } \frac{3\pi}{2} < \beta_o h < 2\pi \end{aligned}\right\} \tag{1.48}$$

and is given by

$$I_z(0) = \frac{jE_o}{30\beta_o}\left[\frac{(1-\cos\beta_o h)^2}{C_a(h,0)\cos\beta_o h - E_a(h,0)\cos^2\beta_o h - C_a(h,h) + E_a(h,h)\cos\beta_o h}\right] \tag{1.49}$$

or

$$I_z(\lambda/2) = \frac{jE_o}{30\beta_o}\left[\frac{-\sin^2\beta_o h}{C_a(h,0)\cos\beta_o h - E_a(h,0)\cos^2\beta_o h - C_a(h,h) + E_a(h,h)\cos\beta_o h}\right]. \tag{1.50}$$

Theoretical and experimental results of $I_z(0)$ as a function of h are compared in Fig. 1-2. The theoretical results were obtained from (1.49) by the use of a high speed computer. The experimental results were obtained by measuring the current induced at the center of a cylinder whose radius is 3/16" and whose length varied between $\lambda/4$ and 2λ. The cylinder was illuminated by a plane wave with a frequency of 1.088 Gc. Except near $h = 0.7\lambda$, where a resonant peak occurs, the agreement between theory and experiment is good. The discrepancy near $h = 0.7\lambda$ may be due to a deficiency in the theoretical treatment or it may have its origin in the experiment, i.e. the incident electromagnetic wave may not be uniform along the cylinder for all cylinder lengths.

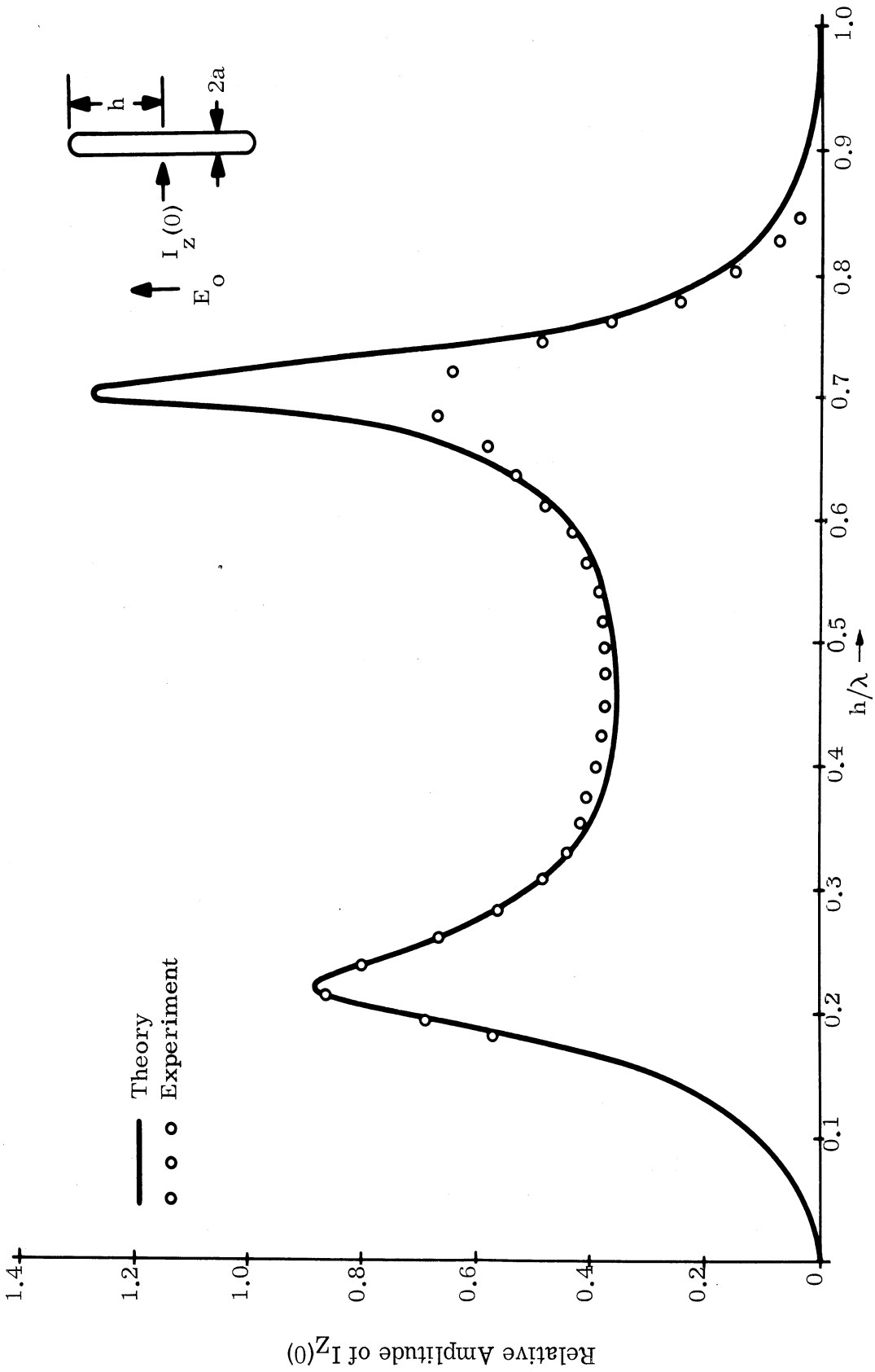

FIG. 1-2: $I_z(0)$ vs h/λ WHEN $\beta_o a = 0.11$, f = 1.088 Kmc, $Z_L = 0$

However, in view of the good general agreement the discrepancy does not appear serious. In Fig. 1-3 the current distributions for cylinders of various lengths are shown. Good agreement between theoretical predicution and experimental results is evident.

For a cylinder whose length is 0.43λ or 1.4λ the induced current reaches a resonant peak for $\beta_o a = 0.11$. Since these current peaks imply large radar cross sections we propose to decrease the cross sections by eliminating these current peaks by using suitable impedance loading. This will be carried out in section 1-3.1. Before proceeding, we consider another example.

1-1.3 Induced Current on a Cylinder with an Infinite Midpoint Impedance

The second case to be studied is that of a cylinder with an infinite midpoint impedance. Theoretically, the induced current can be obtained from (1.34) by setting $Z_L = \infty$. Experimentally, an infinite impedance is approximated by a coaxial cavity tuned at its antiresonant position. This coaxial cavity is built inside the cylinder as described in section 1-2.1. A small probe then measures the induced current.

When $Z_L = \infty$, we have from (1.35) and (1.36)

$$\frac{N}{M} = \frac{-(1-\cos\beta_o h)}{\sin\beta_o h}, \qquad \text{for } \beta_o h \neq n\pi. \tag{1.51}$$

Substituting (1.51) into (1.34) then gives

$$I_z(z) = \frac{-jE_o}{30\beta_o} \cdot \frac{(1-\cos\beta_o h)\left[\sin\beta_o|z| - \sin\beta_o h + \sin\beta_o(h-|z|)\right]}{\left[\sin\beta_o h\left[C_a(h,0)-(2-\cos\beta_o h)C_a(h,h)-\cos\beta_o h\, E_a(h,0)+E_a(h,h)\right]-(1-\cos\beta_o h)^2 S_a(h,h)\right]} \tag{1.52}$$

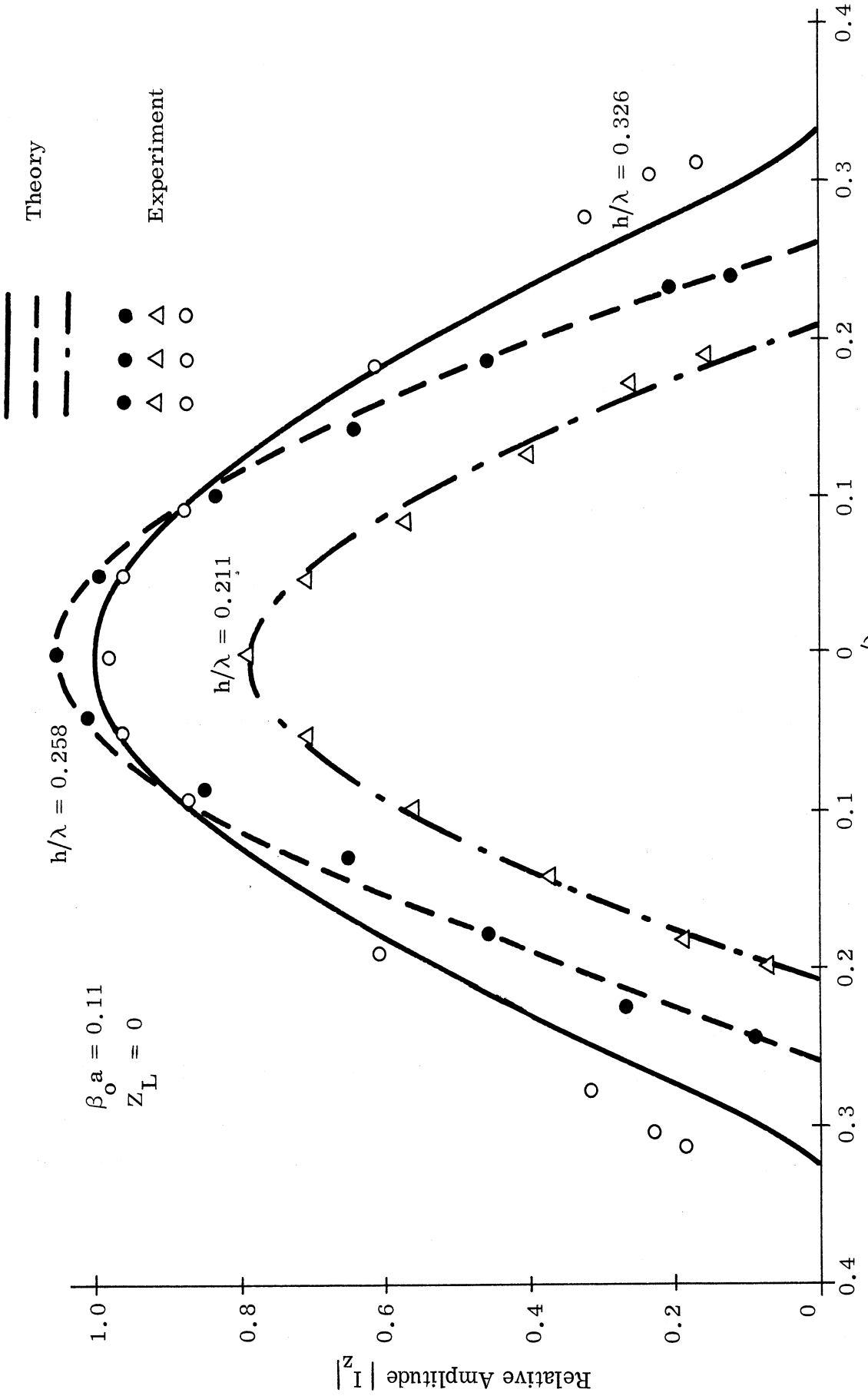

FIG. 1-3: CURRENT DISTRIBUTION ON UNLOADED CYLINDERS

In this case the induced current is zero at the center of the cylinder and its distribution along the cylinder is a combination of a sine and shifted sine curves.

The maximum induced current occurs at

$$z = h/2 \qquad \text{for } \beta_o h < 2\pi \tag{1.53}$$

and is given by

$$I_z(h/2) = \frac{-jE_o}{30\beta_o} \cdot \tag{1.54}$$

$$\frac{2\sin\frac{\beta_o h}{2}\left(1-\cos\frac{\beta_o h}{2}\right)(1-\cos\beta_o h)}{\left[\sin\beta_o h\left[C_a(h,0)-(2-\cos\beta_o h)C_a(h,h)-\cos\beta_o h\,E_a(h,0)+E_a(h,h)\right]-(1-\cos\beta_o h)^2 S_a(h,h)\right]}$$

The theoretical value of $I_z(h/2)$ as a function of h/λ is compared with the experimental curve in Fig. 1-4. The agreement between the theoretical predictions and the experimental observations is only fair. This lack of agreement is probably due to the difficulty in experimentally obtaining an infinite impedance from a coaxial cavity structure. The fact that closer agreement between theory and experiment is obtained for $Z_L = j\,2000\,\Omega$ tends to support this explanation.

For three cylinders of different lengths the induced current distribution for the case of infinite impedance loading is shown graphicall in Fig. 1-5. The agreement between theory and experiment is good.

Moreover, with infinite impedance loading at the center, the induced currents at resonant lengths (namely $2h = 0.43\lambda$ and $2h = 1.4\lambda$) are greatly reduced. However, the induced current appears to have a peak when $2h = 0.9\lambda$, and if a small cross section over a wide frequency band is desired, this current peak must also be suppressed. Thus we conclude that an infinite (or very high) impedance is not optimum for minimizing the scattering over a wide range of frequencies. We shall take up this problem again in section 1-3.1.

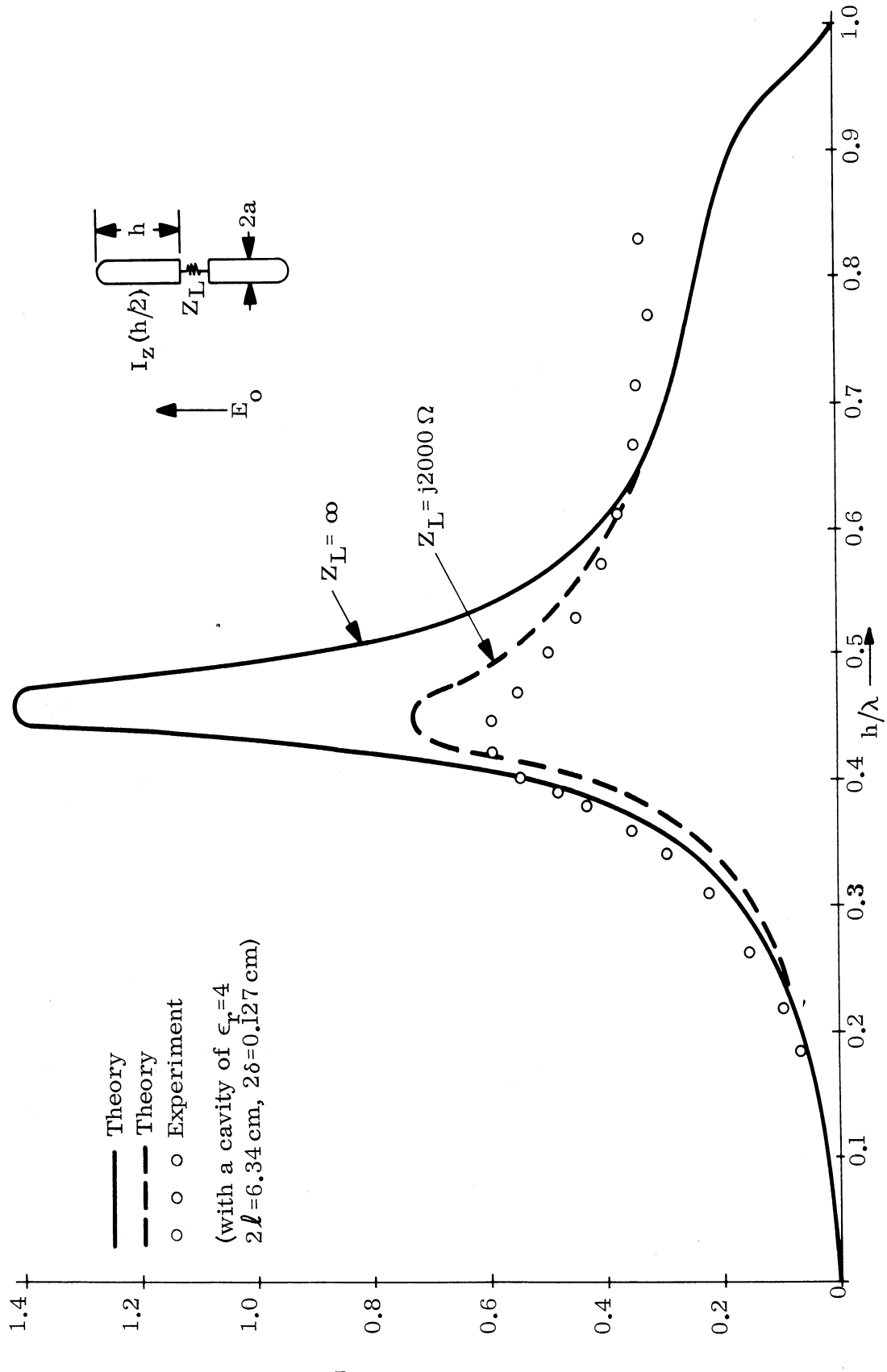

FIG. 1-4: $I_z(h/2)$ vs h/λ WHEN β_o=0.11, f=1.088 Kmc, Z_L= LARGE.

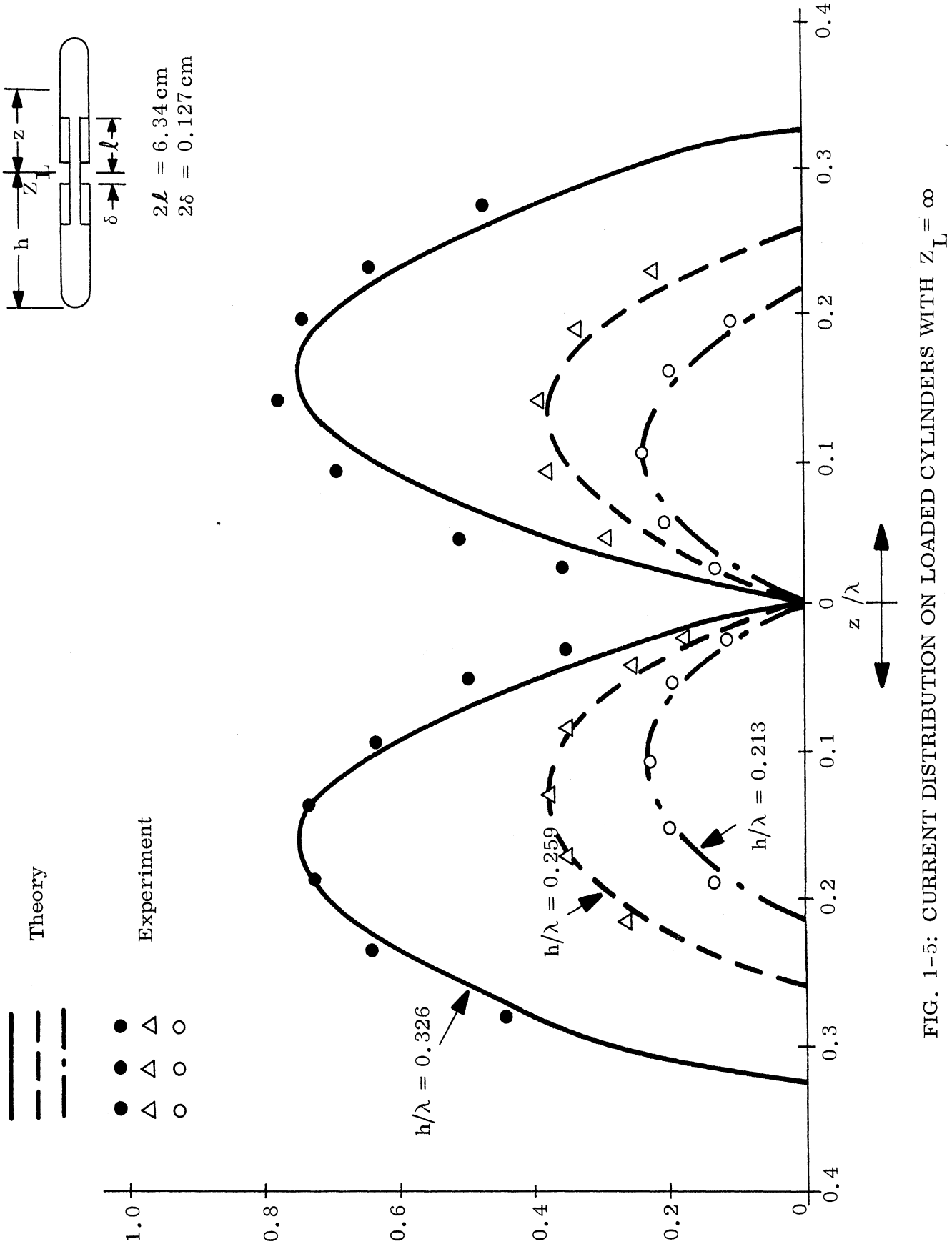

FIG. 1-5: CURRENT DISTRIBUTION ON LOADED CYLINDERS WITH $Z_L = \infty$

1-1.4 Induced Current on a Cylinder of Near-Resonant Length with Various Central Impedances

In this section we study the induced currents when the cylinder length is chosen to be a resonant length. For experimental convenience we select the following specific case:

$$a = 0.173\lambda$$

$$2h = 0.43\lambda$$

$$Z_L = jX_L \quad .$$

This last condition restricts the central impedance to be purely reactive, and is chosen because only a reactive impedance can be obtained experimentally from a coaxial cavity. With these conditions the theoretical value of the induced current can be expressed as

$$I_z(z) \doteq \frac{jE_o}{30\beta_o} M \left[\frac{(\cos\beta_o z - 0.216) + \frac{N}{M}\sin(77.5^o - |\beta_o z|)}{j0.215 - \frac{N}{M}(0.218 - j0.25)} \right] \qquad (1.55)$$

where

$$\frac{N}{M} \doteq \frac{-0.765X_L}{0.955X_L - 24.6} \qquad (1.56)$$

Values of $I_z(z)$ are calculated for values of Z_L equal to 0, ∞, $-j1600\Omega$, $-j800\Omega$, $-j600\Omega$, $j1600\Omega$, $j800\Omega$, $j600\Omega$ and $j400\Omega$ and shown in Figs. 1-6a and 1-6b. From the graphs we may observe the following:

(1) When $Z_L = 0$ (no loading) the induced current is very large and is distributed along the cylinder as a shifted cosine curve.

(2) When $Z_L = \infty$ the induced current is greatly reduced in magnitude. Its distribution curve becomes double-humped with a null at the center.

(3) When Z_L is capacitive and finite the induced current is smaller than the case of $Z_L = 0$ but larger than for $Z_L = \infty$.

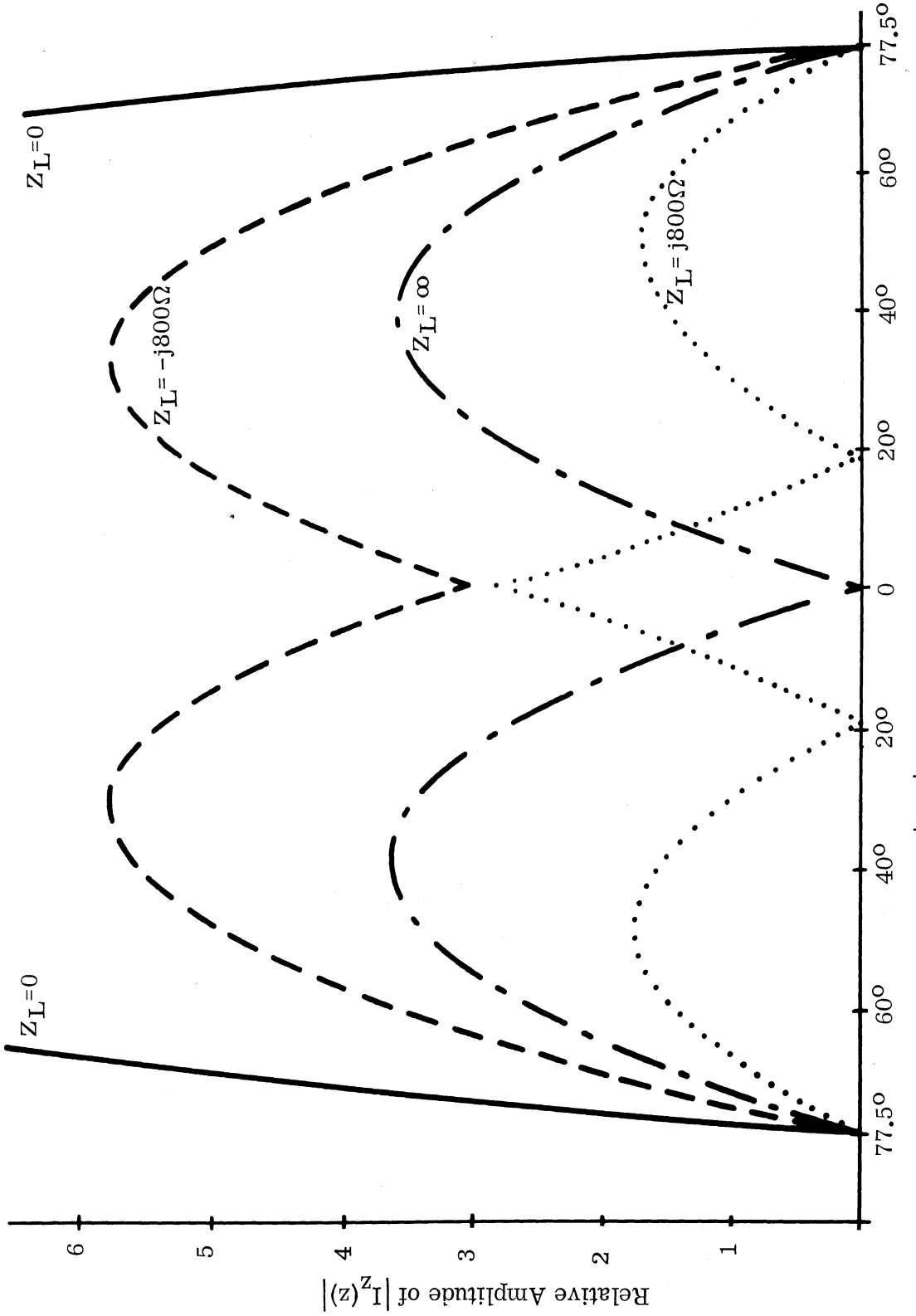

FIG. 1-6a: CURRENT DISTRIBUTION, $I_z(z)$, ON CYLINDER OF h=0.215λ, a=0.0173λ FOR DIFFERENT CENTRAL LOADS, Z_L (THEORETICAL)

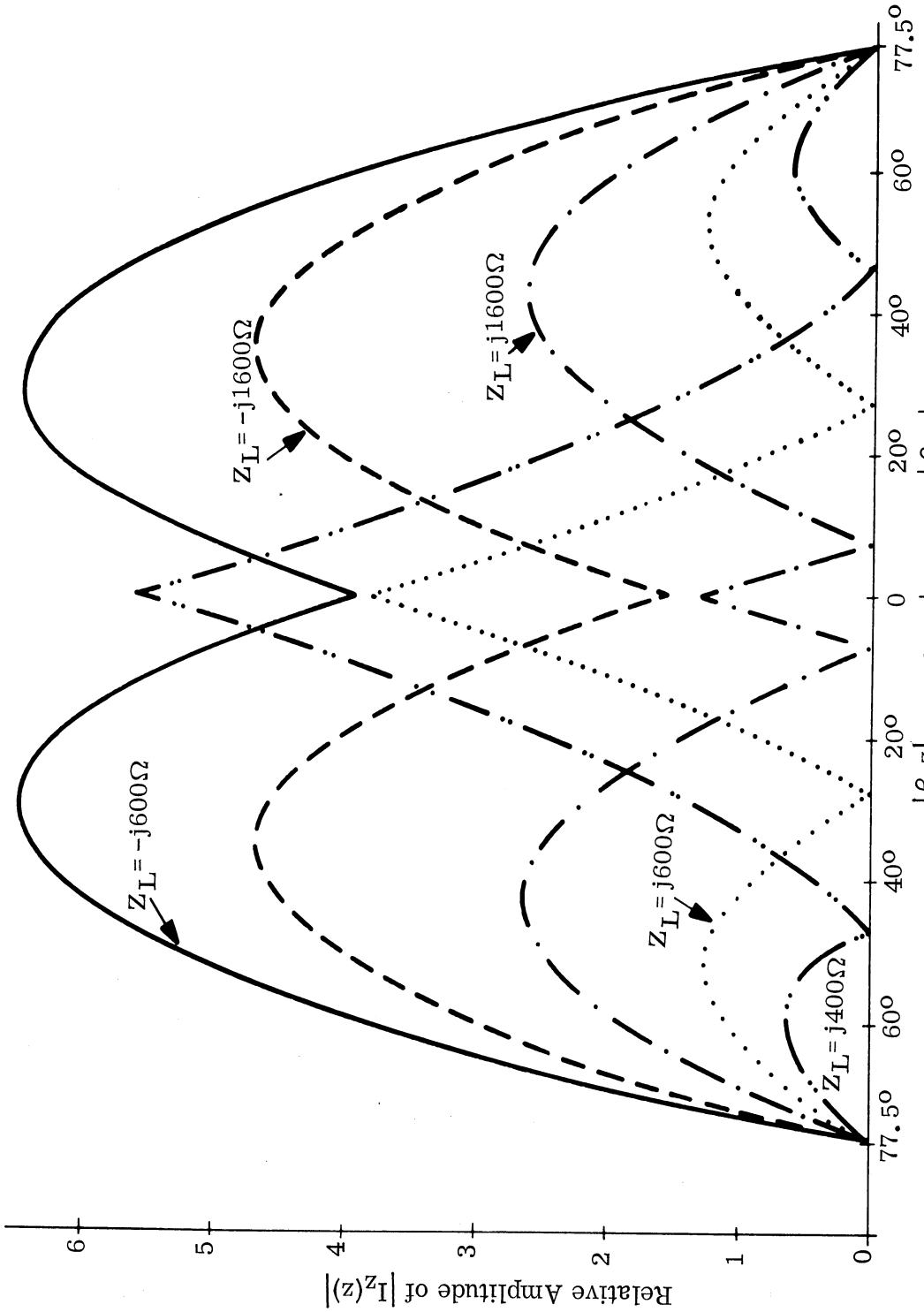

FIG. 1-6b: CURRENT DISTRIBUTION, $I_z(z)$, ON CYLINDER OF h=0.215λ, a=0.0173λ FOR DIFFERENT CENTRAL LOADS, Z_L (THEORETICAL)

(4) When Z_L is inductive and finite, the magnitude of the induced current is smaller than the case of $Z_L = \infty$ and is distributed in the form of three loops along the cylinder. It is of interest to note that the phase of the current at the center loop is reversed.

The most significant result is (4). From it we conclude that it is possible to reduce the broadside back scattering from a cylinder to zero by properly adjusting the value of Z_L. As we shall see in a later section (1-3), the optimum impedance for zero broadside back scattering with a cylinder of this size is inductive and has a small resistive component.

To compare the theoretical predictions of Figs. 1-6a and 1-6b the induced current along a cylinder of the specified dimension and with various cavity lengths was determined experimentally. The results are shown in Figs. 1-14a and 1-14b. The experimental curves closely resemble their theoretical counterparts. When the cavity length (total length) is longer than 6.2 cm, the impedance of the cavity is capacitive; when the length is less than 6.2 cm, the impedance is inductive. It should be noted that the effective cavity length is greater than these values since it is loaded with a dielectric material for which $\epsilon_r = 4.0$. The approximate value of the cavity impedance is calculated by using a standard impedance formula for a transmission line and assuming that a capacitance of 0.4 $\mu\mu$f is shunted across the gap at the center of the cylinder.

The comparison between theory and experiment is made in Fig. 1-7, where theoretical curves for $Z_L = -j\,800\,\Omega$, ∞, and $j\,800\,\Omega$ are shown. These curves are compared with experimental results for $\ell = 3.32$ cm, 3.10 cm and 2.91 cm (where ℓ is the half-length of the coaxial cavity). The agreement between theory and experiment is very good, indicating that the calculated value of the cavity impedance is quite close to the corresponding theoretical impedance.

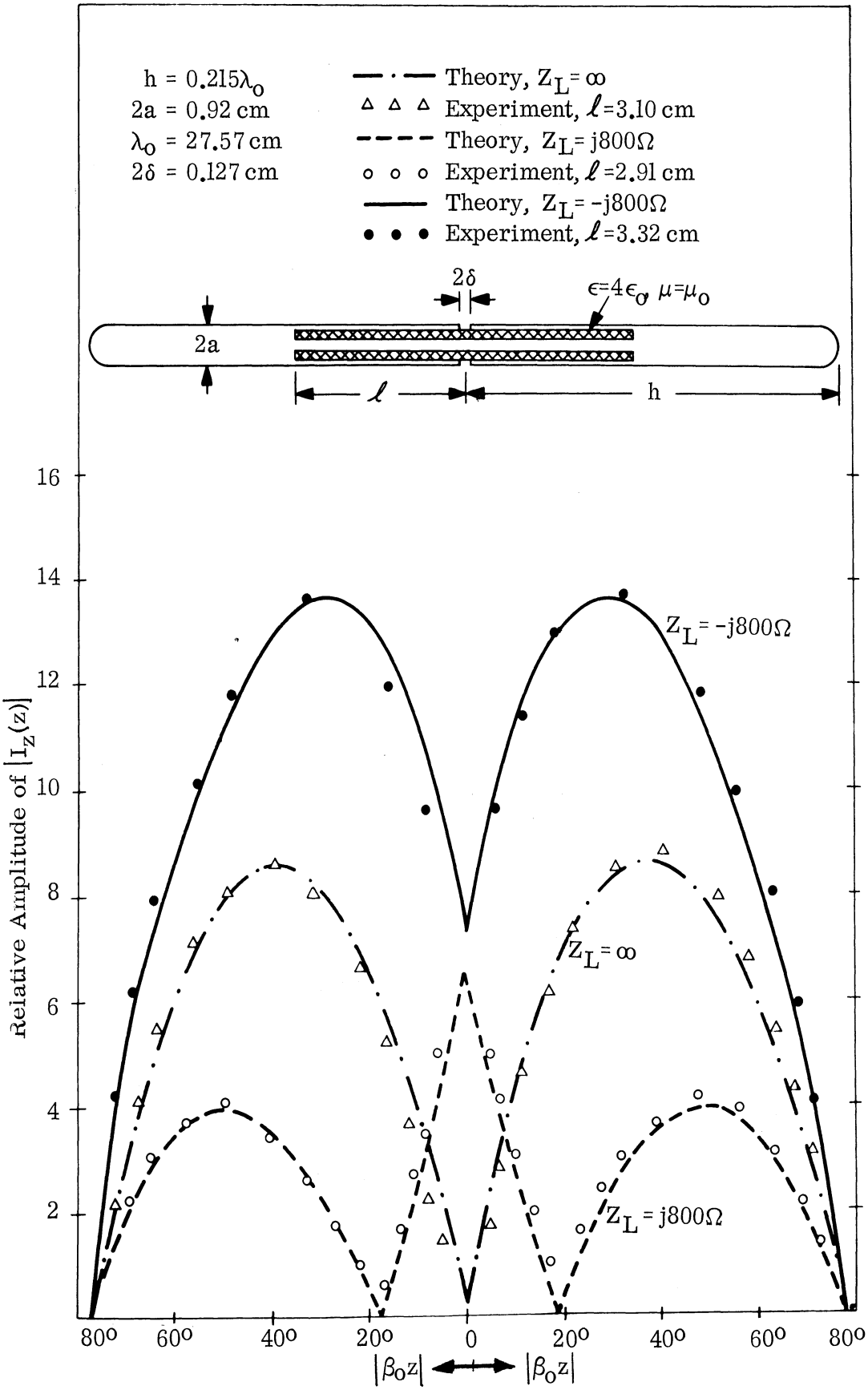

FIG. 1-7: CURRENT DISTRIBUTION ALONG A CYLINDER AS A FUNCTION OF CENTRAL LOAD FOR $h=0.215\lambda_o$ (THEORETICAL AND EXPERIMENTAL)

1-1.5 Induced Current on a Cylinder of Near Anti-Resonant Length with Various Central Impedances

In this section we study the induced current when the cylinder length is an antiresonant length. The following specific case is chosen:

$$a = 0.173\lambda$$

$$2h = 0.9\lambda$$

$$Z_L = jX_L$$

where we again consider only the reactive loading case.

For these conditions the theoretical value of the induced current is

$$I_z(z) \doteq \frac{jE_o}{30\beta_o} M \left[\frac{(\cos\beta_o z + 0.951) + \frac{N}{M}\sin(162^o - |\beta_o z|)}{-0.911 + j0.217 - \frac{N}{M}(0.111 - j0.128)} \right] \qquad (1.57)$$

where

$$\frac{N}{M} \doteq \frac{-0.604X_L}{0.096X_L + 71 - j52.2} \cdot \qquad (1.58)$$

The magnitude of $I_z(z)$ is calculated for values of Z_L equal to 0, ∞, $-j1600\Omega$, $-j800\Omega$, $-j600\Omega$, $j1600\Omega$, $j800\Omega$, $j600\Omega$ and shown graphically in Figs. 1-8a and 1-8b. This family of curves is quite different from those of the preceeding section. Although a purely reactive impedance reduces the magnitude of the induced current and tends to reverse the phase of the induced current, it is not possible to reduce the radar cross section to zero because current nulls do not occur in this case. Actually, as will be shown in 1-3.1, the optimum impedance for zero broadside back scattering from a cylinder of this size should have a large resistive component.

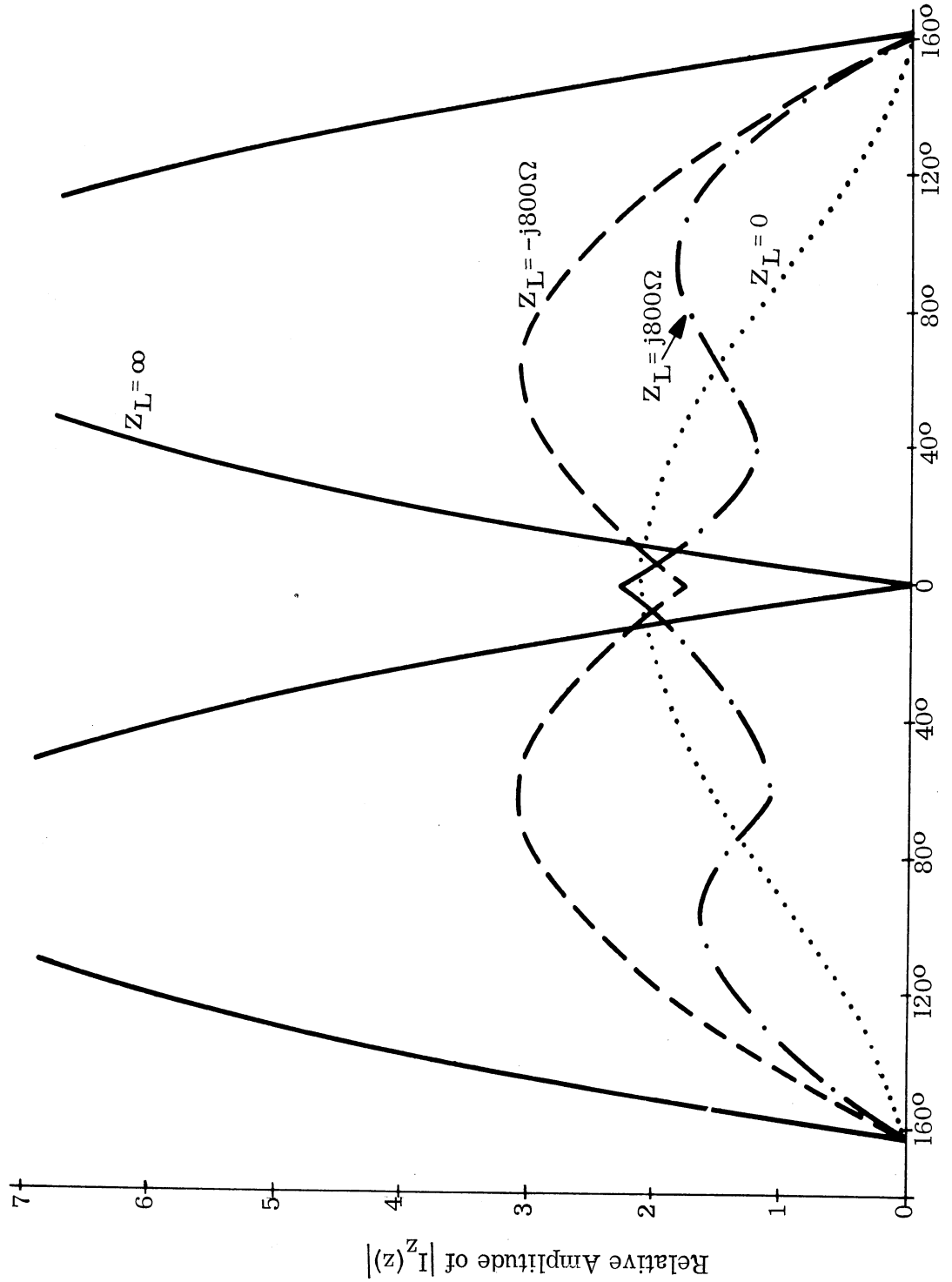

FIG. 1-8a: CURRENT DISTRIBUTION, $I_z(z)$, ON A CYLINDER OF h=0.45λ, a=0.0173λ FOR DIFFERENT CENTRAL LOAD (THEORETICAL)

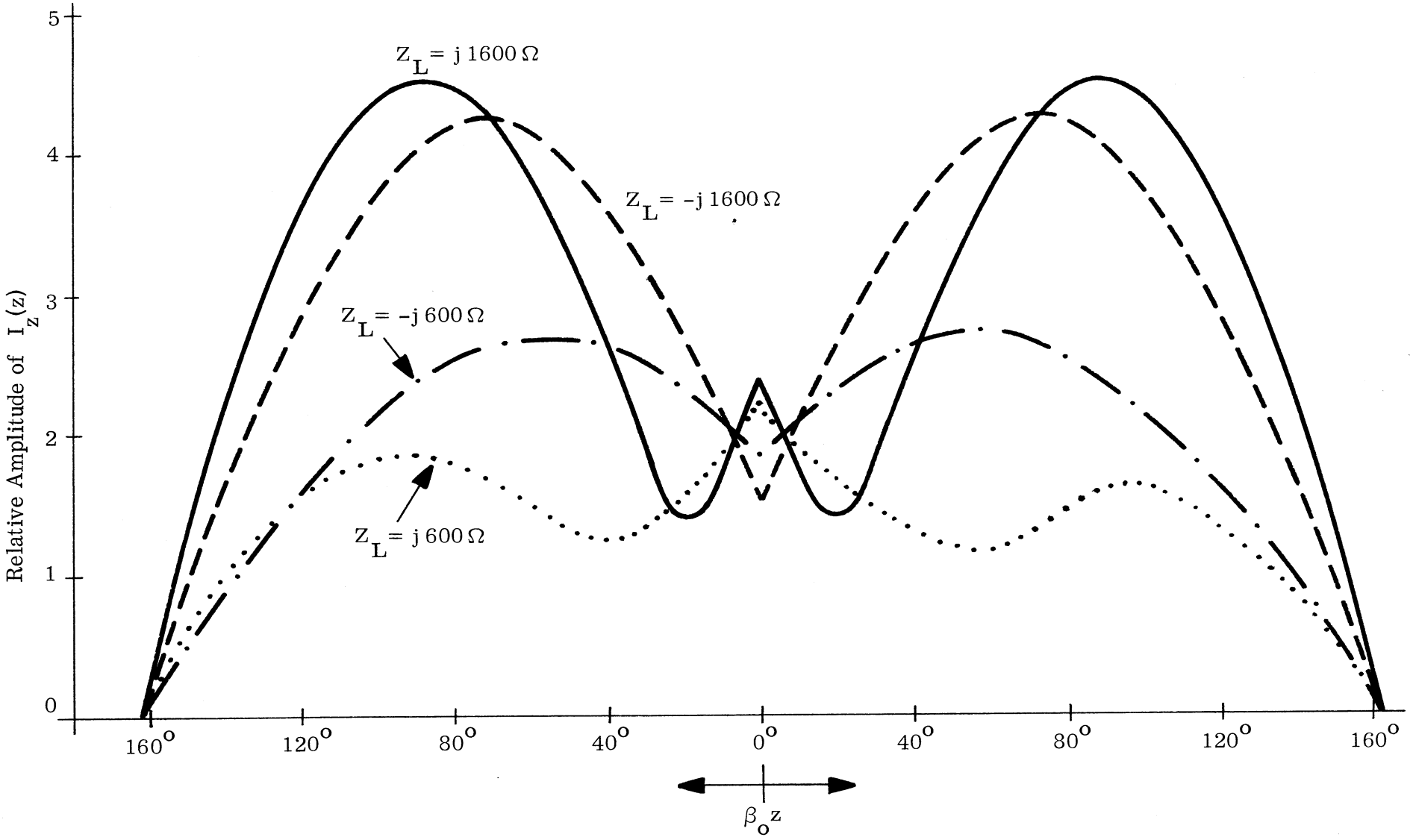

FIG. 1-8b: CURRENT DISTRIBUTION ON A CYLINDER FOR DIFFERENT CENTRAL LOAD
$h = 0.45\lambda$, $a = 0.0173\lambda$ (THEORETICAL)

In Figs. 1-15a and 1-15b the experimental results for the currents induced on this cylinder are summarized. The general shapes of the experimental curves are similar to the theoretical curves. A comparison between theory and experiment is made in Fig. 1-9 for three typical theoretical curves and their experimental counterparts. The agreement between theory and experiment is again good, although not as good as in the case of a shorter cylinder.

1-2 CURRENT MEASUREMENT ON A CENTER-LOADED CYLINDER

1-2.1 Experimental Setup

A block diagram of the equipment used for the current measurement is shown in Fig. 1-10. The cylinder was illuminated at broadside by a plane wave of 1.088 Gc from an L-band horn antenna with the electric field polarized in the direction parallel to the cylinder. A conventional probing method with a small current probe was employed to measure the induced current amplitude on the cylinder.

The coaxial line leading from the probe was covered with radar absorbing material (RAM) and oriented perpendicular to the E field to minimize its interaction with the E field. The measurement area was also lined with RAM to reduce unwanted reflections. This is shown in Fig. 1-11.

Figs. 1-12 and 1-13 show partially disassembled components of the loaded cylinder. The cylinder diameter is about 0.95 cm and its length can be changed from 10 cm ($h = 0.182\lambda$) to 51.29 cm ($h = 0.93\lambda$) by the combination of center and end pieces of different lengths. The center sections of the cylinder contain a symmetric coaxial cavity with an input gap at the center of the cylinder. The diameters of the center and outer conductors of the cavity are 0.32 cm and 0.79 cm respectively. By varying the cavity length, various input reactances are obtained. The coaxial cavity is filled with a dielectric (Stycast Hi K: $\epsilon_r = 4$, $\delta \cong 0.0001$) in order to reduce the cavity length to fit within the cylinder.

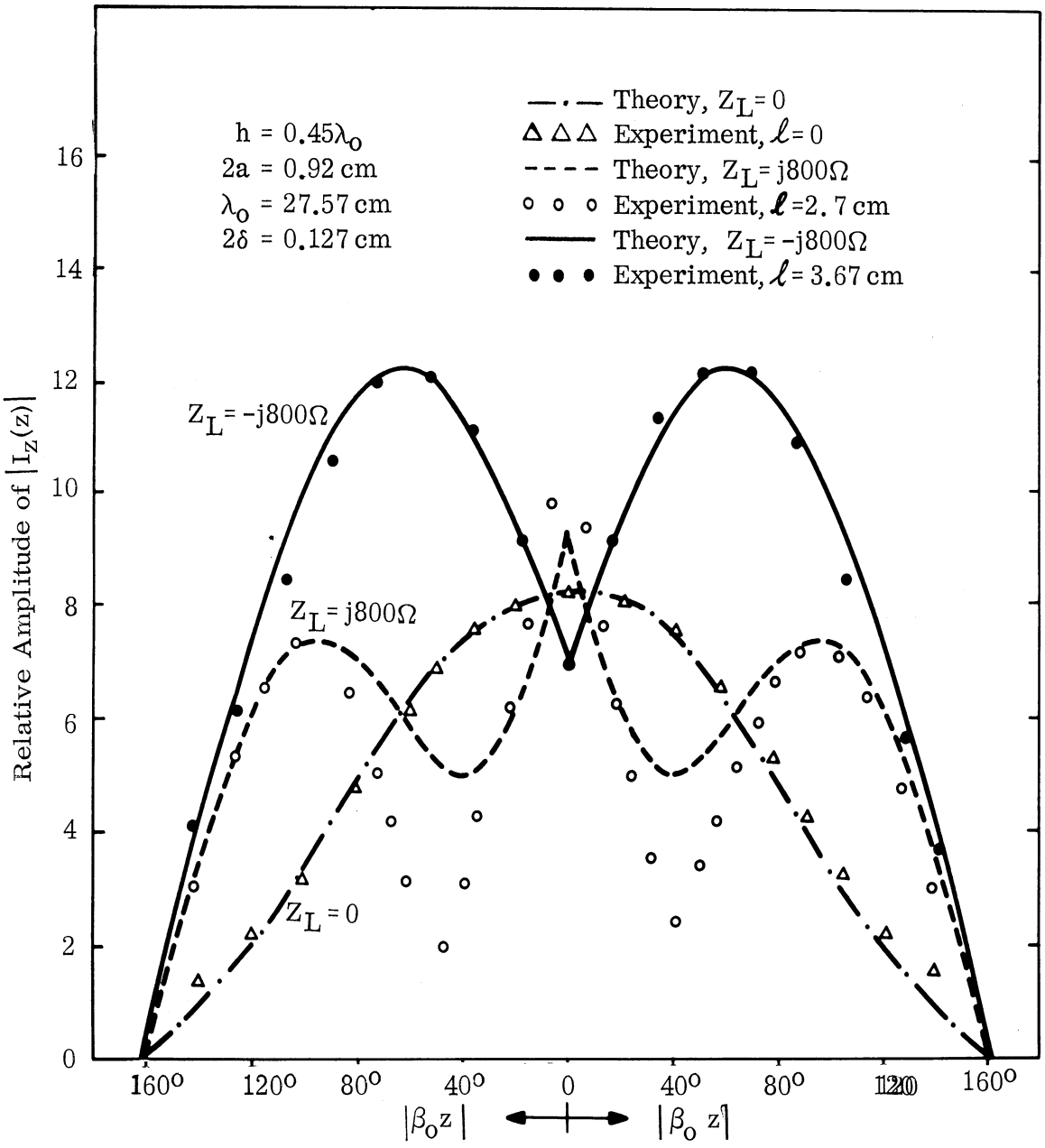

FIG. 1-9: CURRENT DISTRIBUTION ALONG A CYLINDER AS A FUNCTION OF CENTRAL LOAD FOR $h=0.45\lambda_0$ (THEORETICAL AND EXPERIMENTAL)

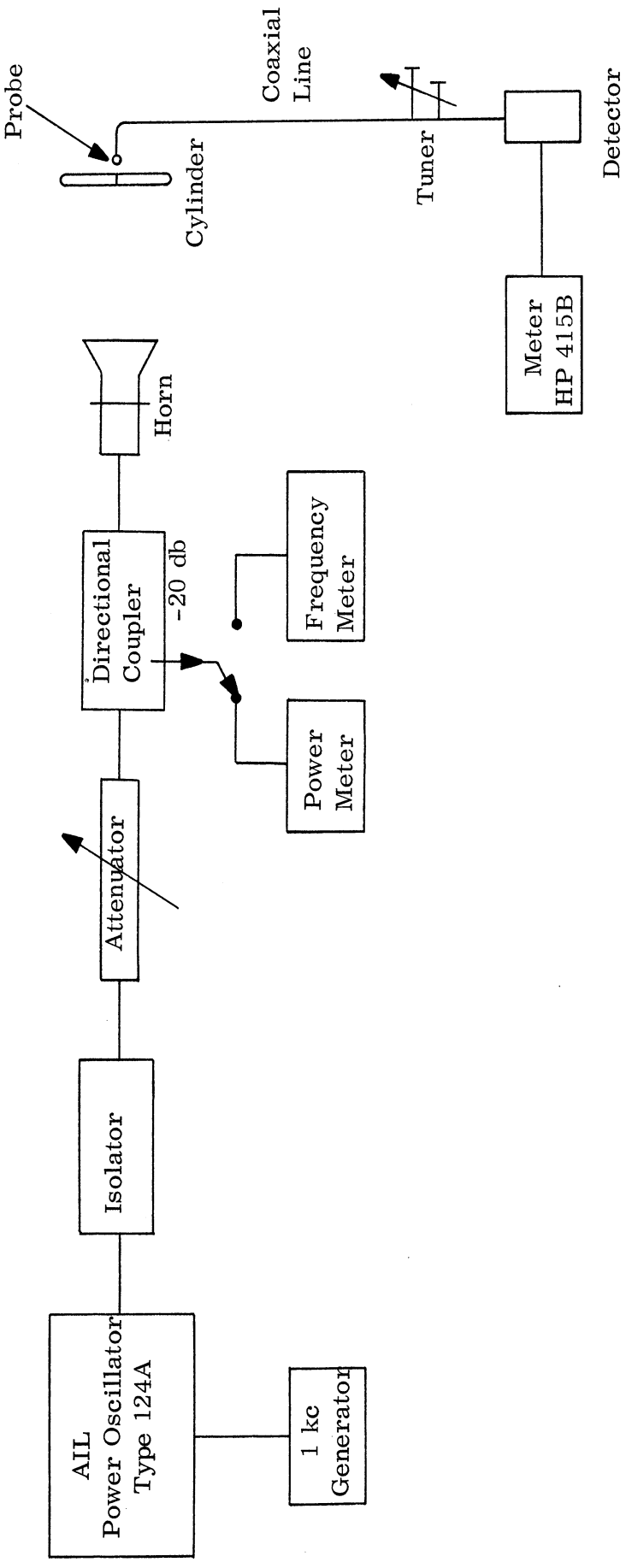

FIG. 1-10: BLOCK DIAGRAM OF THE EXPERIMENTAL SETUP

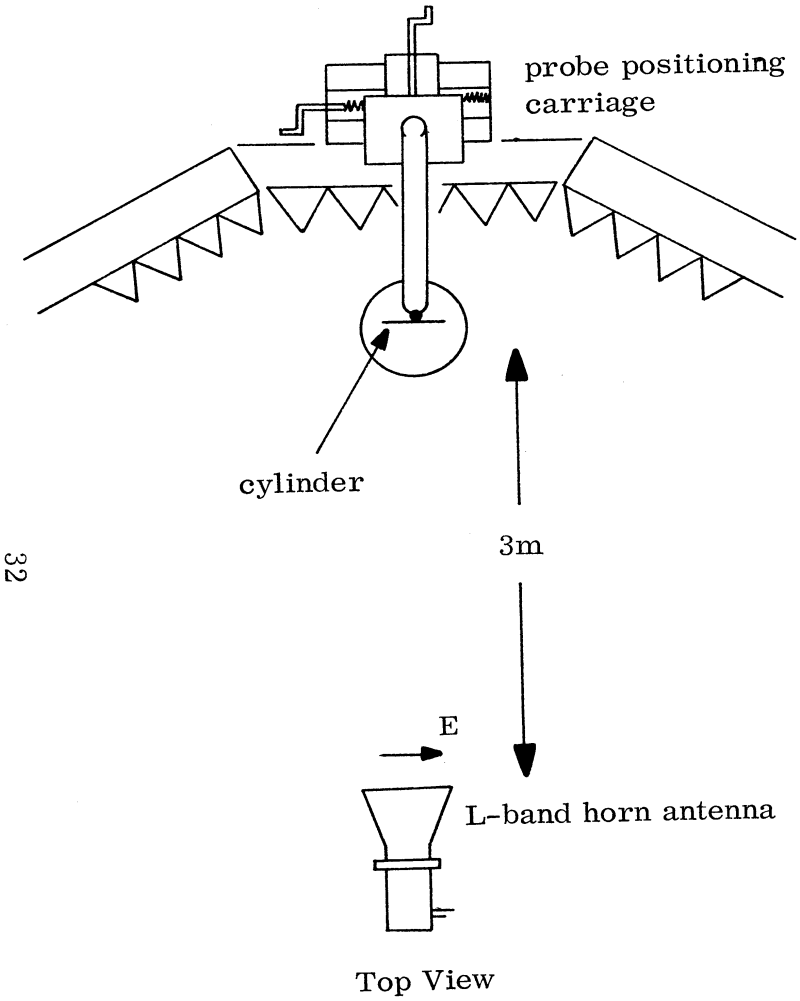

Top View

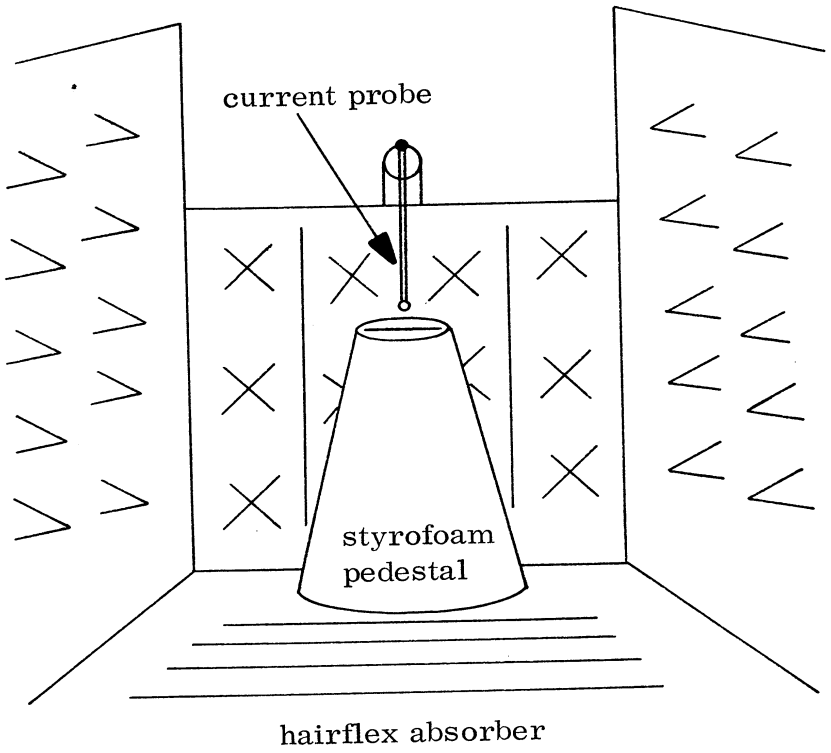

Side View

FIG. 1-11: ROOM LAYOUT

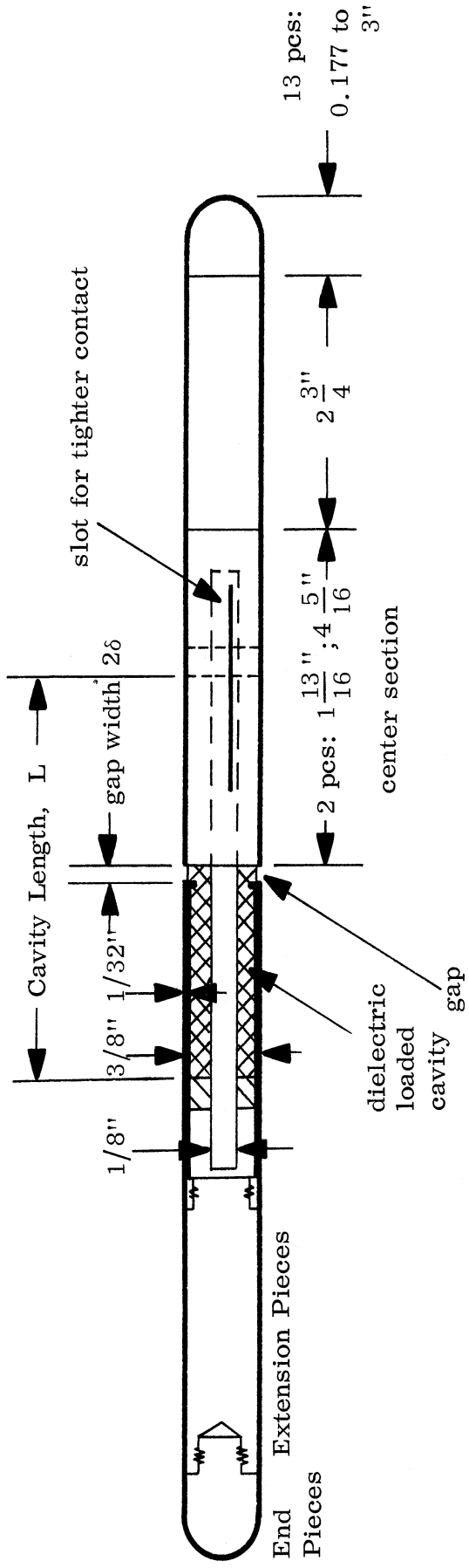

Material: Brass
Dielectric: Stycast Hi K ($\epsilon_r = 4$)
Minimum Dipole Length = 10.03 cm = 0.362λ at 1.088 Gc ($\delta = 0$)
Maximum Dipole Length = 51.19 cm = 1.91λ at 1.088 Gc ($\delta = 0$)

FIG. 1-12: CYLINDER WITH VARIABLE OVERALL LENGTH AND CAVITY LENGTH

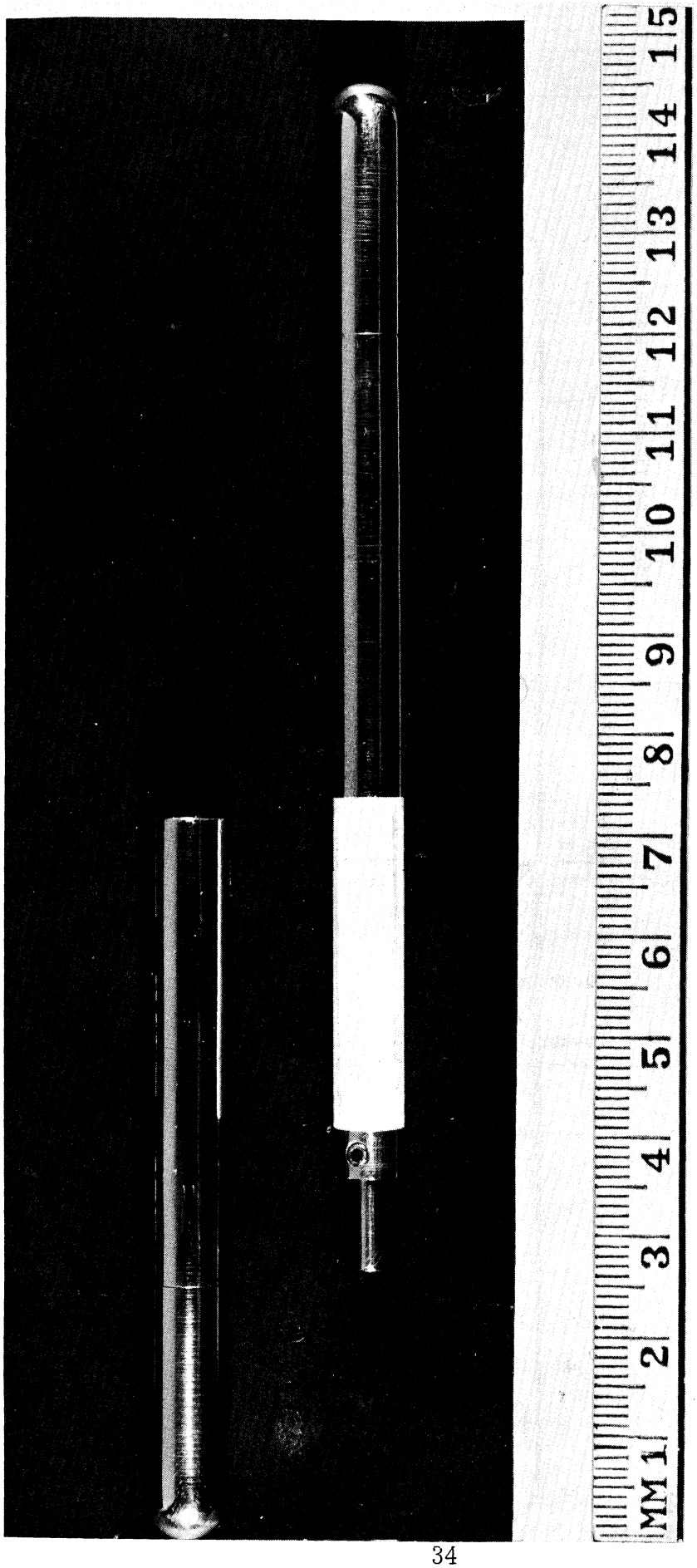

FIG. 1-13: CYLINDER WITH COAXIAL CAVITY

1-2.2 Experimental Results

Figs. 1-14a and 1-14b show the cylinder current distributions with $h = 0.215\lambda$ for various central loadings. The curves are given in terms of the cavity length L. The central impedance Z_L is not explicitly defined here, but its relation to the cavity length L is given in the next section (1-2.3). When $L = 0$, $Z_L = 0$; Z_L achieves its maximum ("infinite") when L is about 6.21 cm. For $0 < L < 6.21$ cm Z_L is inductive while for $L > 6.21$ cm but less than a certain critical length, Z_L is capacitive.

The maximum current on a cylinder with $h = 0.215\lambda$ and $Z_L = 0$ corresponds to a resonant current. The relative amplitude of the current is normalized to this maximum current. For the case of $L = 5.83$ cm the current distribution is close to optimum, i.e. the cross section is close to zero. For other cavity lengths the current distributions are also in good agreement with the theoretical predictions.

In Figs. 1-15a and 1-15b we have the current distributions for a cylinder with various cavity lengths and $h = 0.444\lambda$. This particular cylinder length corresponds to an antiresonant length. The manner in which this affects the induced current may be seen from the graphs: the introduction of a central impedance increases, rather than decreases, the induced current in general. This implies an increase in back scattering. Although the current distribution corresponding to $L = 5.58$ cm is close to the optimum distribution, it is impossible to reduce the broadside cross section to zero by purely reactive loading. This is due to the fact that the phase of the current is not completely reversed at the center part of the cylinder and no current null appears with this loading. The asymmetries which exist in the measured currents are caused by room reflections.

Fig. 1-16 shows the current distributions on a cylinder with fixed central impedance but whose length varies from $2h = 10.03$ cm to $2h = 39.73$ cm. The

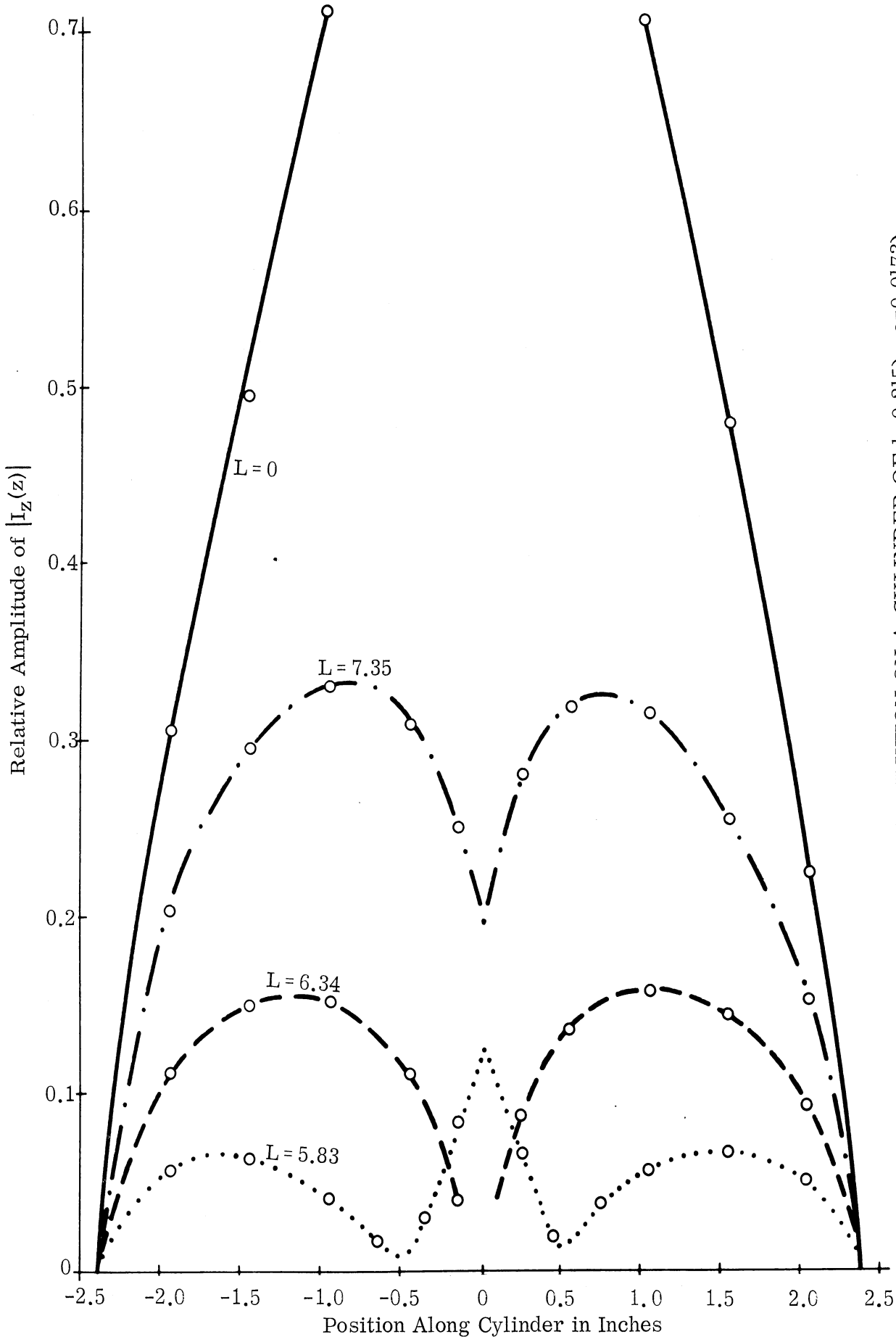

FIG. 1-14a: CURRENT DISTRIBUTION ON A CYLINDER OF h=0.215λ, a=0.0173λ WITH CAVITY LENGTHS, L (cm) (EXPERIMENTAL

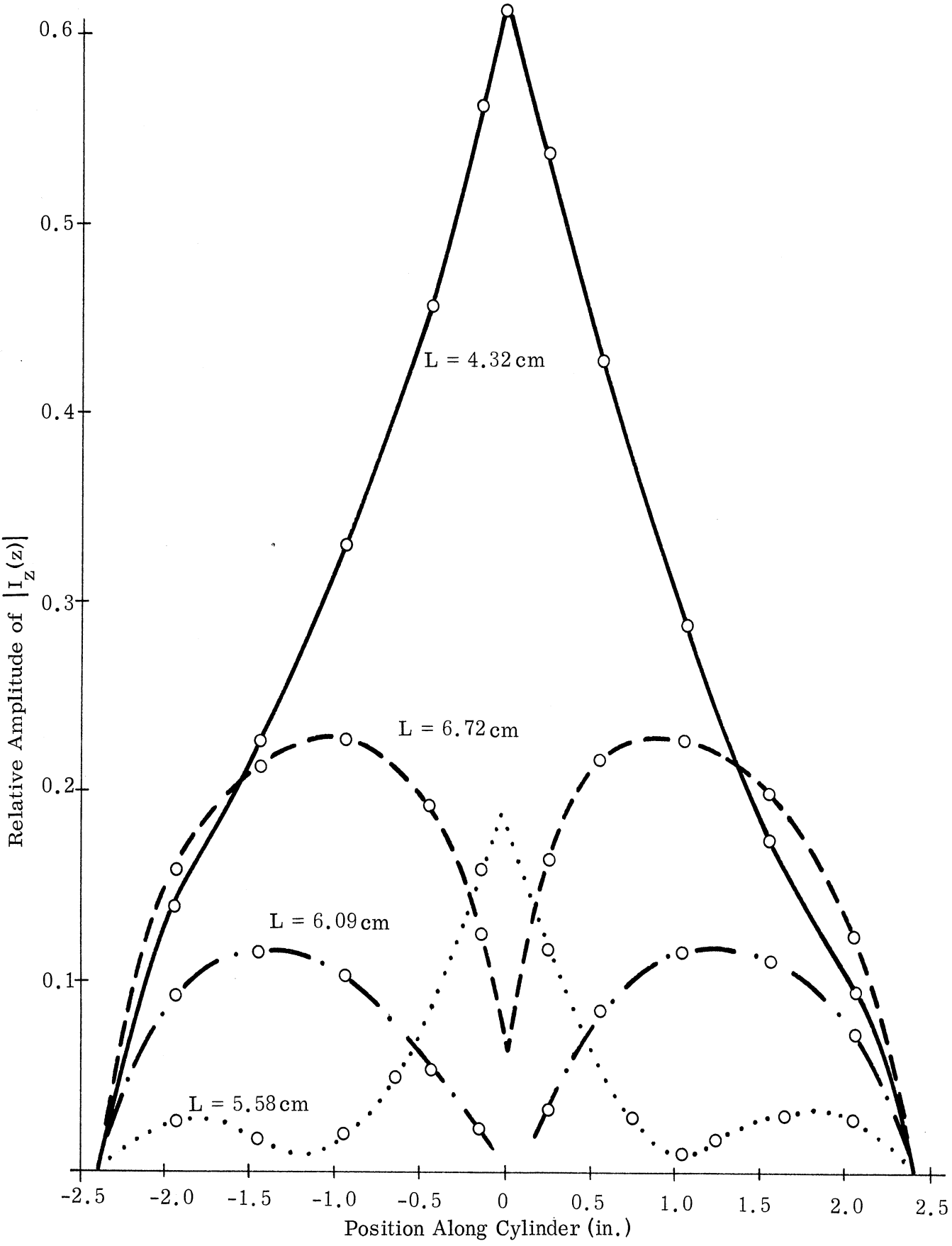

FIG. 14b: CURRENT DISTRIBUTION ON A CYLINDER WITH VARIOUS CAVITY LENGTHS h = 0.215λ, a = 0.0173λ. (EXPERIMENTAL)

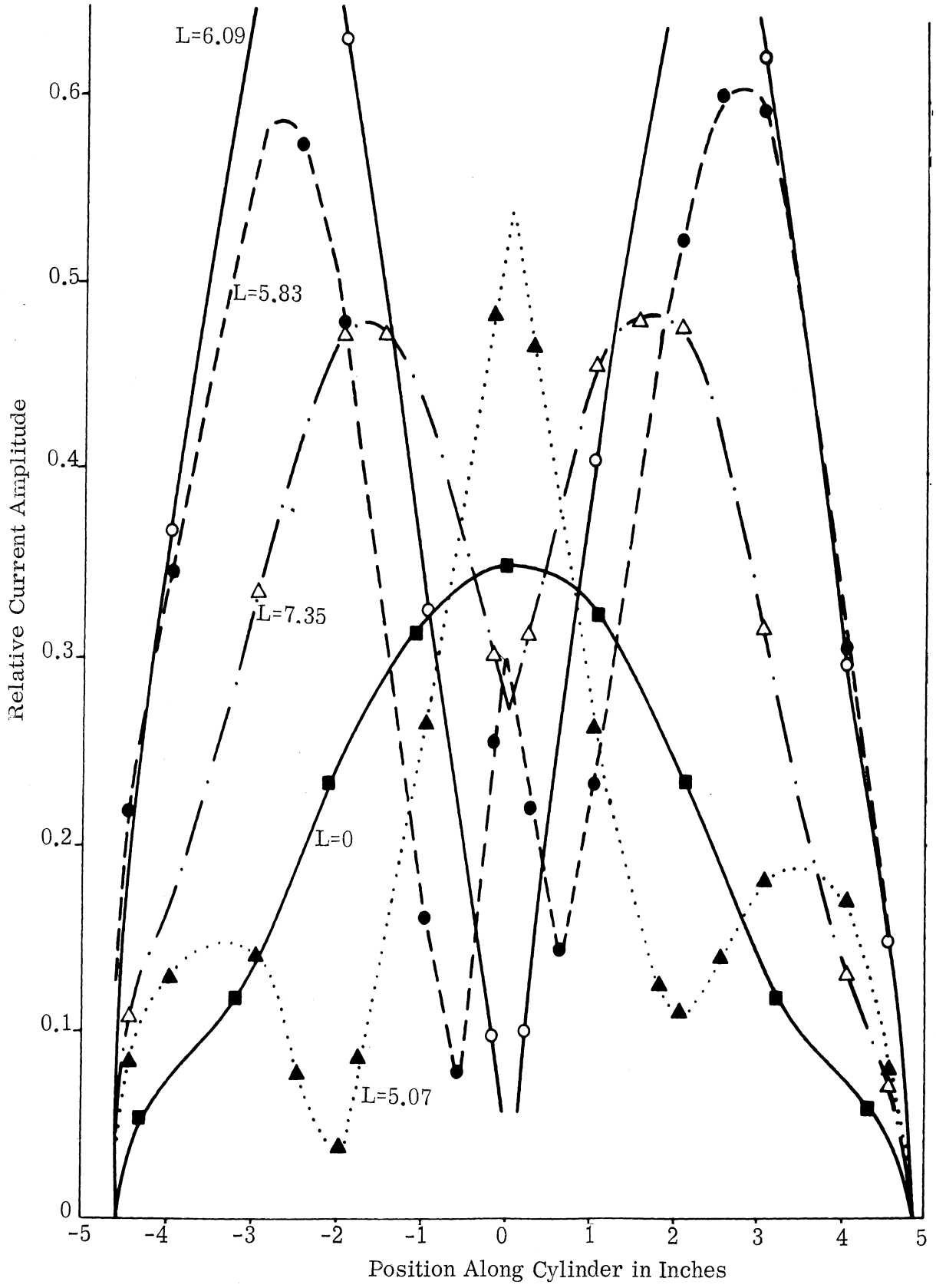

FIG. 1-15a: CURRENT DISTRIBUTION ON A CENTER-LOADED CYLINDER WITH VARIOUS CAVITY LENGTHS. $h=0.444\lambda_o$, $2\delta=0.050$ in, $\epsilon_r=4$. CURRENT SCALE IS RELATIVE TO MAXIMUM CURRENT (1.0) ON $h=0.215\lambda_o$, UNLOADED CYLINDER (EXPERIMENTAL)

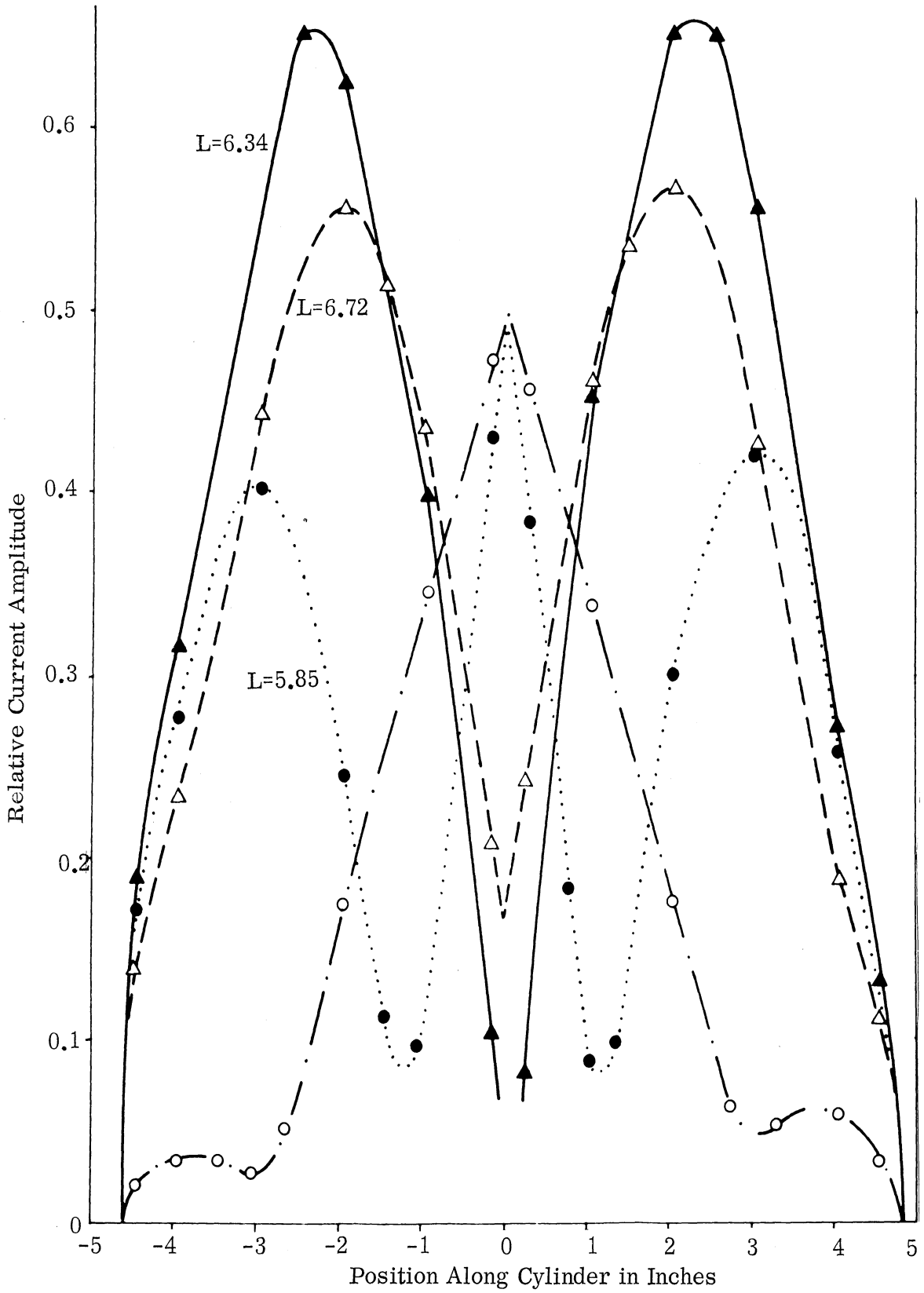

FIG. 1-15b: CURRENT DISTRIBUTION ON CENTER-LOADED CYLINDER WITH VARIOUS CAVITY LENGTHS. $h=0.444\lambda_o$, $2\delta=0.050$ in., $\epsilon_r = 4$. CURRENT SCALE IS RELATIVE TO MAXIMUM CURRENT (1.0) ON $h=0.215\lambda_o$ UNLOADED CYLINDER (EXPERIMENTAL)

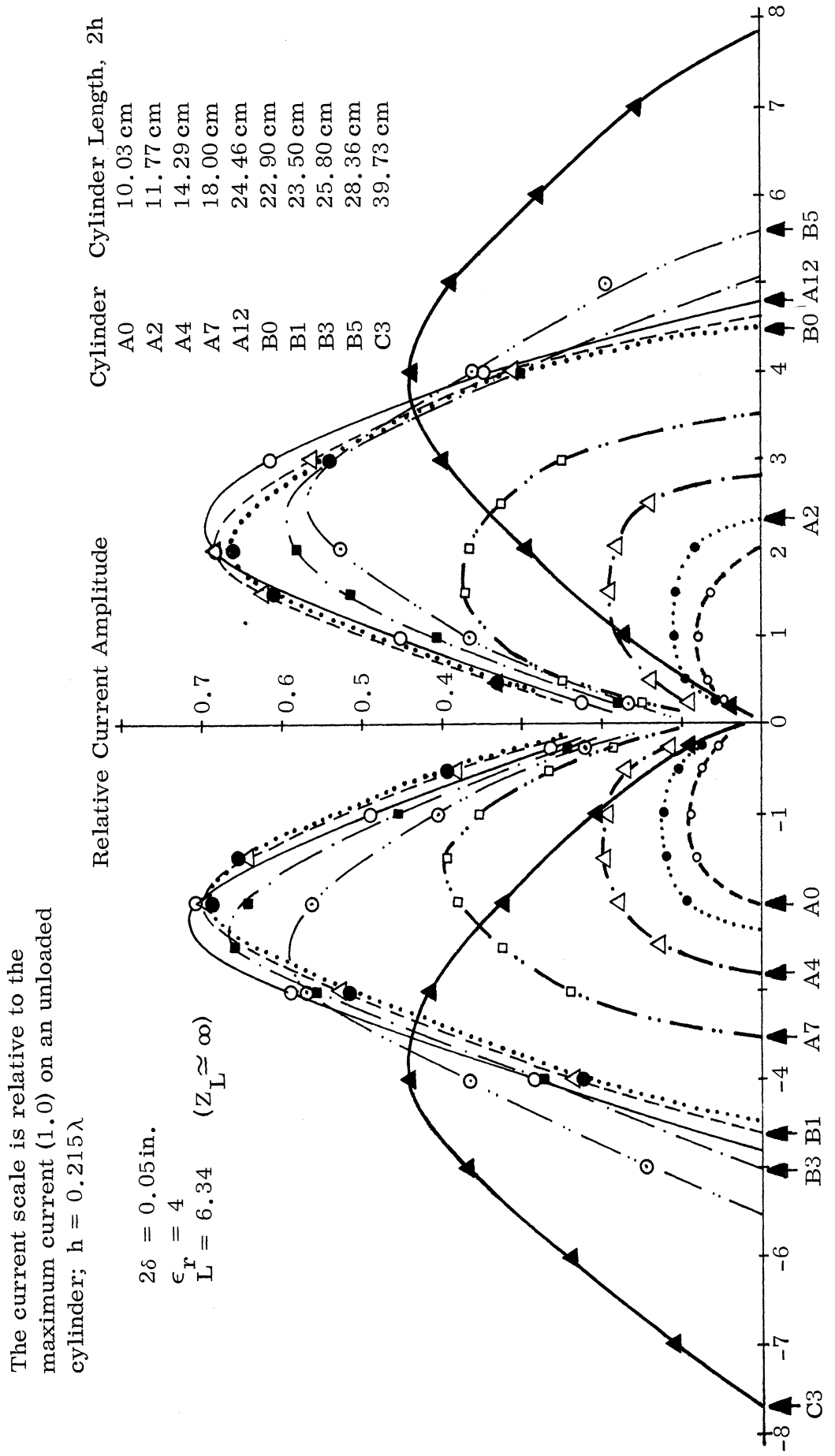

FIG. 1-16: CURRENT DISTRIBUTION ON CENTER LOADED CYLINDER FOR FIXED CAVITY LENGTH (EXPERIMENTAL)

cavity length is kept at L = 6.34 cm. The cavity length is rather arbitrary, but it appears to give a high central impedance. An accurate antiresonant length of the cavity was later found to be L = 6.21 cm.

1-2.3 Equivalent Circuit for Coaxial Cavity and Gap Capacitance

An approximate value for the input impedance of the coaxial cavity can be obtained from the following observations.

In Fig. 1-17a the dielectric loaded coaxial cavity is schematically represented. The input terminals are at the center of the outer conductor and a stray capacitance is assumed to be shunted across the input terminals. If a voltage V is applied at the input terminals the input current i is

$$i = i_t + i_c \tag{1.59}$$

where i_t is the transmission line current which flows inside the coaxial cavity and i_c is the current which flows through the stray capacitance.

It is evident that

$$i_c = j\omega C_s V \tag{1.60}$$

but the transmission line current i_t requires a more involved argument for its determination:

As shown in Fig. 1-17b, the coaxial cavity can first be simplified to the case of a transmission line driven by a voltage V at the center of one wire of the line. This transmission line can then be considered as the superposition of two modes, as shown in Fig. 1-17c. Hence

$$i_t = i^s + i^a \tag{1.61}$$

where i^s is the current of the symmetrical mode and i^a is the current of the antisymmetrical mode. Since i^s can be assumed to be a usual TEM mode current

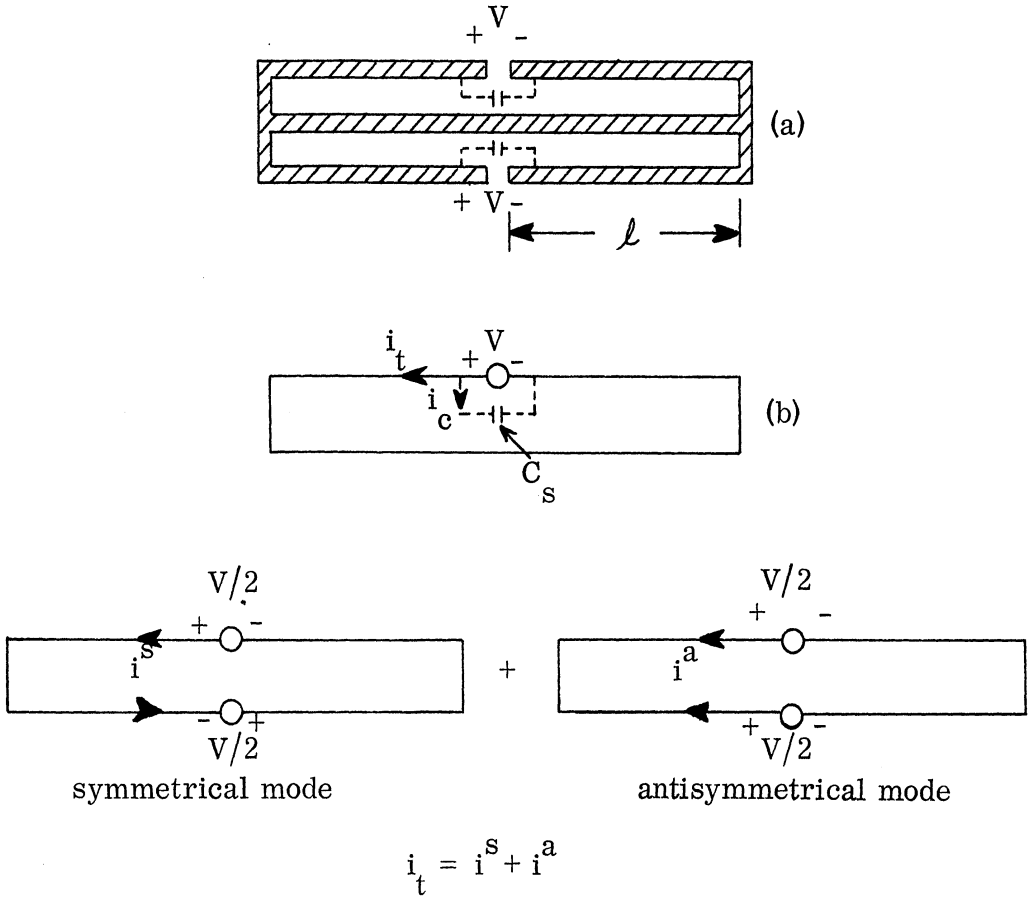

$$i_t = i^s + i^a$$

FIG. 1-17: EQUIVALENT CIRCUITS FOR COAXIAL CAVITY

it can be obtained simply as

$$i^s = \frac{V/2}{jZ_o \tan\beta\ell} \tag{1.62}$$

where Z_o is the characteristic impedance of the (assumed) lossless cavity, β is a propagation constant, and ℓ is the half-length. Furthermore, a coaxial cavity does not allow the existence of the antisymmetrical mode and so the antisymmetrical current is small. Thus, neglecting i^a the total input current i becomes

$$i = i_t + i_c = \frac{V/2}{jZ_o \tan\beta\ell} + j\omega C_s V \tag{1.63}$$

The input impedance of the coaxial cavity is

$$Z_L = \frac{V}{i} = \frac{j2Z_o \tan\beta\ell}{1 - 2\omega C_s Z_o \tan\beta\ell} \tag{1.64}$$

where Z_o is known to be

$$Z_o = \frac{60}{\sqrt{\epsilon_r}} \ln\left(\frac{r_2}{r_1}\right) \tag{1.65}$$

and ϵ_r is the dielectric constant of the dielectric in the cavity and r_1 and r_2 are the inner and outer cavity radii respectively. The value of the stray capacitance C_s in (1.64) is difficult to determine either theoretically or experimentally and an indirect method was used:

We know that corresponding to $Z_L = \infty$ the current distribution has a null at $z = 0$ and maxima at $z = \pm h/2$. From the current distributions of Figs. 1-14a and

For the cavity used in the experiment,

$$Z_o = 27.2\Omega, \qquad \omega = 2\pi \times 1.088 \times 10^9, \qquad \epsilon_r = 4,$$

and we obtain from (1.66)

$$C_s = 0.402\,\mu\mu f \tag{1.67}$$

Using this value of C_s, other input impedances have been obtained as functions of $L\,(= 2\ell)$

L(cm)	$Z_L\,(\Omega)$
5.07	j 212
5.86	j 600
6.04	j 800
6.10	j 1600
6.21	j ∞
6.39	-j 1600
6.55	-j 800
6.64	-j 600

The effect of the gap width on the induced current is shown in Fig. 1-18. Since the amplitude of the induced current is greatly affected by the gap width, the stray capacitance at the cavity input cannot be neglected in the calculation of the input impedance.

1-3. THE RADAR CROSS SECTION OF A CENTER-LOADED CYLINDER

In the preceding sections we found the induced current on a center-loaded cylinder as a function of cylinder dimension and the central impedance. We now proceed to study the scattering from such a cylinder and determine the optimum impedance for reducing the broadside cross section.

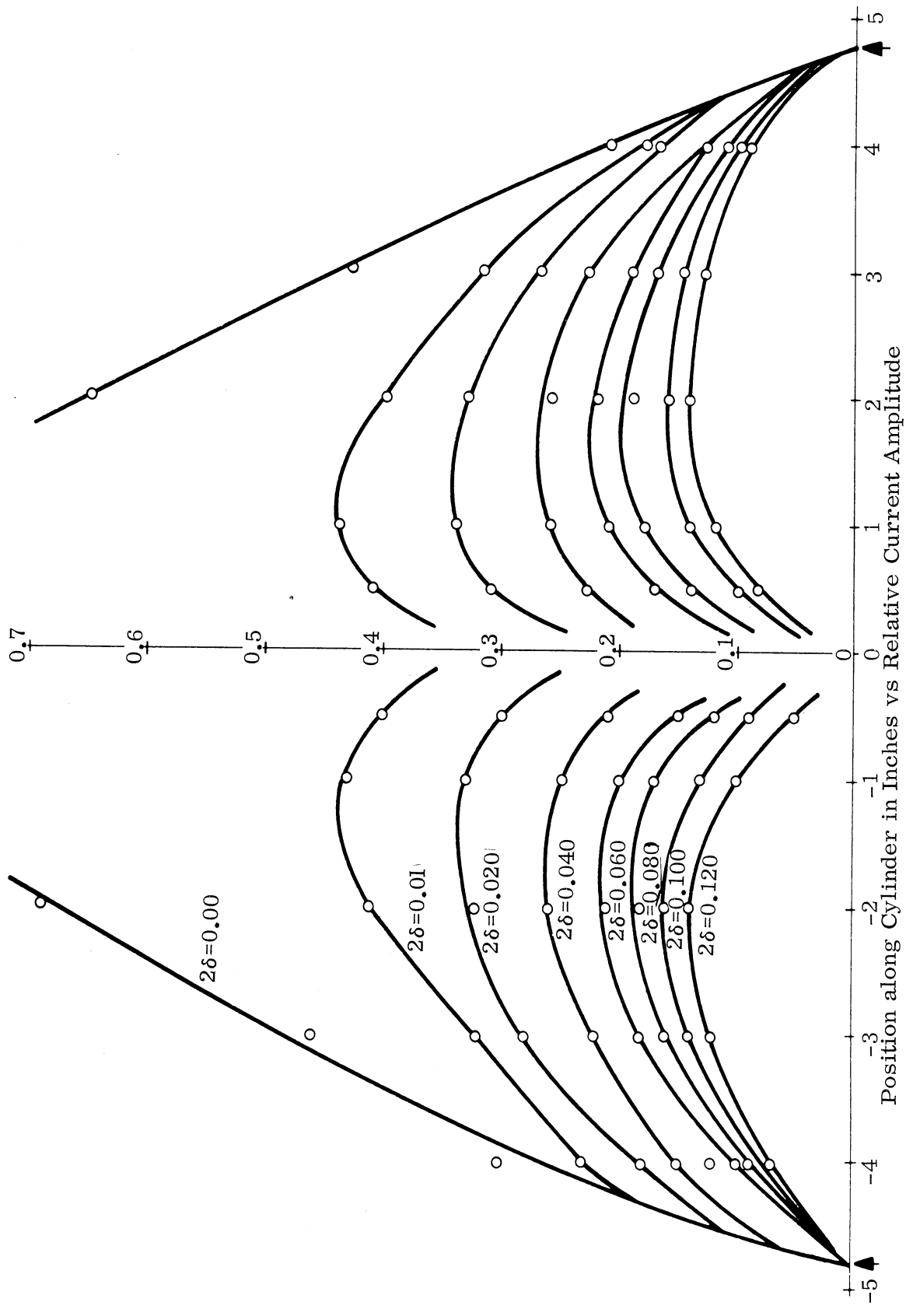

FIG. 1-18: CURRENT DISTRIBUTION ON CENTER-LOADED CYLINDER FOR VARIOUS GAP THICKNESS, 2δ. CURRENT SCALE IS RELATIVE TO MAXIMUM CURRENT (1.0) ON UNLOADED CYLINDER h=0.215λ, ϵ_r=4, L=6.85 cm.

1-3.1 Optimum Impedance for Zero Broadside Back Scattering from a Thin Cylinder

Since the induced currents give rise to a vector potential from which the scattered field may be computed, we use the expressions for the induced current in (1.34) through (1.36) to first determine the associated vector potential.

For the far zone of the cylinder the vector potential is

$$A_z = \frac{\mu_o}{4\pi}\frac{jE_o}{30\beta_o}\left(\frac{1}{\cos\beta_o h - MT_{ca} - NT_{sa}}\right)\left[M\int_{-h}^{h}(\cos\beta_o z - \cos\beta_o h)\frac{e^{-j\beta_o R}}{R}\,dz + N\int_{-h}^{h}\sin\beta_o(h-|z|)\frac{e^{-j\beta_o R}}{R}\,dz\right] \quad (1.68)$$

where

$R = R_o - z\cos\theta$ = distance between a point on the cylinder and the observation point.

The scattered electric field in the far zone is then

$$E_\theta^s = -j\omega A_\theta = j\omega A_z \sin\theta \ . \quad (1.69)$$

and the corresponding Poynting vector is

$$P^s = \frac{1}{2\zeta_o}\left|E_\theta\right|^2 \quad (1.70)$$

The scattered field in the broadside direction is obtained when

$$\theta = 90^o \qquad \text{and} \qquad R = R_o \ . \quad (1.71)$$

We then obtain

$$E_\theta^s(\theta=90^o) = \frac{2}{\beta_o}E_o\frac{e^{-j\beta_o R_o}}{R_o}\left[\frac{M(\sin\beta_o h - \beta_o h\cos\beta_o h) + N(1-\cos\beta_o h)}{\cos\beta_o h - MT_{ca} - NT_{sa}}\right] \quad (1.72)$$

and

$$P^s(\theta=90^o) = \frac{2}{\zeta_o}\frac{E_o^2}{\beta_o^2 R_o^2}\left|\frac{M(\sin\beta_o h - \beta_o h\cos\beta_o h) + N(1-\cos\beta_o h)}{\cos\beta_o h - MT_{ca} - NT_{sa}}\right|^2 . \quad (1.73)$$

Equation (1.36) gives N as a function of Z_L. Hence (1.73) expresses the Poynting power density as a function of the central impedance.

Thus to reduce the back scattering ($\theta = 90^o$) radar cross section to zero we simply make P^s equal to zero. This gives the condition

$$\frac{N}{M} = -\frac{\sin\beta_o h - \beta_o h\cos\beta_o h}{1-\cos\beta_o h} . \quad (1.74)$$

Using (1.35) and (1.36), (1.74) can be rewritten as

$$\frac{Z_L \sin\beta_o h(1-\cos\beta_o h)}{Z_L\sin^2\beta_o h - j60T_{sd}\cos\beta_o h} = \frac{\sin\beta_o h - \beta_o h\cos\beta_o h}{1-\cos\beta_o h} . \quad (1.75)$$

By solving for Z_L in (1.75) we obtain the optimum central impedance

$$\left[Z_L\right]_o = \frac{-j60T_{sd}(1-\beta_o h\cot\beta_o h)}{2\cos\beta_o h - 2 + \beta_o h\sin\beta_o h} \quad (1.76)$$

where T_{sd} is expressed in (1.38).

Equation (1.76) gives the complete expression for optimum central impedance as a function of the cylinder dimension. In view of its simplicity, the expression should prove useful in practical design.

In Fig. 1-19 the calculated values of $\left[Z_L\right]_o$ for a cylinder with $a = 0.0173\lambda$ are plotted as a function of the cylinder length h/λ. Certain observations are evident:

(1) In general, the optimum central impedance for zero broadside back scattering should have both resistive and reactive components.

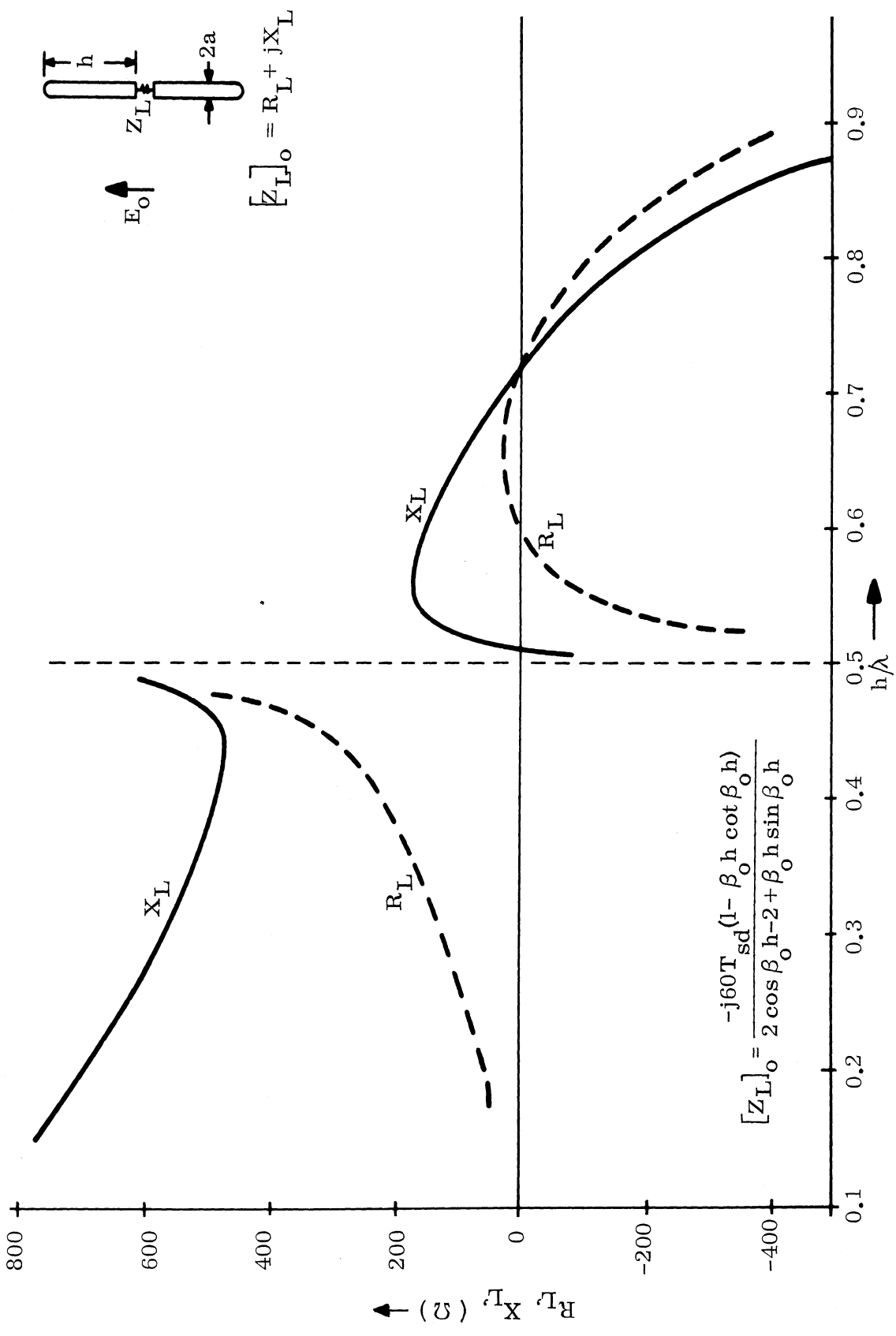

FIG. 1-19: OPTIMUM CENTRAL IMPEDANCE $[Z_L]_o$ FOR ZERO BACKSCATTERING FROM CYLINDER OF RADIUS a=0.0173λ AS FUNCTION OF CYLINDER LENGTH

(2) For a cylinder shorter than one wavelength ($h < 0.5\lambda$) the optimum impedance is inductive and requires a resistive component.

(3) For a cylinder longer than one wavelength ($h > 0.5\lambda$) the optimum impedance is inductive or capacitive but it requires a negative resistive component.

These results indicate that for cylinders shorter than one wavelength a passive impedance can reduce the cross section to zero, but for cylinders longer than one wavelength an active impedance is required. However, in the latter case an active impedance may not be needed if the cylinder is loaded at two points.

In Fig. 1-20 the cylinder parameter is changed to $a = 0.0517\lambda$ and $[Z_L]_o$ is again obtained as a function of cylinder length h/λ. The similarity to Fig. 1-19 is evident. For the thicker cylinder the resistive component remains relatively constant but the reactive component is reduced—almost by a factor of two.

Another property which can be studied from (1.76) is the bandwidth characteristic of this technique. To do this we consider a cylinder with $h = 4$ cm, $a = 0.476$ cm and calculate the optimum impedance for a range of frequencies between 1 Gc and 3 Gc. The results are shown in Fig. 1-21. From the graph it is seen that within this frequency range the optimum impedance is inductive and requires a resistive component. For a wider range of frequencies an active impedance is needed. This impedance appears to be obtainable by a simple network synthesis.

1-3.2 Scattered Fields of a Center-Loaded Cylinder

In this section we calculate the bistatic scattered field of a center loaded cylinder which is illuminated by a normally incident plane wave.

When a center loaded cylinder is illuminated by a plane wave at normal incidence, the induced currents are given by equations (1.34) to (1.36). In turn, these induced currents give rise to a vector potential in the far zone of the cylinder. Using (1.68) which expresses the vector potential and (1.69) which express the

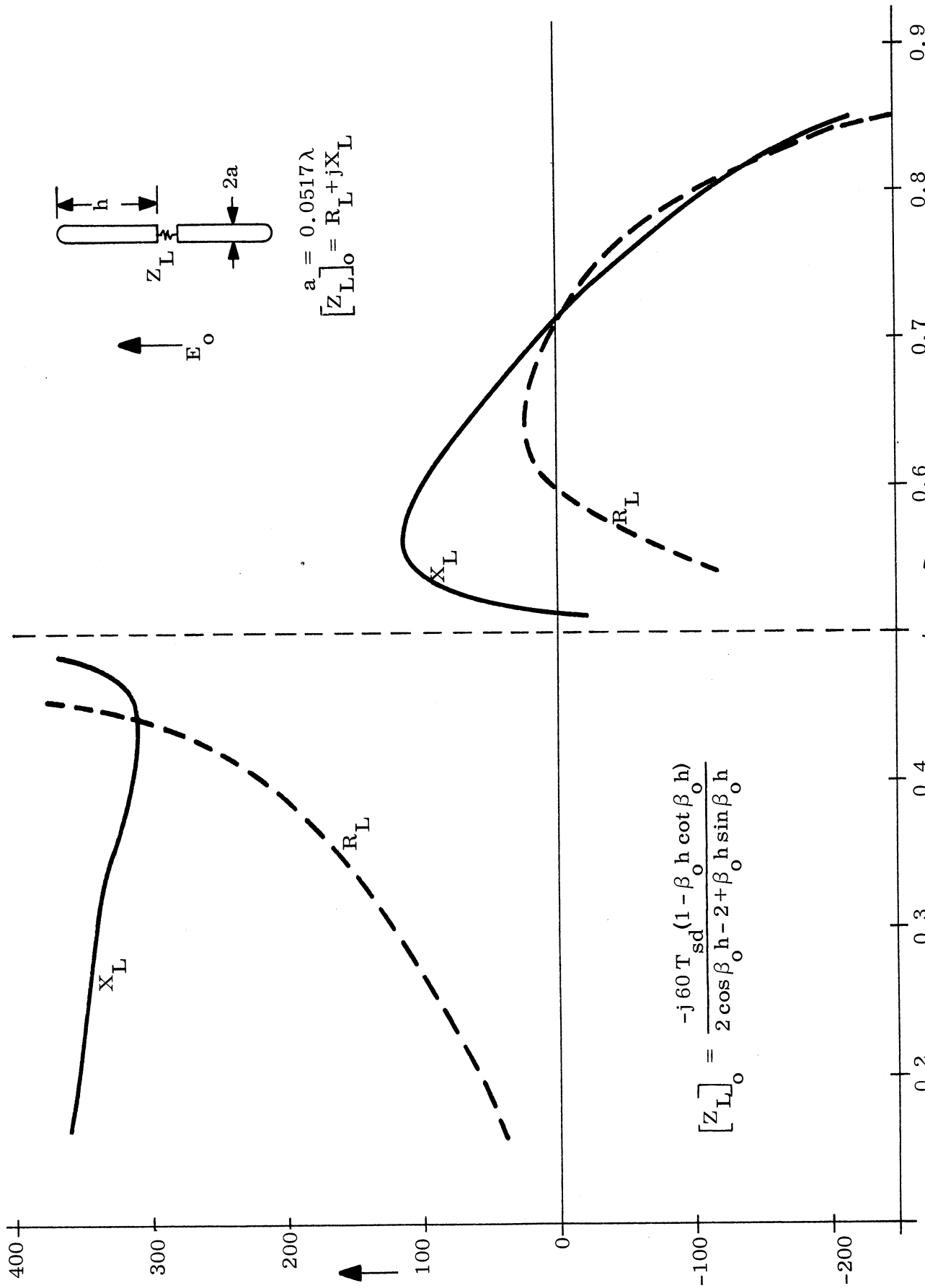

FIG. 1-20: OPTIMUM CENTRAL IMPEDANCE, $[Z_L]_o$, FOR ZERO BACK SCATTERING FROM A CYLINDER

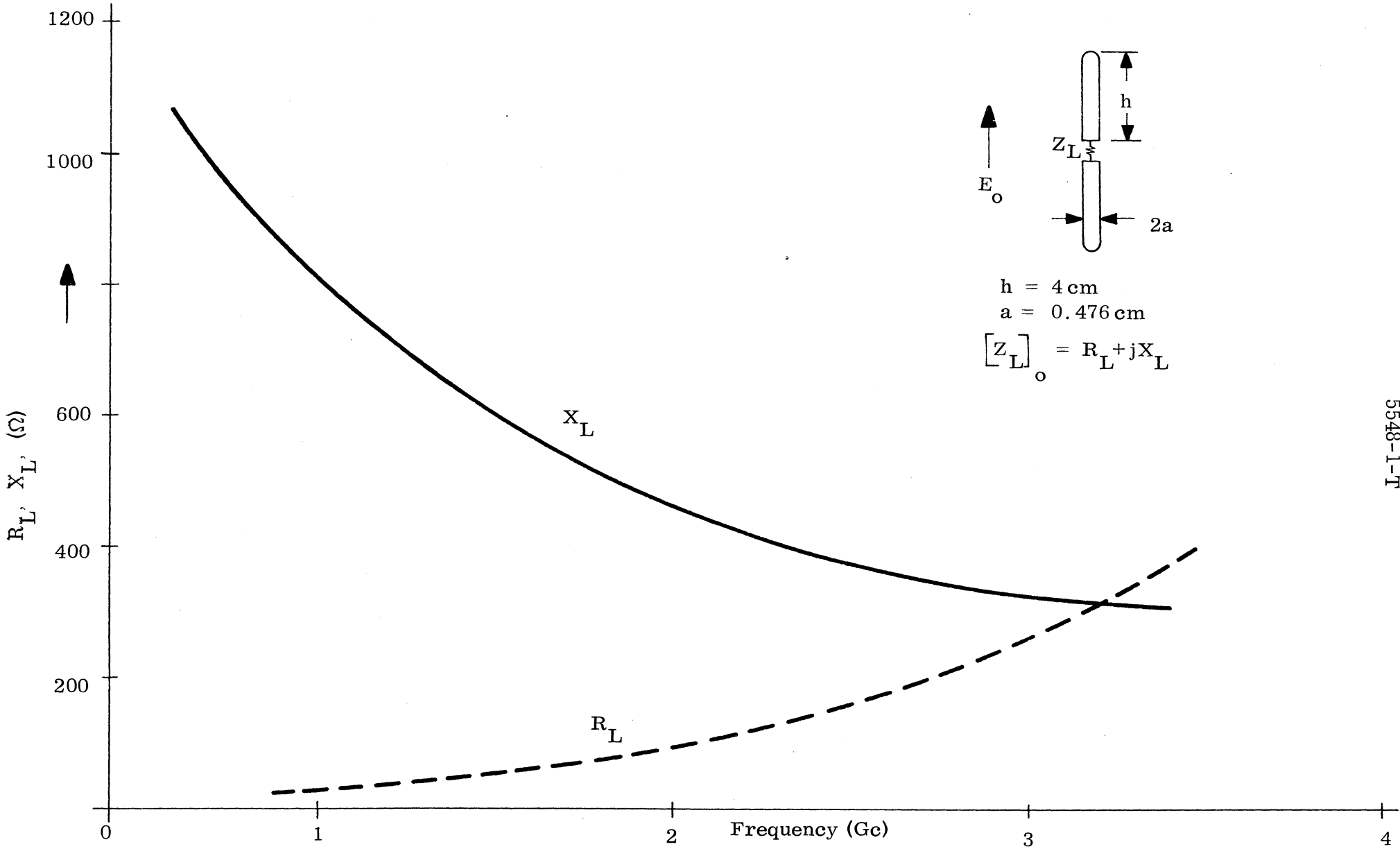

FIG. 1-21: OPTIMUM CENTRAL IMPEDANCE, $[Z_L]_o$, FOR ZERO BACK SCATTERING FROM A CYLINDER

THE UNIVERSITY OF MICHIGAN
5548-1-T

scattered electric field we perform the indicated integration and obtain

$$E_\theta^s = \frac{\omega\mu_o}{4\pi}\frac{e^{-j\beta_o R_o}}{R_o}\frac{E_o}{30\beta_o}\left(\frac{Mh}{\cos\beta_o h - MT_{ca} - NT_{sa}}\right)\left\{\sin\theta\left[\frac{\sin[\beta_o h(1+\cos\theta)]}{\beta_o h(1+\cos\theta)} + \right.\right.$$

$$+\frac{\sin[\beta_o h(1-\cos\theta)]}{\beta_o h(1-\cos\theta)} - 2\cos\beta_o h\,\frac{\sin(\beta_o h\cos\theta)}{\beta_o h\cos\theta}\Bigg]$$

$$\left. + \frac{N}{M}\frac{2}{\beta_o h}\,\frac{\cos(\beta_o h\cos\theta) - \cos\beta_o h}{\sin\theta}\right\}. \qquad (1.77)$$

By plotting E_θ^s as a function of θ we obtain the bistatic scattered field. An example will be considered.

For the case of a cylinder of resonant length we choose the following parameters:

$$h = 0.213\lambda, \qquad a = 0.0173\lambda$$

$$T_{cd} = 3.17 - j0.327$$

$$T_{sd} = 0.696 - j1.071$$

$$T_{ca} = 0.62 - j0.928$$

$$T_{sd} = 3.63 - j0.377$$

where the T's are calculated with the aid of a computer. We choose several different central loads: $Z_L = 0,\ \infty,\ j800\Omega,\ -j800\Omega,\ -j600\Omega,\ j626\Omega$ and the optimum central load $Z_L = 65 + j626\Omega$ (which can be obtained from Fig. 1-19 or from (1.76)).

For these seven cases of Z_L the back scattered field ($\theta = 90^o$) are calculated and listed in Table I. In the table the field strengths are normalized to the value of $E^s_\theta(\theta = 90^o)$ when $Z_L = 0$.

TABLE I

Impedance Z_L	Field Strength $E^s_\theta(\theta = 90^o)$	Power $[E^s_\theta]^2$	db
0	1.0	1.0	0
∞	.0841	.00707	-21.5
j 800	.022	.000484	-33.2
-j 800	.149	.0222	-16.5
-j 650	.144	.0207	-16.8
j 626	.00943	.0000889	-40.5
65+j 626	0	0	$-\infty$

In Fig. 1-22 is shown the bistatic field patterns for the cylinder with $Z_L = 0$, j 800 Ω, -j 800 Ω and ∞ Ω. Although the scattered field is greatly reduced by the introduction of the center loading, since none of these is the optimum loading, the scattered field can be further reduced.

In Fig. 1-23 where the bistatic field patterns for $Z_L = 65 + j\,626$ and for $Z_L = j\,626$ are shown, the scale is magnified by a factor of 100 with respect to the one used in Fig. 1-22. Even when Z_L is optimum the scattered field is not zero except in the back scatter direction. Instead, the pattern is seen to consist of four loops of very small field intensity with maxima at $\theta = 35^o$ and $\theta = 145^o$. However, the maximum field intensity is 56 db below its value for $Z_L = 0$.

I-4 SUMMARY

The important results obtained in Part I are summarized here.

The induced current on a center-loaded cylinder which is illuminated normally by a plane wave is obtained as a function of the cylinder dimension and the central impedance in (1.34) through (1.36).

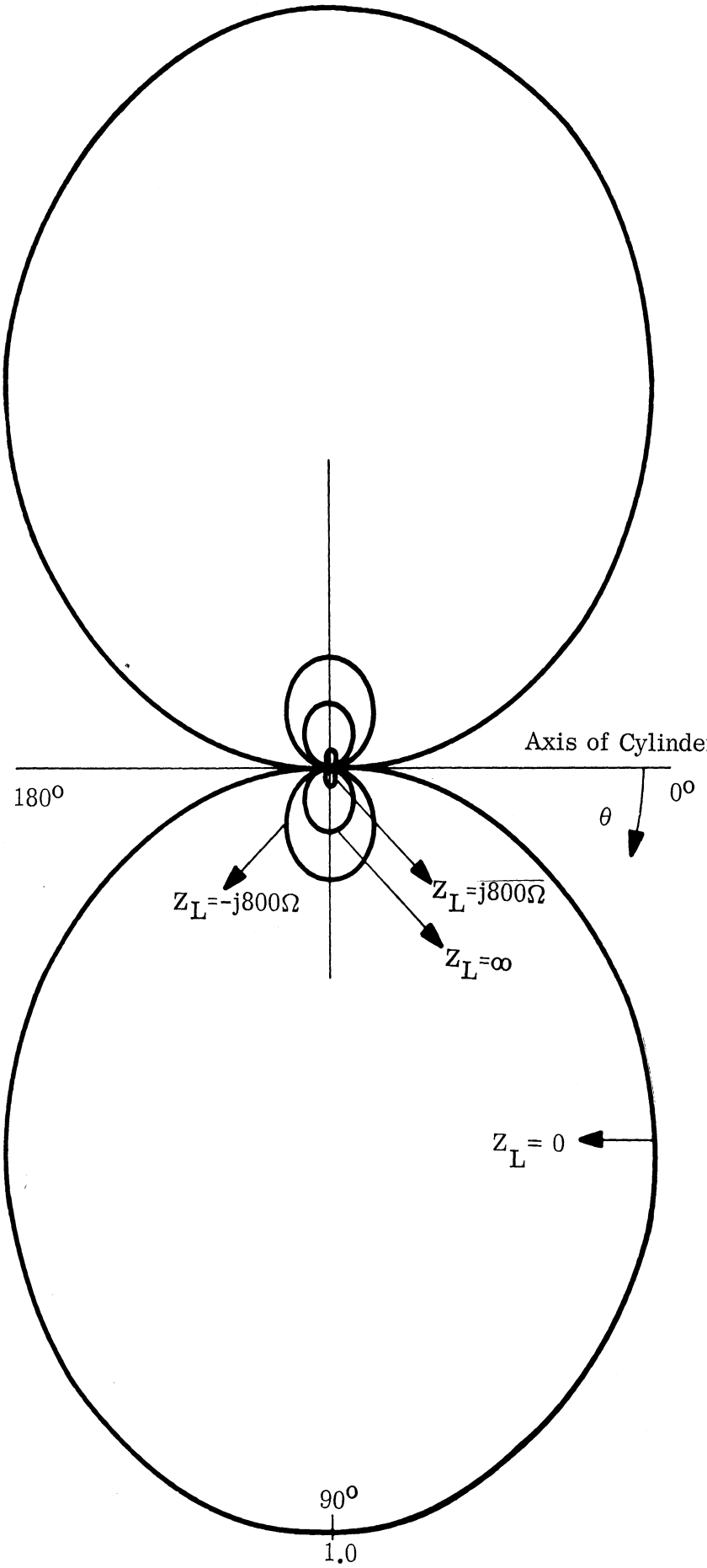

FIG. 1-22: BISTATIC FIELD PATTERNS OF LOADED CYLINDER FOR VARIOUS LOAD IMPEDANCE (THEORETICAL)

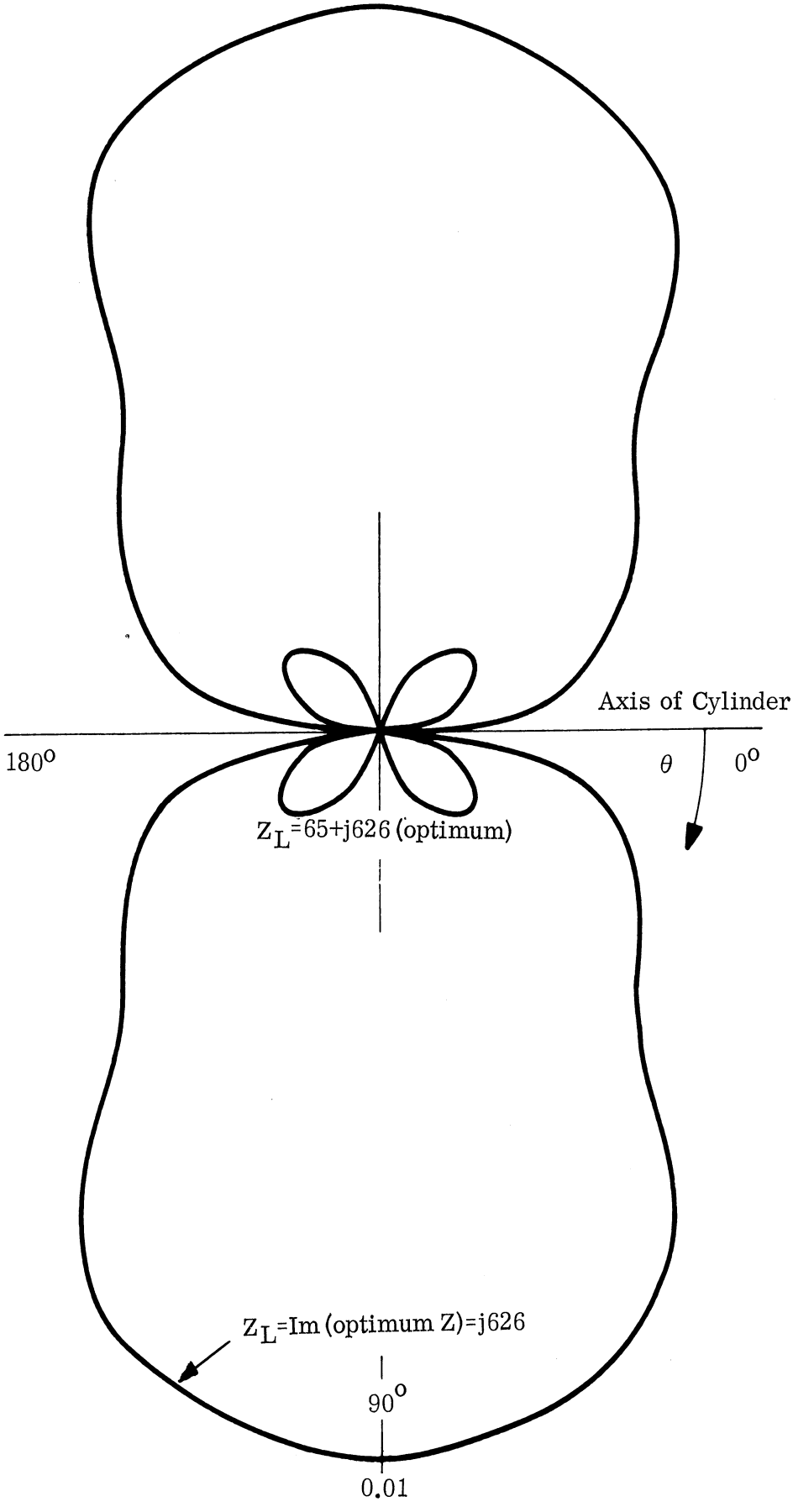

FIG. 1-23: BISTATIC FIELD PATTERNS FOR OPTIMUM LOADING OF CYLINDER
SCALE EXPANDED TO 100 TIMES THAT OF FIG 1-22. (THEORETICAL)

The effect of a central impedance on the induced current on a resonant cylinder is investigated in Section 1-1.4 It is found that there exists an optimum impedance which will reduce the magnitude of the induced current greatly and in addition, reverse the phase of the induced current over the central part of the cylinder. This optimum impedance will give zero broadside back scattering and very low return in other aspects.

The effect of a central impedance on the induced current on an antiresonant cylinder is investigated in section 1-1.5. It is found that the induced current is, in general, not reduced by a central impedance. Although we can make the broadside back scattering vanish the scattering in other aspects may be enhanced.

An experimental study on the induced current has been carried out in parallel with the development of the theory. The theory was carefully checked by experiment at every step and the agreement between theory and experiment is excellent.

The scattering nature of a center-loaded cylinder is studied in section I-3. The optimum impedance which makes the broadside back scattering vanish is obtained in (1.76). The expression for this optimum impedance is very simple and should prove useful in practical design situations. The optimum impedance as a function of the cylinder dimension is shown graphically in Figs. 1-19 and 1-20. The frequency characteristic of an optimum impedance for broadband effect is shown graphically in Fig. 1-21.

II
THE MINIMIZATION OF THE CROSS SECTION OF A CYLINDER BY CENTRAL LOADING (ARBITRARY ASPECT)

In Part I we considered the case of broadside illumination and established optimum loading which results in zero back scatter for the broadside direction. It is natural to ask whether that same optimum loading will minimize the back scattering for off-broadside illumination angles. This question is taken up in part II where we seek to find the induced current on a center-loaded cylinder illuminated by an obliquely incident plane wave. After the induced current is obtained, both the theoretical back scattered field in an arbitrary direction and the radar cross section of the cylinder can be obtained and compared with experimental observations. Good agreement between experiment and theory is obtained.

2-1 INDUCED CURRENT ON A CENTER-LOADED CYLINDER ILLUMINATED BY AN OBLIQUELY INCIDENT PLANE WAVE

When a conducting finite cylinder is illuminated by a plane EM wave at oblique incidence, the induced current does not have symmetry with respect to the center of the cylinder. Nonetheless the induced current along the cylinder can be divided into a symmetrical and an antisymmetrical component. Although a central load will greatly change the symmetrical component of the induced current, such a load has no effect on the antisymmetrical component. On a cylinder with a resonant length, the symmetrical component of the induced current dominates the antisymmetrical component; therefore, back scattering can be modified greatly by a single load. On the other hand, on a cylinder with an antiresonant length, the antisymmetrical component of the induced current dominates its symmetrical component; hence a single center load can only modify the back scattering very slightly.

The same integral equation method of Part I will be used. It is perhaps worthwhile to note that King (1956) solved a similar problem of a center-loaded receiving antenna but he ignored the antisymmetrical component of the antenna

current. His results are also rather complicated for our purpose. We use a somewhat different method in order to obtain a reasonably simple solution with an accuracy which is satisfactory for our purpose.

2-1.1 Integral Equation for the Induced Current on the Cylinder

The geometry of the problem is as shown in Fig. 2-1. A cylinder with a radius a and length 2h is assumed to be perfectly conducting. A plane EM wave is incident to the cylinder at an angle θ. A lumped impedance Z_L is connected at the center of the cylinder. The dimensions of interest are

$$\frac{1}{4}\lambda < 2h < 2\lambda$$

$$\beta_o^2 a^2 \ll 1.$$

where λ is the wavelength and β_o is the wave number. The second condition implies that the cylinder is thin and only the axial current is induced.

The tangential component of the incident EM wave along the cylinder is assumed to be

$$E_z^{in} = E_o \cos\theta \, e^{-j\beta_o \sin\theta z} \tag{2.1}$$

where E_o is a constant and the time-dependent factor $e^{j\omega t}$ is omitted.

The current and the charge on the cylinder maintain a tangential electric field at the surface which can be expressed as

$$E_z^a = -\frac{\partial \phi}{\partial z} - j\omega A_z \tag{2.2}$$

where ϕ is the scalar potential maintained by the charge and A_z is the tangential component of the vector potential maintained by the current. By using the Lorentz condition,

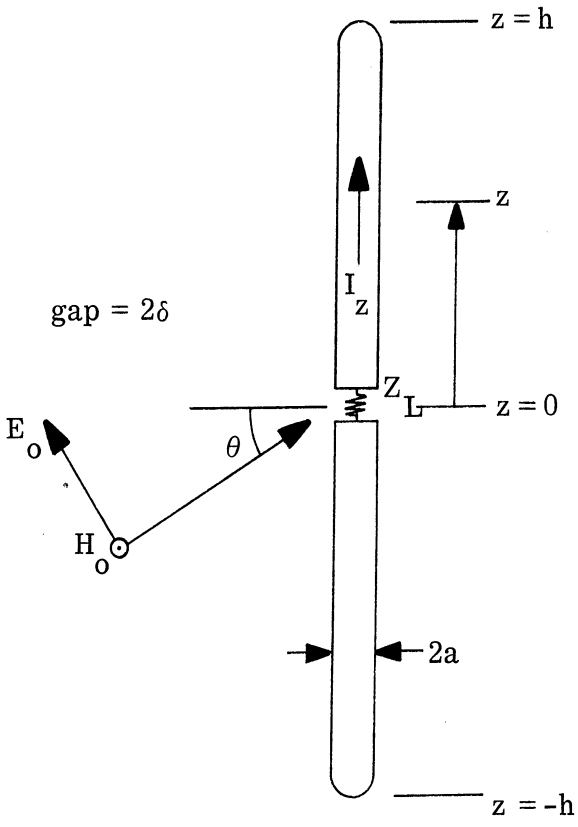

FIG. 2-1: A CENTRALLY LOADED CYLINDER ILLUMINATED OBLIQUELY BY AN EM WAVE

$$\phi = j \frac{\omega}{\beta_o^2} \nabla \cdot \vec{A} \tag{2.3}$$

(2.2) can be expressed as

$$E_z^a = -j \frac{\omega}{\beta_o^2} \left(\frac{\partial^2}{\partial z^2} + \beta_o^2 \right) A_z \ . \tag{2.4}$$

The electric field maintained across the gap at the center of the cylinder can be expressed as

$$E_z^g = Z_L I_o \delta(z) \tag{2.5}$$

where Z_L is the center load, I_o is the induced current at the center of the cylinder and $\delta(z)$ is a delta function.

Since the tangential electric field should be continuous at the boundary we obtain the following equation

$$E_z^a + E_z^{in} = Z_L I_o \delta(z) \tag{2.6}$$

$$\text{for } -h \leqslant z \leqslant h \ .$$

Equation (2.6) implies that the total tangential electric field vanishes on the surface of the cylinder and maintains a voltage drop of $Z_L I_o$ across the gap at the center of the cylinder.

The substitution of (2.1) and (2.4) in (2.6) gives

$$\frac{\partial^2}{\partial z^2} A_z + \beta_o^2 A_z = -j \frac{\beta_o^2}{\omega} \left[E_o \cos\theta \, e^{-j\beta_o \sin\theta z} - Z_L I_o \delta(z) \right] \tag{2.7}$$

$$\text{for } -h \leqslant z \leqslant h.$$

The general solution for A_z is the sum of the complementary function and a particular integral

$$A_z = \frac{-j}{v_o}\left[C_1 \cos\beta_o z + C_2 \sin\beta_o z + \Theta(z)\right] \tag{2.8}$$

where v_o is $1/\sqrt{\mu_o \epsilon_o}$, C_1 and C_2 are arbitrary constants, and where the particular integral $\Theta(z)$ can be obtained as

$$\Theta(z) = \frac{E_o}{\beta_o \cos\theta}\, e^{-j\beta_o \sin\theta z} - \frac{1}{2} Z_L I_o \sin\beta_o |z| \quad . \tag{2.9}$$

In (2.8) A_z can be divided into a symmetrical and an antisymmetrical component

$$A_z(z) = A_z^s(z) + A_z^a(z) \tag{2.10}$$

thus

$$A_z^s(z) = \frac{-j}{v_o}\left[C_1 \cos\beta_o z + \frac{E_o}{\beta_o \cos\theta} \cos(\beta_o z \sin\theta) - \frac{1}{2} Z_L I_o \sin\beta_o |z|\right] \tag{2.11}$$

$$A_z^a(z) = \frac{-j}{v_o}\left[C_2 \sin\beta_o z - j \frac{E_o}{\beta_o \cos\theta} \sin(\beta_o z \sin\theta)\right] \quad . \tag{2.12}$$

We also divide the induced current on the cylinder into a symmetrical and an antisymmetrical component:

$$I_z(z) = I_z^s(z) + I_z^a(z)$$

and, by the assumed symmetries,

$$I_z^s(z) = I_z^s(-z), \qquad I_z^a(z) = -I_z^a(-z) \quad . \tag{2.13}$$

From the definition of the vector potential, we can write A_z in terms of I_z as follows:

$$A_z^s(z) = \frac{\mu_o}{4\pi} \int_{-h}^{h} I_z^s(z') K_z(z, z')\, dz'$$

$$= \frac{-j}{v_o} \left[C_1 \cos\beta_o z + \frac{E_o}{\beta_o \cos\theta} \cos(\beta_o z \sin\theta) - \frac{1}{2} Z_L I_o \sin\beta_o |z| \right] \qquad (2.14)$$

$$A_z^a(z) = \frac{\mu_o}{4\pi} \int_{-h}^{h} I_z^a(z') K_a(z, z')\, dz'$$

$$= \frac{-j}{v_o} \left[C_2 \sin\beta_o z - j \frac{E_o}{\beta_o \cos\theta} \sin(\beta_o z \sin\theta) \right] \qquad (2.15)$$

where

$$K_a(z, z') = \frac{e^{-j\beta_o \sqrt{(z-z')^2 + a^2}}}{\sqrt{(z-z')^2 + a^2}} \qquad (2.16)$$

Equations (2.14) and (2.15) are integral equations for the induced currents, $I_z^s(z)$ and $I_z^a(z)$. We will determine $I_z^s(z)$ and $I_z^a(z)$ in sections 2-1.2 and 2-1.3 respectively.

2-1.2 Symmetrical Component of the Induced Current

Instead of solving (2.14) directly for $I_z^s(z)$, for convenience we will start from (2.11), from which C_1 can be expressed as

$$C_1 = \sec\beta_o h \left[j v_o A_z^s(h) - \frac{E_o}{\beta_o \cos\theta} \cos(\beta_o h \sin\theta) + \frac{1}{2} Z_L I_o \sin\beta_o h \right]. \qquad (2.17)$$

With (2.11) and (2.17), we obtain

$$A_z(z) - A_z(h)$$

$$= \frac{-j}{v_o} \sec\beta_o h \left\{ \left[jv_o A_z^s(h) - \frac{E_o}{\beta_o \cos\theta} \cos(\beta_o h \sin\theta) \right] (\cos\beta_o z - \cos\beta_o h) \right.$$

$$\left. + \frac{1}{2} Z_L I_o \sin\beta_o (h - |z|) + \frac{E_o \cos\beta_o h}{\beta_o \cos\theta} \left[\cos(\beta_o z \sin\theta) - \cos(\beta_o h \sin\theta) \right] \right\} \quad (2.18)$$

With the help of (2.14), another integral equation for $I_z^s(z)$ is obtained as follows:

$$\int_{-h}^{h} I_z^s(z') K_d(z, z')\, dz'$$

$$= \frac{-j4\pi}{\zeta_o} \sec\beta_o h \left\{ \left[jv_o A_z^s(h) - \frac{E_o}{\beta_o \cos\theta} \cos(\beta_o h \sin\theta) \right] (\cos\beta_o z - \cos\beta_o h) \right.$$

$$\left. + \frac{1}{2} Z_L I_o \sin\beta_o (h - |z|) + \frac{E_o \cos\beta_o h}{\beta_o \cos\theta} \left[\cos(\beta_o z \sin\theta) - (\beta_o h \sin\theta) \right] \right\} \quad (2.19)$$

where

$$K_d(z, z') = K_a(z, z') - K_z(h, z') \quad (2.20)$$

and ζ_o is 120π. Equation (2.19) is valid for $-h \leqslant z \leqslant h$ but $A_z^s(h)$ and I_o in the right hand side of (2.19) are still unknown.

However, the right hand side of (2.19) suggests a form for the solution of $I_z^s(z)$ as

$$I_z^s(z) = C_c(\cos\beta_o z - \cos\beta_o h) + C_s \sin\beta_o (h - |z|) + C_\theta \left[\cos(\beta_o z \sin\theta) - \cos(\beta_o h \sin\theta) \right] \quad (2.21)$$

It is then reasonable to divide (2.19) into three parts as follows:

$$C_c \int_{-h}^{h} (\cos\beta_o z' - \cos\beta_o h) K_d(z, z')\, dz'$$

$$= \frac{-j4\pi}{\zeta_o} \sec\beta_o h \left[jv_o A_z^s(h) - \frac{E_o}{\beta_o \cos\theta} (\beta_o h \sin\theta) \right] (\cos\beta_o z - \cos\beta_o h), \qquad (2.22)$$

$$C_s \int_{-h}^{h} \sin\beta_o(h - |z'|) K_d(z, z')\, dz' = \frac{-j2\pi}{\zeta_o} \sec\beta_o h Z_L I_o \sin\beta_o(h - |z|), \qquad (2.23)$$

and

$$C_\theta \int_{-h}^{h} \left[\cos(\beta_o z' \sin\theta) - \cos(\beta_o h \sin\theta) \right] K_d(z, z')\, dz'$$

$$= \frac{-j4\pi}{\zeta_o} \frac{E_o}{\beta_o \cos\theta} \left[\cos(\beta_o z \sin\theta) - \cos(\beta_o h \sin\theta) \right]. \qquad (2.24)$$

Equations (2.22) through (2.24) are well matched at the end points, $z = \pm h$. Furthermore, the constants C_c, C_s and C_θ can be determined by matching these equations at the center of the cylinder, $z = 0$. This matching yields

$$C_c = \frac{-j4\pi}{\zeta_o T_{cd}} \sec\beta_o h \left[jv_o A_z^s(h) - \frac{E_o}{\beta_o \cos\theta} \cos(\beta_o h \sin\theta) \right] (1 - \cos\beta_o h) \qquad (2.25)$$

where

$$T_{cd} = \int_{-h}^{h} (\cos\beta_o z' - \cos\beta_o h) K_d(0, z')\, dz' \qquad (2.26)$$

and

$$C_s = \frac{-j2\pi}{\zeta_o T_{sd}} \sec\beta_o h Z_L I_o \sin\beta_o h \qquad (2.27)$$

where

$$T_{sd} = \int_{-h}^{h} \sin\beta_o(h - |z'|)\, K_d(0, z')\, dz' \tag{2.28}$$

and

$$C_\theta = \frac{-j4\pi}{\zeta_o T_{\theta d}} \frac{E_o}{\beta_o \cos\theta} \left[1 - \cos(\beta_o h \sin\theta)\right] \tag{2.29}$$

where

$$T_{\theta d} = \int_{-h}^{h} \left[\cos(\beta_o z' \sin\theta) - \cos(\beta_o h \sin\theta)\right] K_d(0, z')\, dz' . \tag{2.30}$$

The substitution of (2.25), (2.27) and (2.29) in (2.21) gives

$$I_z^s(z) = \frac{-j4\pi}{\zeta_o} \left\{ \frac{1}{T_{cd}} \left[jv_o A_z^s(h) - \frac{E_o}{\beta_o \cos\theta} \cos(\beta_o h \sin\theta) \right] (\sec\beta_o h - 1)(\cos\beta_o z - \cos\beta_o h) \right.$$

$$+ \frac{1}{2T_{sd}} Z_L I_o \tan\beta_o h \sin\beta_o(h - |z|)$$

$$\left. + \frac{1}{T_{\theta d}} \frac{E_o}{\beta_o \cos\theta} \left[1 - \cos(\beta_o h \sin\theta)\right] \left[\cos(\beta_o z \sin\theta) - \cos(\beta_o h \sin\theta)\right] \right\} . \tag{2.31}$$

In (2.31), $A_z^s(h)$ and I_o are still unknown, but I_o can be determined from (2.31).

By definition,

$$I_o \equiv I_z(0) = I_z^s(0) + I_z^a(0), \quad \text{but} \quad I_z^a(0) = 0$$

hence

$$I_o = I_z^s(0) \quad . \tag{2.32}$$

I_o can then be expressed in terms of $A_z^s(h)$ by letting $z = 0$ in (2.31), and after some algebraic manipulation (2.31) itself can be rearranged to give

$$I_z^s(z) = \frac{-j4\pi}{\zeta_o}\left\{\left[jv_o A_z^s(h) - \frac{E_o}{\beta_o \cos\theta}\cos(\beta_o h\sin\theta)\right]\left[M_1'(\cos\beta_o z - \cos\beta_o h) + N_1' \sin\beta_o(h - |z|)\right] + \frac{E_o}{\beta_o\cos\theta}\left[M_2\left[\cos(\beta_o z\sin\theta) - \cos(\beta_o h\sin\theta)\right] + N_2\sin\beta_o(h-|z|)\right]\right\} \quad (2.33)$$

where

$$M_1' = \frac{1}{T_{cd}}(\sec\beta_o h - 1) \quad (2.34)$$

$$N_1' = \frac{-Z_L\tan\beta_o h(\sec\beta_o h + \cos\beta_o h - 2)}{T_{cd}Z_L\tan\beta_o h\sin\beta_o h - j60\,T_{cd}T_{sd}} \quad (2.35)$$

$$M_2 = \frac{1}{T_{\theta d}}\left[1 - \cos(\beta_o h\sin\theta)\right] \quad (2.36)$$

$$N_2 = \frac{-Z_L\sin\beta_o h\left[1-\cos(\beta_o h\sin\theta)\right]^2}{T_{\theta d}Z_L\sin^2\beta_o h - j60\,T_{\theta d}T_{sd}\cos\beta_o h} \quad (2.37)$$

In (2.33) the remaining unknown is $A_z^s(h)$. To determine it we use the definition of the vector potential

$$A_z^s(h) = \frac{\mu_o}{4\pi}\int_{-h}^{h} I_z^s(z')\,K_a(h,z')\,dz' \quad (2.38)$$

After substituting (2.33) in (2.38), $A_z^s(h)$ becomes

$$A_z^s(h) = \frac{jE_o}{v_o \beta \cos\theta} \frac{\left[\cos(\beta_o h \sin\theta)(M_1' T_{ca} + N_1' T_{sa}) - (M_2 T_{\theta a} + N_2 T_{sa})\right]}{1 - M_1' T_{ca} - N_1' T_{sa}} \tag{2.39}$$

where

$$T_{ca} = \int_{-h}^{h} (\cos\beta_o z' - \cos\beta_o h) K_a(h, z')\, dz' \tag{2.40}$$

$$T_{sa} = \int_{-h}^{h} \sin\beta_o (h - |z'|) K_z(h, z')\, dz' \tag{2.41}$$

$$T_{\theta a} = \int_{-h}^{h} \left[\cos(\beta_o z' \sin\theta) - \cos(\beta_o h \sin\theta)\right] K_z(h, z')\, dz' . \tag{2.42}$$

If (2.39) is substituted in (2.33) and the result rearranged, the final form of the solution for $I_z^s(z)$ becomes

$$I_z^s(z) = \frac{jE_o}{30\beta_o \cos\theta} \left\{ \left[\frac{\cos(\beta_o h \sin\theta) - M_2 T_{\theta a} - N_2 T_{sa}}{\cos\beta_o h - M_1 T_{ca} - N_1 T_{sa}} \right] M_1 (\cos\beta_o z - \cos\beta_o h) \right.$$

$$+ \left[\frac{N_1 \cos(\beta_o h \sin\theta) - N_1 M_2 T_{\theta a} + M_1 N_2 T_{ca} - N_2 \cos\beta_o h}{\cos\beta_o h - M_1 T_{ca} - N_1 T_{sa}} \right] \sin\beta_o (h - |z|)$$

$$\left. - M_2 \left[\cos(\beta_o z \sin\theta) - \cos(\beta_o h \sin\theta)\right] \right\} \tag{2.43}$$

where

$$M_1 = \frac{1}{T_{cd}} (1 - \cos\beta_o h) \tag{2.44}$$

$$N_1 = \frac{-Z_L \sin\beta_o h (1 - \cos\beta_o h)^2}{T_{cd} Z_L \sin^2 \beta_o h - j60\, T_{cd} T_{sd} \cos\beta_o h} \tag{2.45}$$

and M_2 and N_2 are expressed in (2.36) and (2.37).

Equation (2.43) expresses $I_z^s(z)$ as a function of the cylinder size, the center load Z_L and the incidence angle θ of an EM wave.

As a matter of completeness and convenience, the integrals T_{cd}, T_{sd}, $T_{\theta d}$, T_{ca}, T_{sa} and $T_{\theta a}$ are expressed in terms of better known integrals:

$$T_{cd} = C_a(h, 0) - C_a(h, h) - \cos\beta_o h \left[E_a(h, 0) - E_a(h, h)\right] \tag{2.46}$$

$$T_{sd} = \sin\beta_o h \left[C_a(h, 0) - C_a(h, h)\right] - \cos\beta_o h \left[S_a(h, 0) - S_a(h, h)\right] \tag{2.47}$$

$$T_{\theta d} = C_a^{\theta}(h, 0) - C_a^{\theta}(h, h) - \cos(\beta_o h \sin\theta) \left[E_a(h, 0) - E_a(h, h)\right] \tag{2.48}$$

$$T_{ca} = C_a(h, h) - \cos\beta_o h E_a(h, h) \tag{2.49}$$

$$T_{sa} = \sin\beta_o h C_a(h, h) - \cos\beta_o h S_a(h, h) \tag{2.50}$$

$$T_{\theta a} = C_a^{\theta}(h, h) - \cos(\beta_o h \sin\theta) E_a(h, h) \tag{2.51}$$

where

$$C_a(h, 0) = \int_{-h}^{h} \cos\beta_o z' K_a(0, z')\, dz' \tag{2.52}$$

$$C_a(h, h) = \int_{-h}^{h} \cos\beta_o z' K_a(h, z')\, dz' \tag{2.53}$$

$$E_a(h, 0) = \int_{-h}^{h} K_a(0, z')\, dz' \tag{2.54}$$

$$E_a(h, h) = \int_{-h}^{h} K_a(h, z')\, dz' \tag{2.55}$$

$$S_a(h, 0) = \int_{-h}^{h} \sin\beta_o |z'|\, K_a(0, z')\, dz' \tag{2.56}$$

$$S_a(h, h) = \int_{-h}^{h} \sin\beta_o |z'|\, K_a(h, z')\, dz' \tag{2.57}$$

$$C_a^{\theta}(h, 0) = \int_{-h}^{h} \cos(\beta_o z' \sin\theta)\, K_a(0, z')\, dz' \tag{2.58}$$

$$C_a^{\theta}(h, h) = \int_{-h}^{h} \cos(\beta_o z' \sin\theta)\, K_a(h, z')\, dz' : \tag{2.59}$$

The integrals of (2.52) through (2.59) can be calculated on a digital computer.

2-1.3 Antisymmetrical Component of the Induced Current

We can determine C_2 from (2.12) as

$$C_2 = \csc\beta_o h \left[j v_o A_z^a(h) + j \frac{E_o}{\beta_o \cos\theta} \sin(\beta_o h \sin\theta) \right] \tag{2.60}$$

Substituting (2.60) in (2.15), we obtain

$$\int_{-h}^{h} I_z^a(z')K_a(z,z')\,dz'$$

$$= \frac{4\pi}{\zeta_o}\csc\beta_o h\left\{\frac{E_o}{\beta_o\cos\theta}\left[\sin(\beta_o h\sin\theta)\sin\beta_o z - \sin\beta_o h\sin(\beta_o z\sin\theta)\right] + v_o A_z^a(h)\sin\beta_o z\right\} \qquad (2.61)$$

If the solution for $I_z^a(z)$ is assumed to be

$$I_z^a(z) = C_a\left[\sin(\beta_o h\sin\theta)\sin\beta_o z - \sin\beta_o h\sin(\beta_o z\sin\theta)\right] \qquad (2.62)$$

equation (2.61) is matched at $z = 0$. We will match (2.61) at two more points.

If we set $z = h/2$ in (2.61) and use the substitution of (2.62), the constant C_a can be expressed as

$$C_a = \frac{1}{T_a(h/2)}\left\{\frac{2\pi E_o}{\zeta_o\beta_o\cos\theta}\left[\sin(\beta_o h\sin\theta)\sec\frac{\beta_o h}{2} - 2\sin\left(\frac{\beta_o h}{2}\sin\theta\right)\right] + \frac{2\pi}{\mu_o}\sec\frac{\beta_o h}{2}A_z^a(h)\right\} \qquad (2.63)$$

where

$$T_a(h/2) = \int_{-h}^{h}\left[\sin(\beta_o h\sin\theta)\sin\beta_o z' - \sin\beta_o h\sin(\beta_o z'\sin\theta)\right]K_a(h/2,z')\,dz'. \qquad (2.64)$$

By definition, $A_z^a(h)$ is

$$A_z^a(h) = \frac{\mu_o}{4\pi} \int_{-h}^{h} I_z^a(z') K_a(h, z')\, dz'$$

$$= \frac{\mu_o}{4\pi} C_a T_a(h) \tag{2.65}$$

where

$$T_a(h) = \int_{-h}^{h} \left[\sin(\beta_o h \sin\theta) \sin\beta_o z' - \sin\beta_o h \sin(\beta_o z' \sin\theta)\right] K_a(h, z')\, dz'. \tag{2.66}$$

From (2.63) and (2.65), $A_z^a(h)$ is determined as

$$A_z^a(h) = \frac{E_o T_a(h) \left[\sin(\beta_o h \sin\theta) \sec\frac{\beta_o h}{2} - 2\sin\left(\frac{\beta_o h}{2}\sin\theta\right)\right]}{\omega\cos\theta \left[2T_a(h/2) - \sec\frac{\beta_o h}{2} T_a(h)\right]} . \tag{2.67}$$

After substituting (2.63) and (2.67) into (2.62) we obtain the final form of the solution for $I_z^a(z)$

$$I_z^a(z) = \frac{E_o}{30\beta_o \cos\theta} \left[\frac{\frac{1}{2}\sin(\beta_o h \sin\theta)\sec\frac{\beta_o h}{2} - \sin\left(\frac{\beta_o h}{2}\sin\theta\right)}{T_a(h/2) - \frac{1}{2}\sec\beta_o h\, T_a(h)}\right] \cdot$$

$$\cdot \left[\sin(\beta_o h \sin\theta)\sin\beta_o z - \sin\beta_o h \sin(\beta_o z \sin\theta)\right] , \tag{2.68}$$

Equation (2.68) gives the complete solution for the antisymmetrical component of the induced current on a cylinder. It is noted that $I_z^a(z)$ is a function of the cylinder size and the incidence angle θ only, and is entirely independent of the center load Z_L.

For convenience the integrals $T_a(h/2)$ and $T_a(h)$ are expressed alternatively as follows:

$$T_a(h/2) = \sin(\beta_o h \sin\theta)\, S_z^{90}(h, h/2) - \sin\beta_o h\, S_a^{\theta}(h, h/2) \tag{2.69}$$

$$T_a(h) = \sin(\beta_o h \sin\theta)\, S_a^{90}(h, h) - \sin\beta_o h\, S_a^{\theta}(h, h) \tag{2.70}$$

where

$$S_a^{\theta}(h, h/2) = \int_{-h}^{h} \sin(\beta_o z' \sin\theta) K_a(h/2, z')\, dz' \tag{2.71}$$

$$S_a^{\theta}(h, h) = \int_{-h}^{h} \sin(\beta_o z' \sin\theta) K_a(h, z')\, dz' \tag{2.72}$$

$$S_a^{90}(h, h/2) = \int_{-h}^{h} \sin\beta_o z' K_a(h/2, z')\, dz' \tag{2.73}$$

$$S_a^{90}(h, h) = \int_{-h}^{h} \sin\beta_o z' K_a(h, z')\, dz' \tag{2.74}$$

The integrals in (2.71) through (2.74) can be readily calculated on a computer.

2-1.4 Numerical Results

To demonstrate the solutions we have obtained in the preceeding sections, numerical calculations are made for two typical cases.

The first case is that of a resonant cylinder for which $h = 0.215\lambda$ and $a = 0.0173\lambda$ and with a central load $Z_L = /j\,800\,\Omega$, as found in Part I. This value of Z_L is close to the optimum value for minimizing the broadside back scattering. Using it, the symmetrical component of the induced current is reduced more than

20 db from the value when $Z_L = 0$. The distribution of the symmetrical component of the induced current, $I_z^s(z)$, is shown in Fig. 2-2 for different incident angles. It is observed that the general behavior of $I_z^s(z)$ is essentially independent of incident angle. This means that an optimum load for reducing the broadside back scattering is also effective in reducing the off-broadside back scattering. As shown in Fig. 2-3, the antisymmetrical component of the induced current, $I_z^a(z)$, on this cylinder is quite small. As already noted, $I_z^a(z)$ is entirely independent of Z_L but is strongly dependent on the cylinder dimension and on the incidence angle. For a cylinder with a resonant length, $I_z^a(z)$ is usually very small compared to $I_z^s(z)$. Hence the fact that the magnitudes of $I_z^s(z)$ and $I_z^a(z)$ are comparable in Figs. 2-2 and 2-3 is a consequence of the large reduction in the symmetrical component produced by the nearly optimum load $Z_L = j\,600\,\Omega$.

The second case is that of an antiresonant cylinder whose dimensions are $h = 0.425\lambda$ and $a = 0.0173\lambda$ and with a central load $Z_L = j\,600\,\Omega$. This Z_L is reather arbitrarily selected for actual numerical calculation. The distribution of the symmetrical component of the induced current, $I_z^s(z)$, for different incidence angles is shown graphically in Fig. 2.4. We observe that the magnitude of $I_z^s(z)$ is only slightly affected by the incidence angle. This also assures that the optimum loading for reducing the broadside back scattering will remain effective in reducing the off-broadside back scattering. The antisymmetrical component of the induced current, $I_z^a(z)$, is very large for this cylinder and its dependence upon the angle of incidence is shown graphically in Fig. 2-5. Comparing Figs. 2-4 and 2-5, we observe that the antisymmetrical component of the induced current dominates the symmetrical component. Since a central load can not change the antisymmetrical component of the induced current, central loading will not be an effective method for reducing the overall back scattering from a cylinder with an antiresonant length.

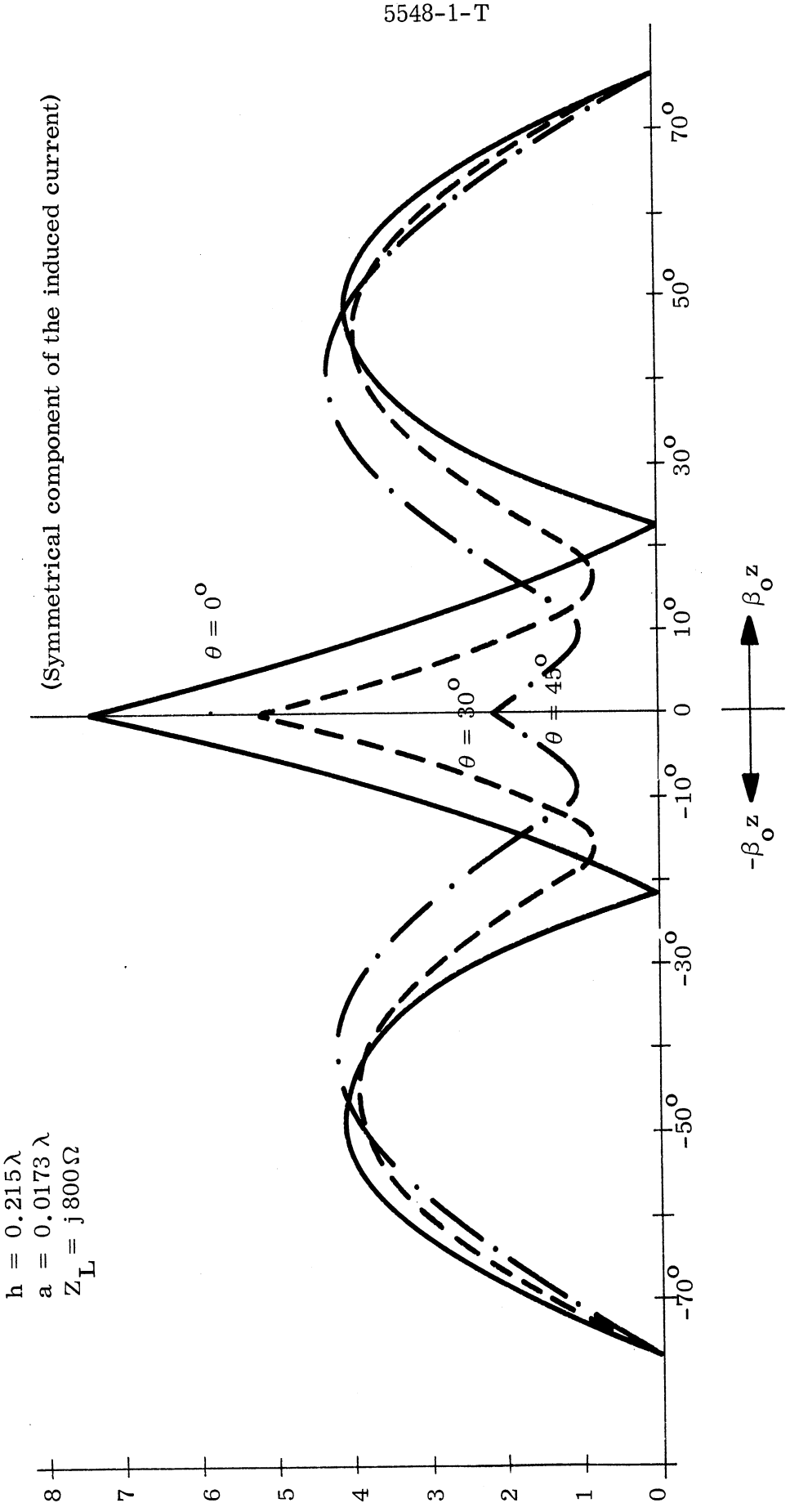

FIG. 2-2: DISTRIBUTION OF $|I_z^s(z)|$ ALONG A CYLINDER WITH A RESONANT LENGTH

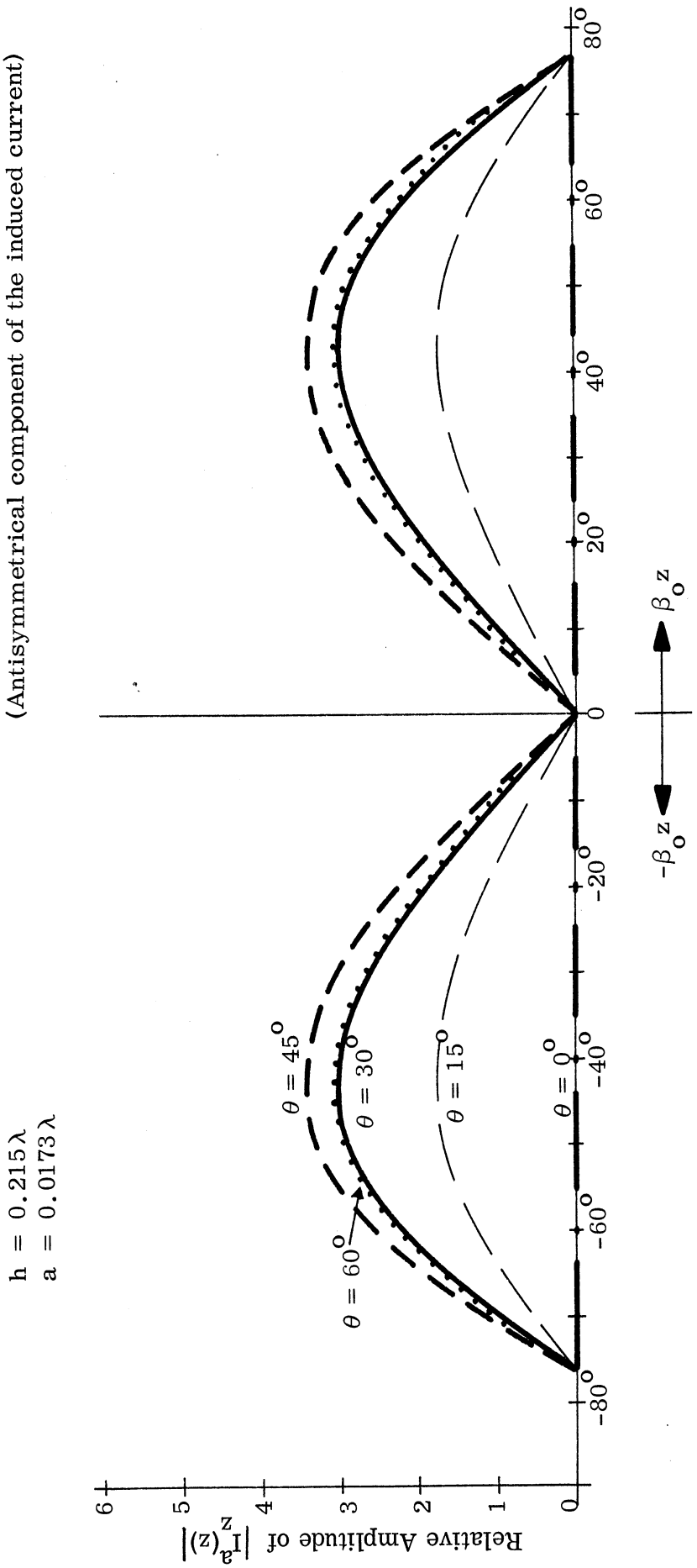

FIG. 2-3: DISTRIBUTION OF $|I_z^a(z)|$ ALONG A CYLINDER WITH A RESONANT LENGTH

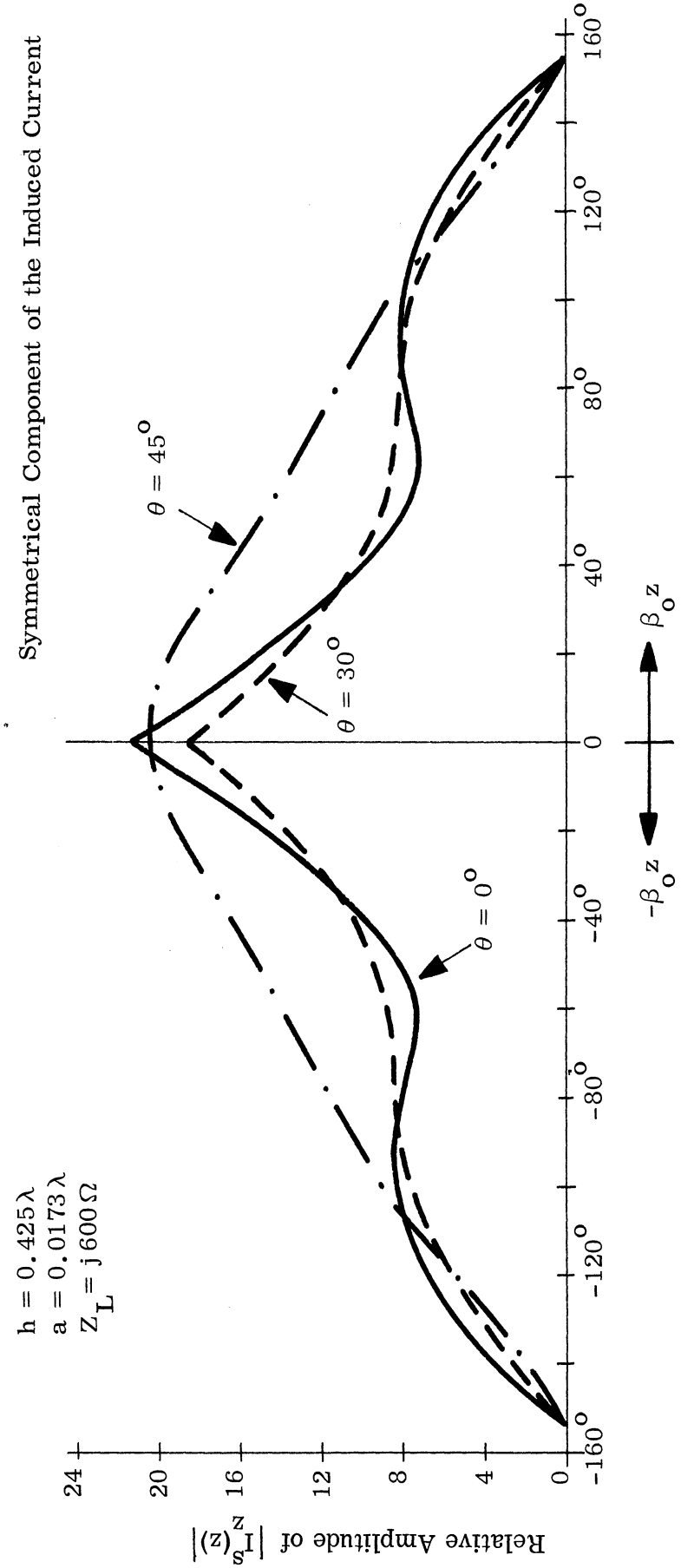

FIG. 2-4: DISTRIBUTION OF $|I_z^s(z)|$ ALONG A CYLINDER WITH AN ANTIRESONANT LENGTH

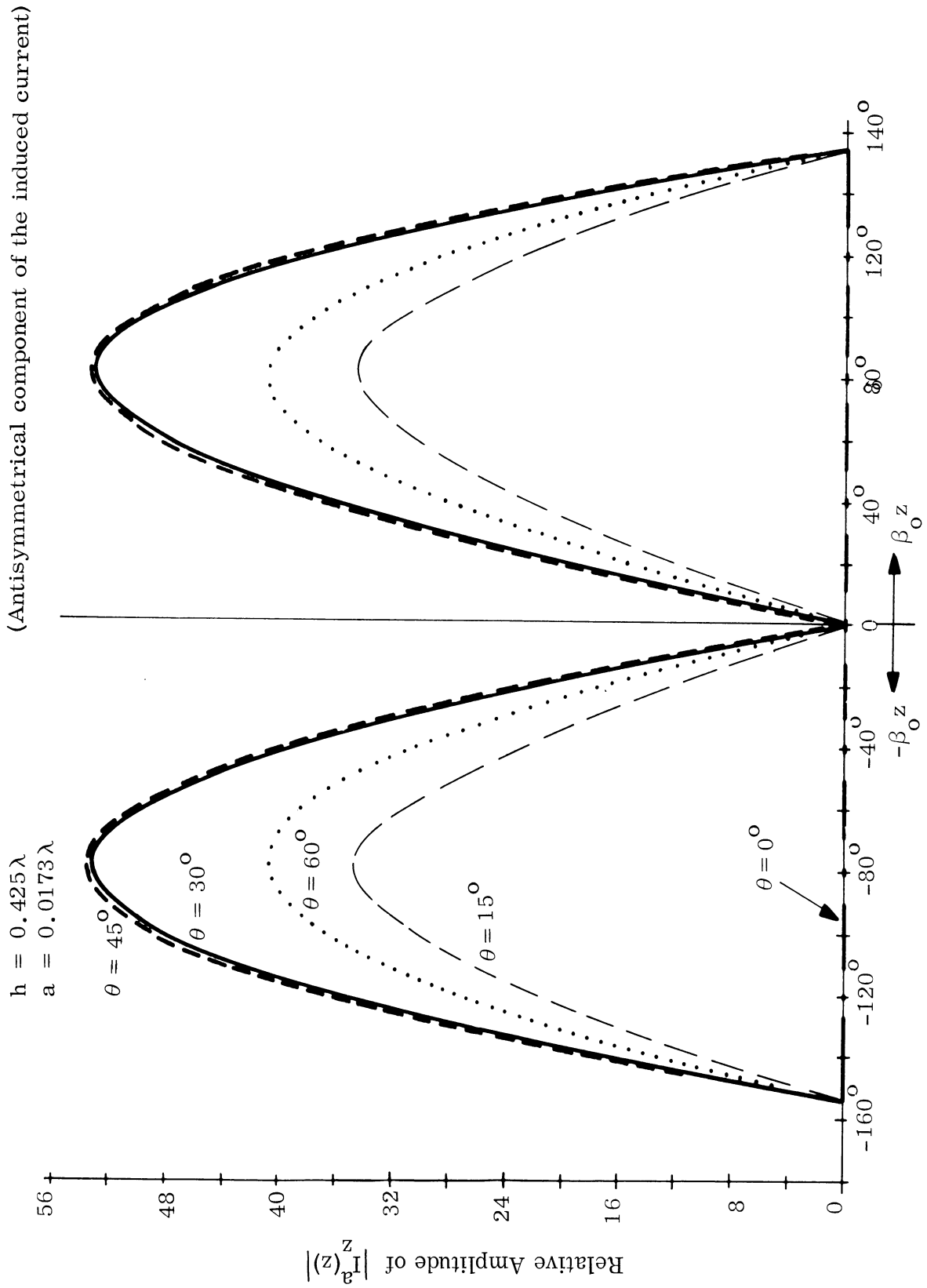

FIG. 2-5: DISTRIBUTION OF $|I_Z^a(z)|$ ALONG A CYLINDER WITH AN ANTIRESONANT LENGTH

It should be remembered that the total induced current is the vector sum of its symmetrical and antisymmetrical components so that a simple addition of $I_z^s(z)$ and $I_z^a(z)$ in Figs. 2-2 through 2-5 does not produce the total induced current, $I_z(z)$.

2-1.5 Comparison Between Theory and Experiment

In order to check the theory, the current distribution was measured on a cylinder with dimensions $h = 0.425\lambda$ and $a = 0.0173\lambda$. A coaxial cavity, built in at the center, was adjusted to simulate the central impedance of about $j\,600\,\Omega$. The actual cavity was filled with a dielectric ($\epsilon_r = 4$) and the length of this cavity was set equal to 5.07 cm. The induced current on the cylinder was measured by a small current loop and the cylinder was illuminated by an EM wave radiated from a horn antenna.

The corresponding theoretical current distribution was calculated on a digital computer and a desk calculator.

The theoretical and the experimental results are compared in Fig. 2-6, and the agreement is quite good. For this particular cylinder whose length is in the antiresonant region, a large antisymmetrical current is predicted by the theory when the incidence angle is other than zero degrees. This was confirmed by experiment, as was the prediction that the antisymmetrical component of the induced current should not be affected by the central load.

The main disagreement between theory and experiment is at the center of the cylinder. One explanation may be that an ideal delta function impedance is assumed in the theory but a finite gap exists on the experimental cylinder. Another may be the difficulty encountered in obtaining a specified impedance by a coaxial cavity.

However, the general behavior of the induced current predicted by theory is confirmed by experiment, and we will assume that our theory is adequate for our purpose.

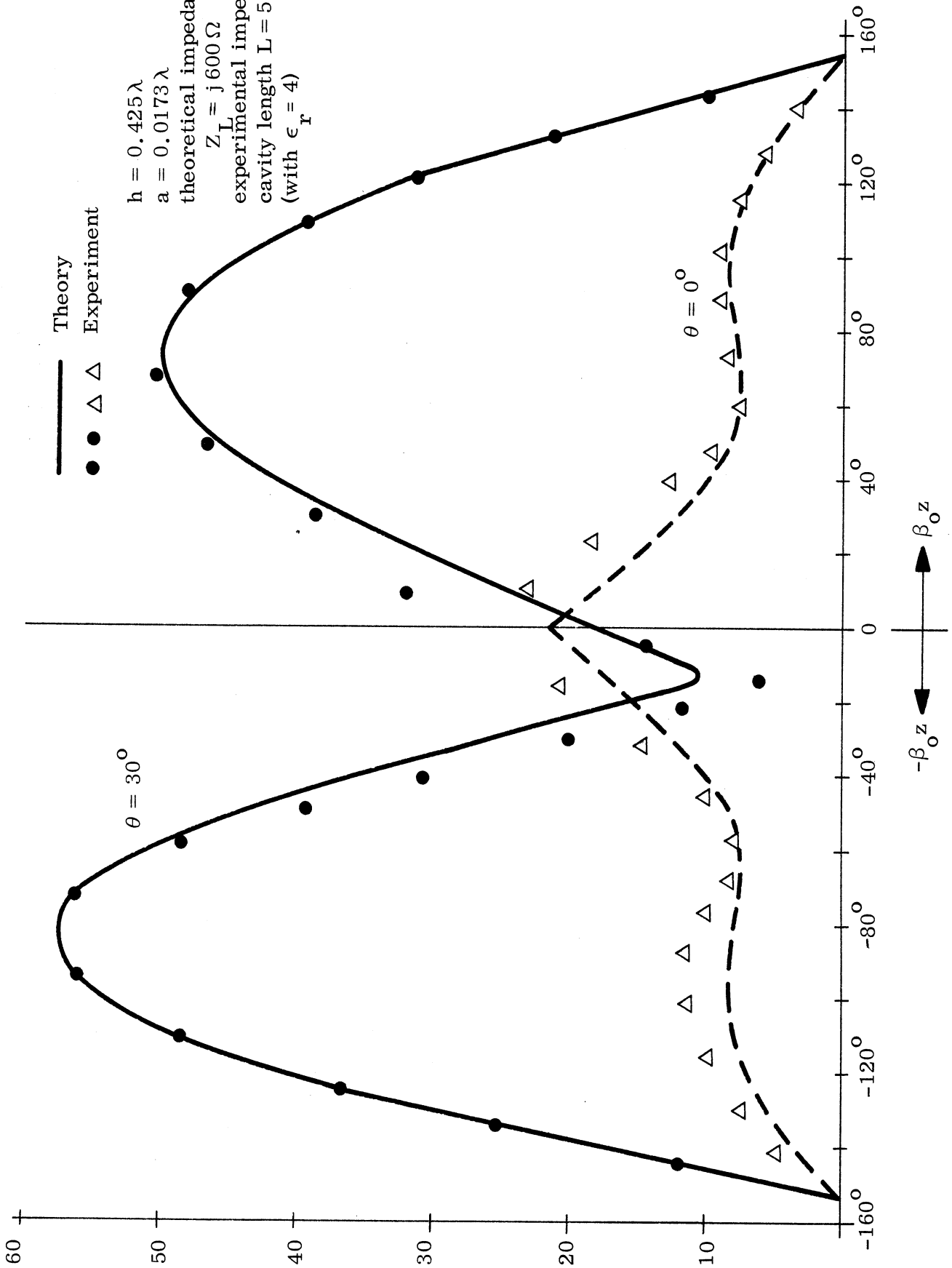

FIG. 2-6: THEORETICAL AND EXPERIMENTAL CURRENT DISTRIBUTION ALONG A CYLINDER

2-2 BACK SCATTERING OF A CENTER-LOADED CYLINDER ILLUMINATED BY A PLANE WAVE AT AN ARBITRARY ANGLE

The induced current on a center-loaded cylinder illuminated by a plane wave at an arbitrary angle was obtained in section 2-1. Using the solution obtained there we can calculate the back scattered field.

2-2.1 Back Scattered Field of a Center-Loaded Cylinder

With the same geometry as in Fig. 2-1 and the solution of the induced current as expressed in (2.43) and (2.68) we proceed as follows:

The symmetrical component of the induced current $I_z^s(z)$ maintains a vector potential at a point in the far zone of the cylinder in the direction of θ:

$$A_z^s = \frac{\mu_o}{4\pi} \frac{e^{-j\beta_o R_o}}{R_o} \int_{-h}^{h} I_z^s(z)\, e^{j\beta_o z \sin\theta}\, dz \qquad (2.75)$$

where $I_z^s(z)$ can be obtained from (2.43) and where R_o is the distance between the center of the cylinder and an observation point. It is important to note that in this part of the study θ is defined as shown in Fig. 2-1 and differs by 90^o from the θ defined in Part I.

Performing the indicated integration in (2.75), the final expression for A_z^s becomes

$$A_z^s(\theta) = \frac{j\mu_o E_o}{120\pi\beta_o^2} \frac{e^{-j\beta_o R_o}}{R_o} \left\{ \left[\frac{\cos(\beta_o h \sin\theta) - M_2 T_{\theta a} - N_2 T_{sa}}{\cos\beta_o h - M_1 T_{ca} - N_1 T_{sa}} \right] \frac{2M_1}{\cos^3\theta \sin\theta} \right.$$

$$\cdot \left[\sin\beta_o h \sin\theta \cos(\beta_o h \sin\theta) - \cos\beta_o h \sin(\beta_o h \sin\theta) \right]$$

$$\left. + \left[\frac{N_1 \cos(\beta_o h \sin\theta) - N_1 M_2 T_{\theta a} + M_1 N_2 T_{ca} - N_2 \cos\beta_o h}{\cos\beta_o h - M_1 T_{ca} - N_1 T_{sa}} \right] \frac{2\left[\cos(\beta_o h \sin\theta) - \cos\beta_o h\right]}{\cos^3\theta} \right\}$$

(cont'd)

$$- \frac{M_2}{2\sin\theta\cos\theta} \left[2\beta_o h\sin\theta - \sin(2\beta_o h\sin\theta)\right] \Bigg\} . \qquad (2.76)$$

Similarly, the antisymmetrical component of the induced current $I_z^a(z)$ maintains a vector potential at a point in the far zone of the cylinder in the direction of θ:

$$A_z^a = \frac{\mu_o}{4\pi} \frac{e^{-j\beta_o R_o}}{R_o} \int_{-h}^{h} I_z^a(z)\, e^{j\beta_o z\sin\theta}\, dz \qquad (2.77)$$

where I_z^a can be obtained from (2.68). After the integration in (2.77) is performed,

$$A_z^a(\theta) = \frac{j\mu_o E_o}{120\pi\beta_o^2} \frac{e^{-j\beta_o R_o}}{R_o} \left[\frac{\frac{1}{2}\sin(\beta_o h\sin\theta)\sec\frac{\beta_o h}{2} - \sin\left(\frac{\beta_o h}{2}\sin\theta\right)}{T_a(h/2) - \frac{1}{2}\sec\beta_o h\, T_a(h)} \right]$$

$$\frac{1}{2\cos^3\theta\sin\theta} \Big[\sin\beta_o h \left[(1+\sin^2\theta)\sin(2\beta_o h\sin\theta) - 2\beta_o h\sin\theta\cos^2\theta\right]$$

$$- 4\cos\beta_o h\sin\theta\sin^2(\beta_o h\sin\theta)\Big] \qquad (2.78)$$

To obtain an expression for the back scattered field, the following argument is employed:

The total vector potential maintained by the induced current on the cylinder is

$$A_z(\theta) = A_z^s(\theta) + A_z^a(\theta) \qquad (2.79)$$

The scattered electric field in the far zone of the cylinder due to the induced current is

$$E_\theta = -j\omega A_\theta = j\omega A_z \cos\theta \tag{2.80}$$

and the Poynting power density of the scattered field is

$$P = \frac{1}{2\zeta_o} \left| E_\theta \right|^2 \quad . \tag{2.81}$$

Hence, using the values of $A_z^s(\theta)$ from (2.76) and $A_z^a(\theta)$ from (2.78), the final expression for the back scattered field becomes

$$E_\theta(\theta) = -\frac{E_o}{\beta_o} \frac{e^{-j\beta_o R_o}}{R_o} \left\{ \left[\frac{\cos(\beta_o h \sin\theta) - M_2 T_{\theta a} - N_2 T_{sa}}{\cos\beta_o h - M_1 T_{ca} - N_1 T_{sa}} \right] \frac{2M_1}{\cos^2\theta \sin\theta} \cdot \right.$$

$$\cdot \left[\sin\beta_o h \sin\theta \cos(\beta_o h \sin\theta) - \cos\beta_o h \sin(\beta_o h \sin\theta) \right]$$

$$+ \left[\frac{N_1 \cos(\beta_o h \sin\theta) - N_1 M_2 T_{\theta a} + M_1 N_2 T_{ca} - N_2 \cos\beta_o h}{\cos\beta_o h - M_1 T_{ca} - N_1 T_{sa}} \right] \cdot$$

$$\cdot \frac{2\left[\cos(\beta_o h \sin\theta) - \cos\beta_o h\right]}{\cos^2\theta} - \frac{M_2}{2\sin\theta} \left[2\beta_o h \sin\theta - \sin(2\beta_o h \sin\theta) \right]$$

$$+ \left[\frac{\frac{1}{2}\sin(\beta_o h \sin\theta) \sec\frac{\beta_o h}{2} - \sin\left(\frac{\beta_o h}{2}\sin\theta\right)}{T_a(h/2) - \frac{1}{2}\sec\beta_o h\, T_a(h)} \right] \frac{1}{2\cos^2\theta \sin\theta} \cdot$$

$$\cdot \left[\sin\beta_o h \left[(1+\sin^2\theta)\sin(2\beta_o h \sin\theta) - 2\beta_o h \sin\theta \cos^2\theta \right] \right.$$

$$\left. \left. - 4\cos\beta_o h \sin\theta \sin^2(\beta_o h \sin\theta) \right] \right\} . \tag{2.82}$$

Equation (2.82) gives the complete expression for the back scattered electric field of a center-loaded cylinder when illuminated by a plane wave with an electric field E_o at an angle θ with respect to the normal to the cylinder. When typical values are calculated from (2.82) and compared with the experimental results, the agreement is excellent, as will be seen in section 2-2.3.

It is noted that the radar cross section is usually defined as

$$\sigma = \lim_{R_o \to \infty} 4\pi R_o^2 \left| \frac{E_\theta(\theta)}{E_o} \right|^2 . \qquad (2.83)$$

The experimental procedure will now be described.

2-2.2 Measurements of the Back Scattered Field of a Center-Loaded Cylinder

The radar cross section measurements were made at a range of 10 feet at a frequency of 1.088 Gc, the same as used for the current distribution measurements. The center-loaded cylinders were illuminated by a plane wave whose electric field vector was in the plane containing the cylinders. The back scattered fields from the cylinders were recorded as a function of aspect angle, where the zero degree aspect was chosen to represent the broadside direction.

Fig. 2-7 shows three scattering patterns for a resonant length cylinder with $h = 0.2134\lambda$ for three different coaxial cavities of $L = 0$ ($Z_L = 0$), $L = 6.22$ cm ($Z_L \simeq \infty$) and $L = 5.83$ cm ($Z_L \simeq j\,600\,\Omega$). We observe that the introduction of an impedance of $Z_L \simeq j\,600\,\Omega$ reduces the cross section of a resonant cylinder by more than 30 db. This impedance is only approximately optimum and it is believed that an optimum impedance, which is about $Z_L = 65 + j\,626\,\Omega$, would reduce the cross section even more. Actually, in the experiment a maximum reduction of 35 db was achieved by a purely reactive loading using a dielectric loaded coaxial cavity.

Figs. 2.8 through 2.11 show the scattering patterns for an anti-resonant length cylinder with $h = 0.4435\lambda$ for four different coaxial cavities: $L = 0$ ($Z_L = 0$)

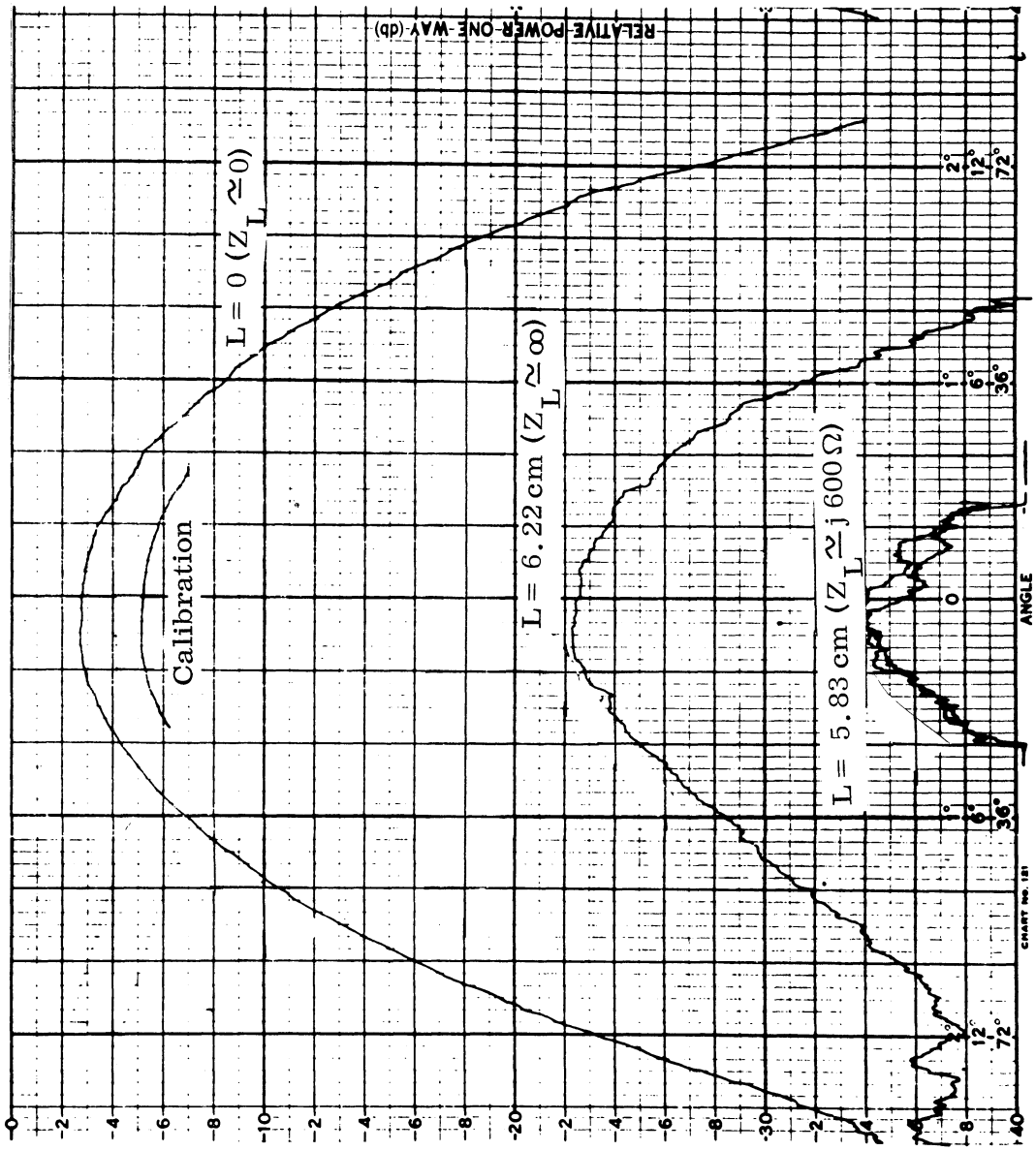

FIG. 2-7: SCATTERING PATTERN FOR h = 0.2134λ CYLINDER

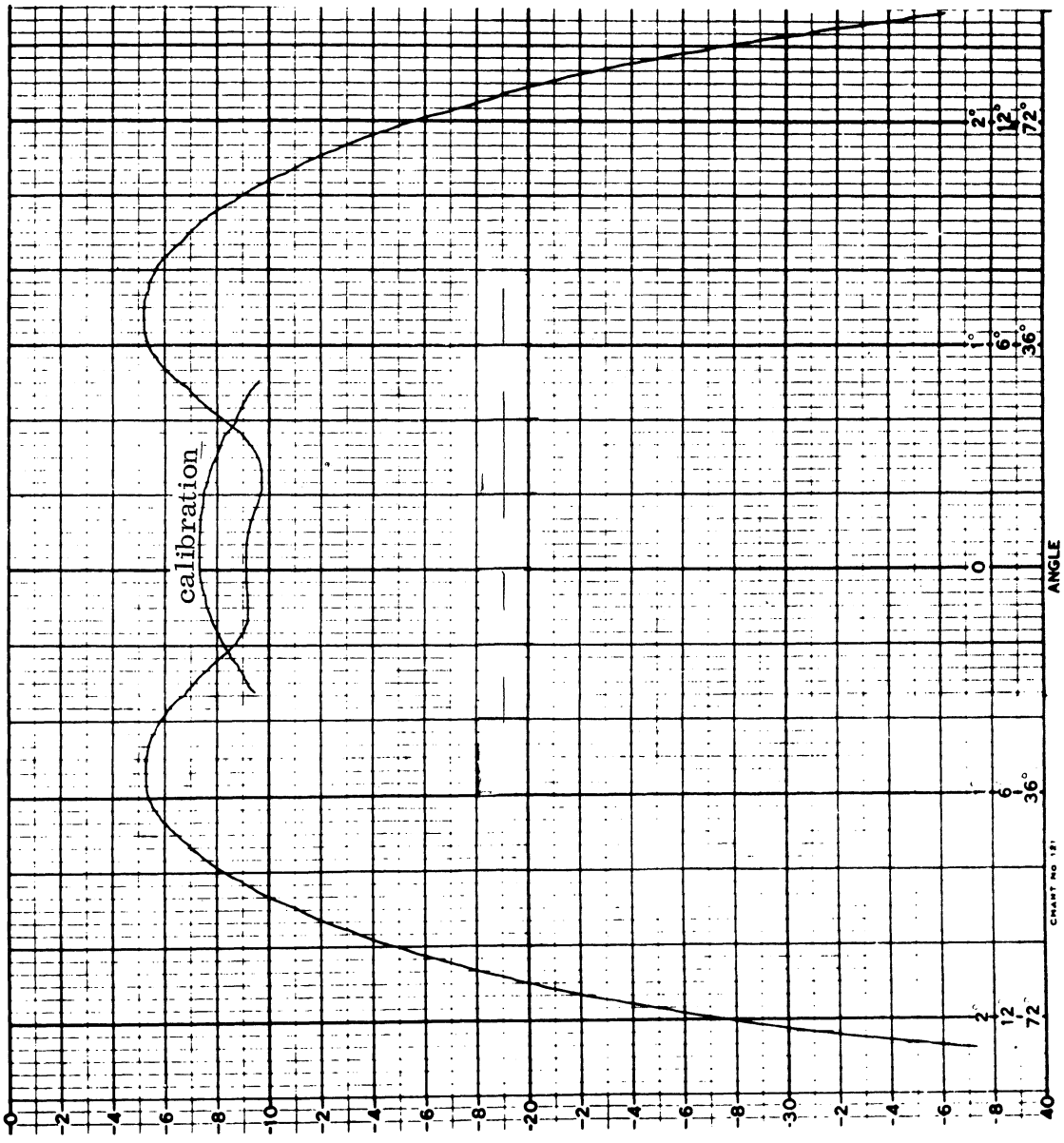

FIG. 2-8: SCATTERING PATTERN FOR h = 0.4435λ CYLINDER
L = 0cm ($Z_L \simeq 0$)

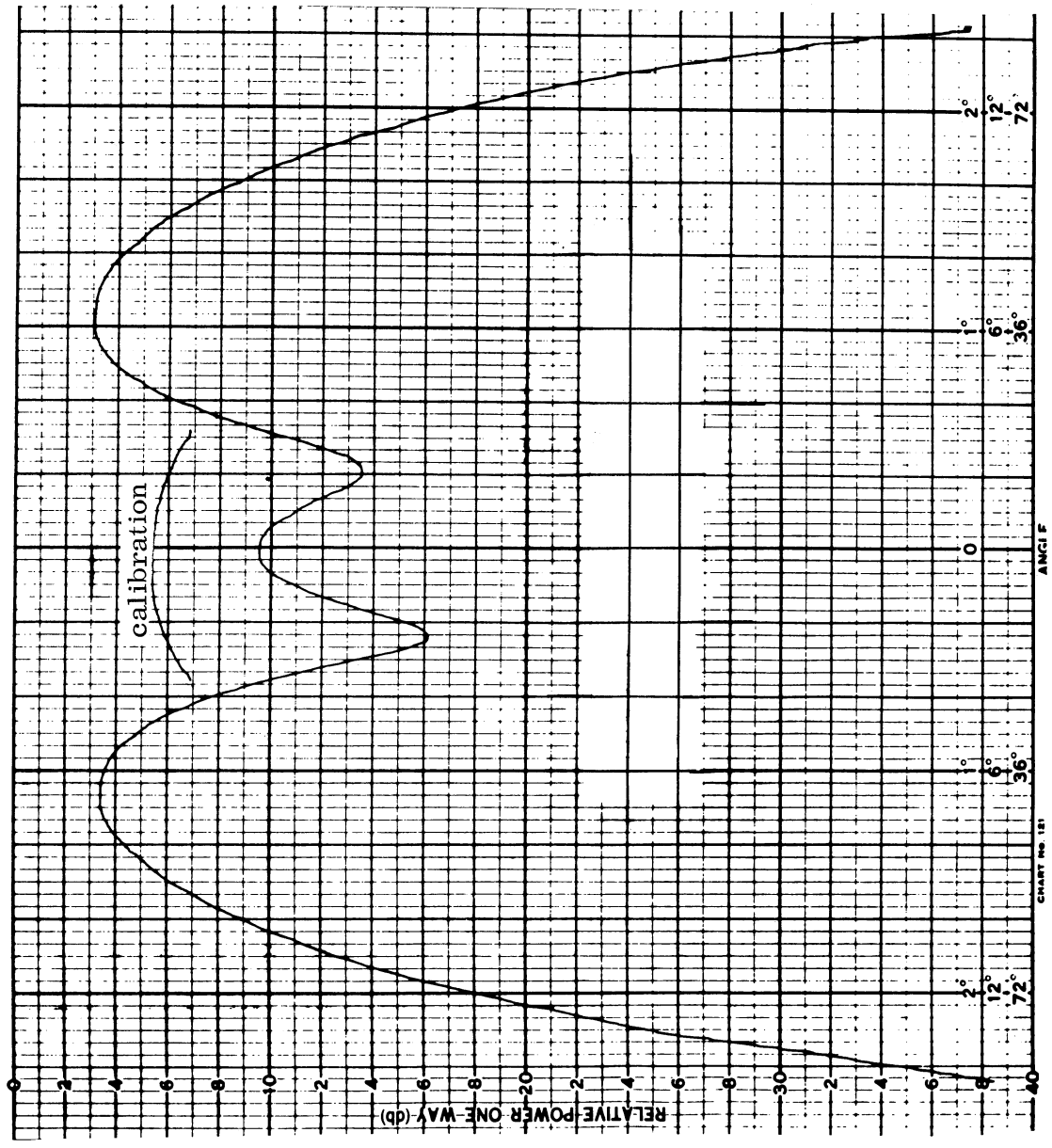

FIG. 2-9: SCATTERING PATTERN FOR $h = 0.4435\lambda$ CYLINDER
$L = 5.58\,\text{cm}$ ($Z_L \simeq j415\Omega$)

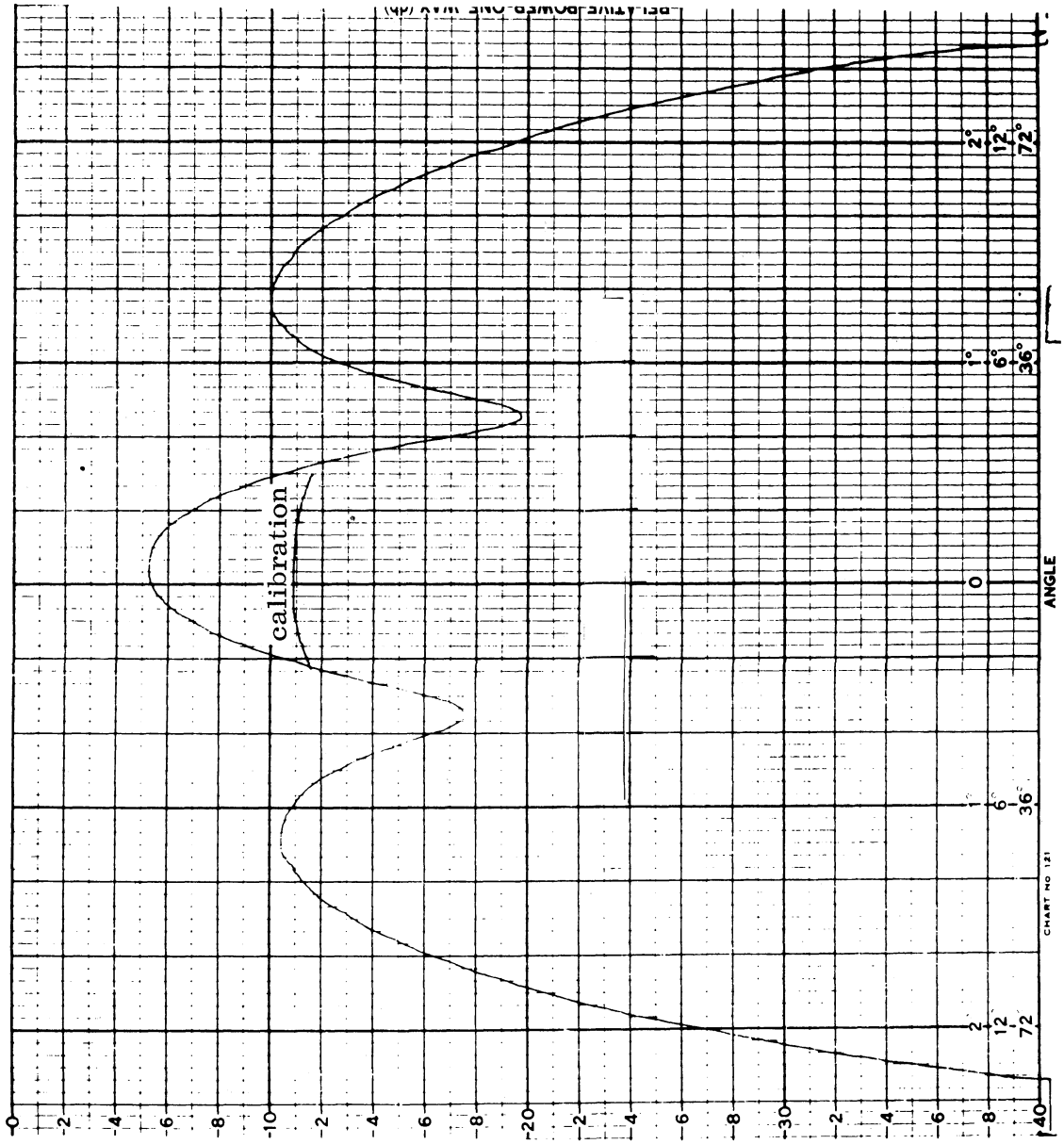

FIG. 2-10: SCATTERING PATTERN FOR h = 0.4435λ CYLINDER
L = 6.22 cm ($Z_L \simeq \infty$)

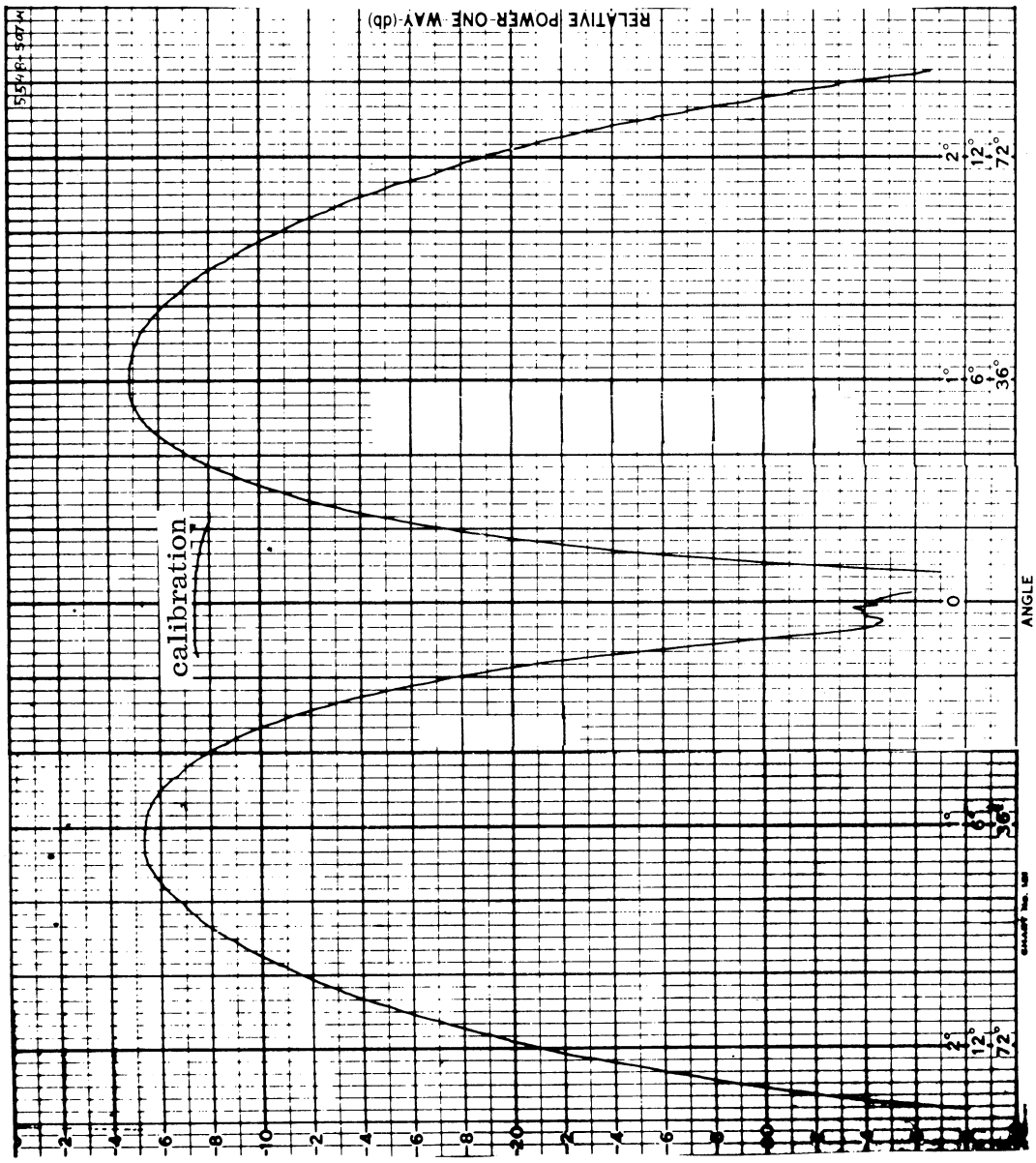

FIG. 2-11: SCATTERING PATTERN FOR h = 0.4435λ CYLINDER
L = 5.07 cm (Z_L = j 212 Ω)

$L = 5.58\,cm$ ($Z_L \simeq j\,415\,\Omega$), $L = 6.22\,cm$ ($Z_L \simeq \infty$) and $L = 5.07\,cm$ ($Z_L \simeq j\,212\,\Omega$). In these figures, we see that the back scatter lobes for some off-broadside aspects are not reduced by central loading. In particular, the large cross sections at about 40^o off-broadside are due to a large antisymmetrical current induced on the cylinder at this angle of incidence. Since the antisymmetrical current is not affected by a change in the central impedance, the only advantage with an antiresonant cylinder is the large reduction of the cross section at broadside incidence which results from the modification of the symmetrical component of the induced current.

Some additional measurements of the maximum reduction of the back scattered cross section as a function of the cavity length are summarized in Table II. In Table II, ϵ_r is the dielectric constant of the dielectric inside the coaxial cavity, σ_{max} is the maximum back scattered cross section of the loaded cylinder and σ_o is the maximum broadside back scattered cross section of a particular non-loaded cylinder for which $h = 0.2134\lambda$.

The variation of the maximum back scattered cross section as a function of the cavity length is shown in Fig. 2-12 where three curves show the information summarized in Table II. It is interesting to compare curve 1 and curve 3. Since the dielectric constant of the dielectric of the cavity changes from 4 to 16, one would expect the required physical length of the cavity to decrease by a factor of 2. In the experiment the required physical length of the cavity was decreased by a factor of 1.5. This tends to indicate that the shunt capacitance across the input of the cavity may change if the cavity is filled with different dielectric.

Fig. 2-13 shows the maximum back scattering cross section as a function of cavity length for a cylinder with $h = 0.215\lambda$. The three curves in the figure are obtained by three different methods. Curve 1 is directly obtained from a back scattering measurement; curve 2 is obtained from the measured current distribution by means of a graphical integration; and curve 3 is the theoretical curve with an

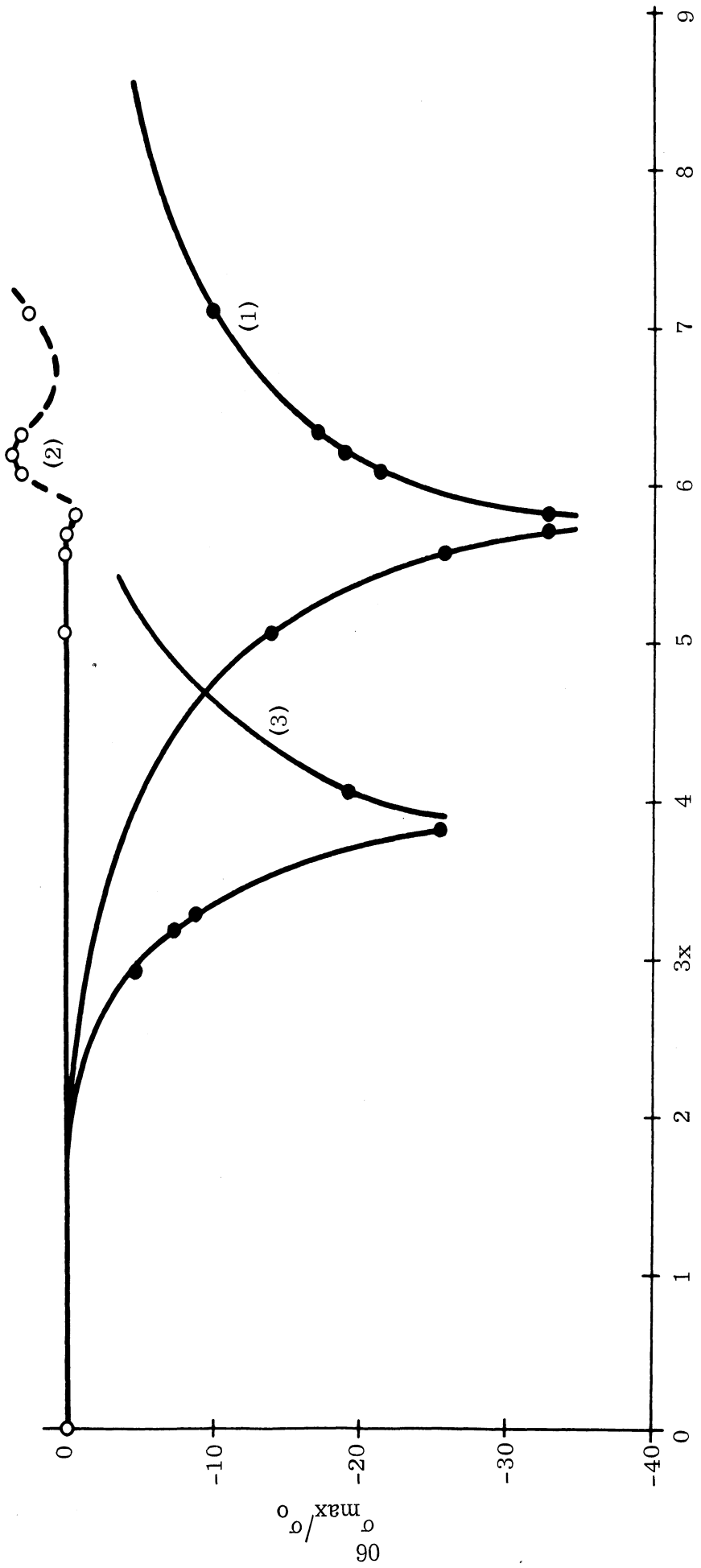

FIG. 2-12: MAXIMUM BACK SCATTERING CROSS SECTION VS CAVITY LENGTH
(1) $h = 0.2134\lambda$, $\epsilon_r = 4$; (2) $h = 0.4435\lambda$, $\epsilon_r = 4$; (3) $h = 0.2134\lambda$, $\epsilon_r = 16$

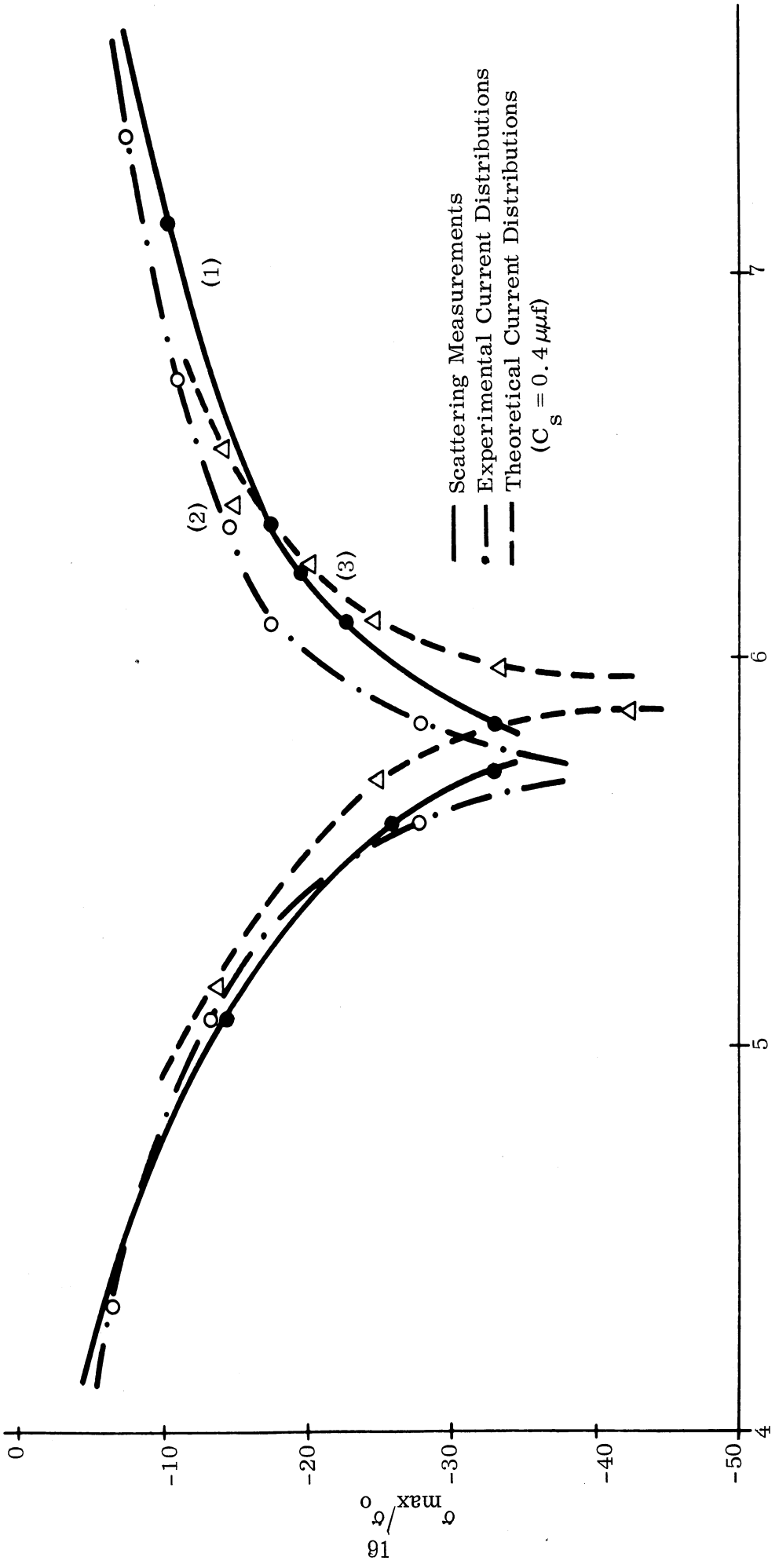

FIG. 2-13: MAXIMUM BACK SCATTERING CROSS SECTION VS CAVITY LENGTH
$h = 0.215\lambda$, $\epsilon_r = 4$

assumption of a shunt capacitance $C_s = 0.4\,\mu\mu f$ which was deduced in section 1-2.3. However, if $C_s = 0.46\,\mu\mu f$ had been chosen, curve (3) would shift to the left and coincide with (1) and (2).

TABLE II

Cylinder Length h	ϵ_r	Cavity Length L (cm)	$\frac{\sigma_{max}}{\sigma_o}$, db
		0	0
		5.07	-14.3
		5.58	-25.7
0.2134λ	4	5.71	-34.9
		5.83	-32.9
		6.10	-22.5
		6.22	-19.1
		6.35	-17.4
		7.12	-10.0
		0	0.1
		5.07	0.1
		5.58	0.0
0.4435λ	4	5.71	-0.2
		5.83	-0.7
		6.10	3.0
		6.22	3.6
		6.35	3.0
		7.12	2.5
		2.92	-4.8
		3.18	-7.5
0.2134λ	16	3.29	-8.9
		3.81	-25.6
		4.07	-19.3

2-2.3 Comparison Between Theory and Experiment

In this section we compare the theoretical predictions and experimental observations of the back scattering cross section dependence on aspect angle. Fig. 2-14 shows the back scattering cross section of a resonant cylinder (h = 0.215λ)

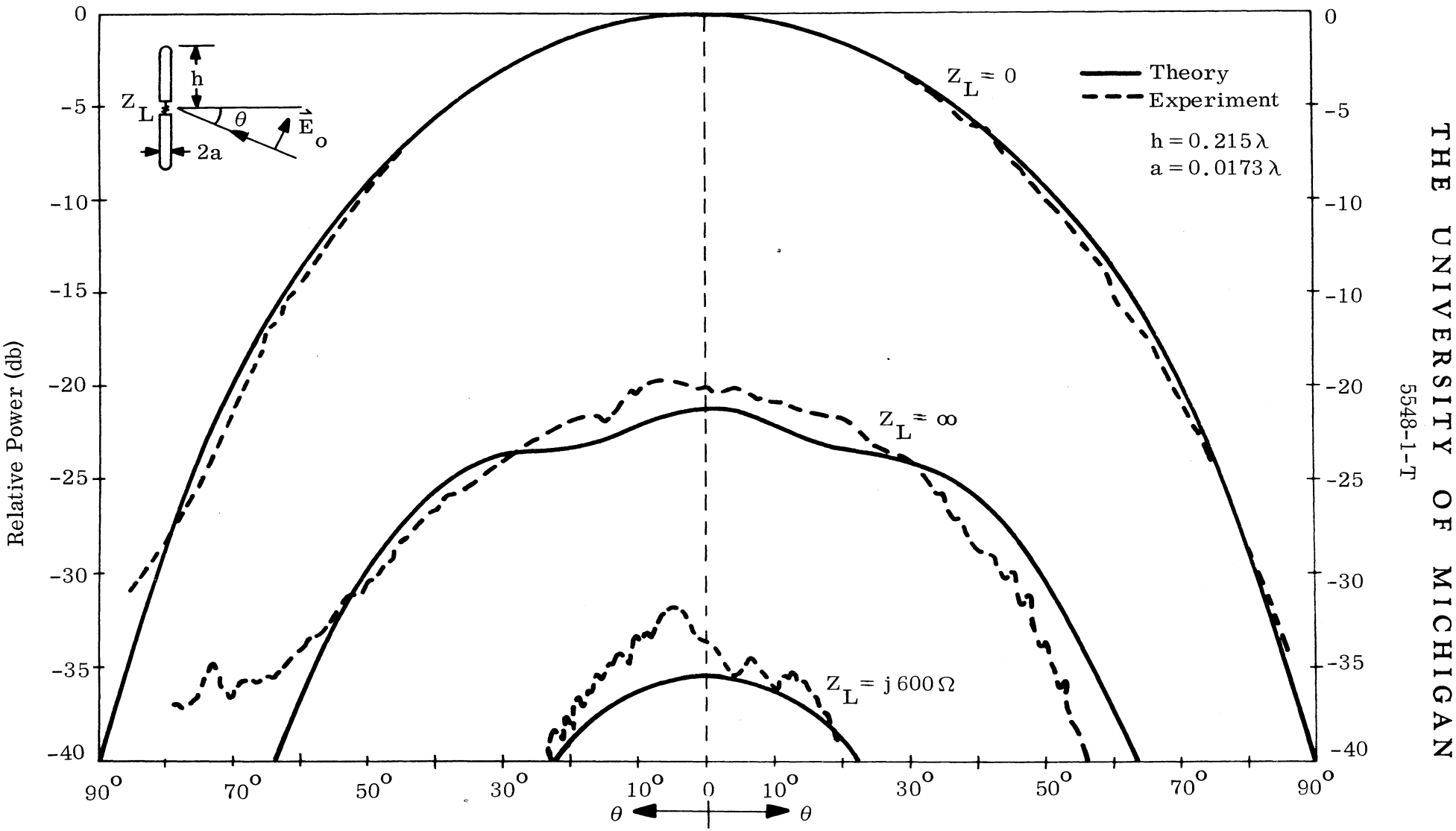

FIG. 2-14: BACK SCATTERING CROSS SECTIONS OF LOADED CYLINDERS VS ASPECT ANGLE (θ)

THE UNIVERSITY OF MICHIGAN
5548-1-T

as a function of the aspect angle for three different loadings. When $Z_L = 0$ (unloaded cylinder) the cross section is very large. When the same cylinder is loaded with an infinite impedance ($Z_L = \infty$), the back scattering cross section is reduced about 20 db. If the loading is adjusted close to the optimum value ($Z_L = j\,600\,\Omega$), a reduction of more than 30 db is obtained. The agreement between theory and experiment is excellent.

Figs. 2-15 through 2-17 show the radar cross sections of an antiresonant cylinder as a function of the aspect angle for three different loadings. When the cylinder is not loaded ($Z_L = 0$), the back scattering is approximately constant over the aspect angle range of $0 \leqslant \theta \leqslant 50^\circ$ with a slight maximum at $\theta = 40^\circ$. The theoretical and the experimental results for this case are compared in Fig. 2-15 in which the zero db level is chosen to have the same absolute scale as in Fig. 2-14.

Fig. 2-16 shows the theoretical curve for $Z_L = j\,300\,\Omega$ compared with an experimental curve for $Z_L = j\,212\,\Omega$. The point of interest is that for this loading the back scattering in the broadside direction is reduced considerably. These two curves, though with different loadings, agree quite well over most of the aspect range except for small θ. The maximum back scattering occurs at $\theta = 42^\circ$ and its amplitude is not reduced by the loading.

Fig. 2-17 shows the theoretical curve for $Z_L = j\,600\,\Omega$ and a comparison with an experimental curve for $Z_L = j\,415\,\Omega$. The general behavior of these curves agrees very well. The maximum back scattering occurs at $\theta = 42^\circ$ and again its amplitude is not reduced by loading.

In these three figures we find that the maximum cross section for an antiresonant cylinder at $\theta \simeq 40^\circ$ is not modified at all by a central loading. As mentioned before, this is due to the fact that this maximum back scattering is produced by the antisymmetrical component of the induced current which is not affected by a central impedance.

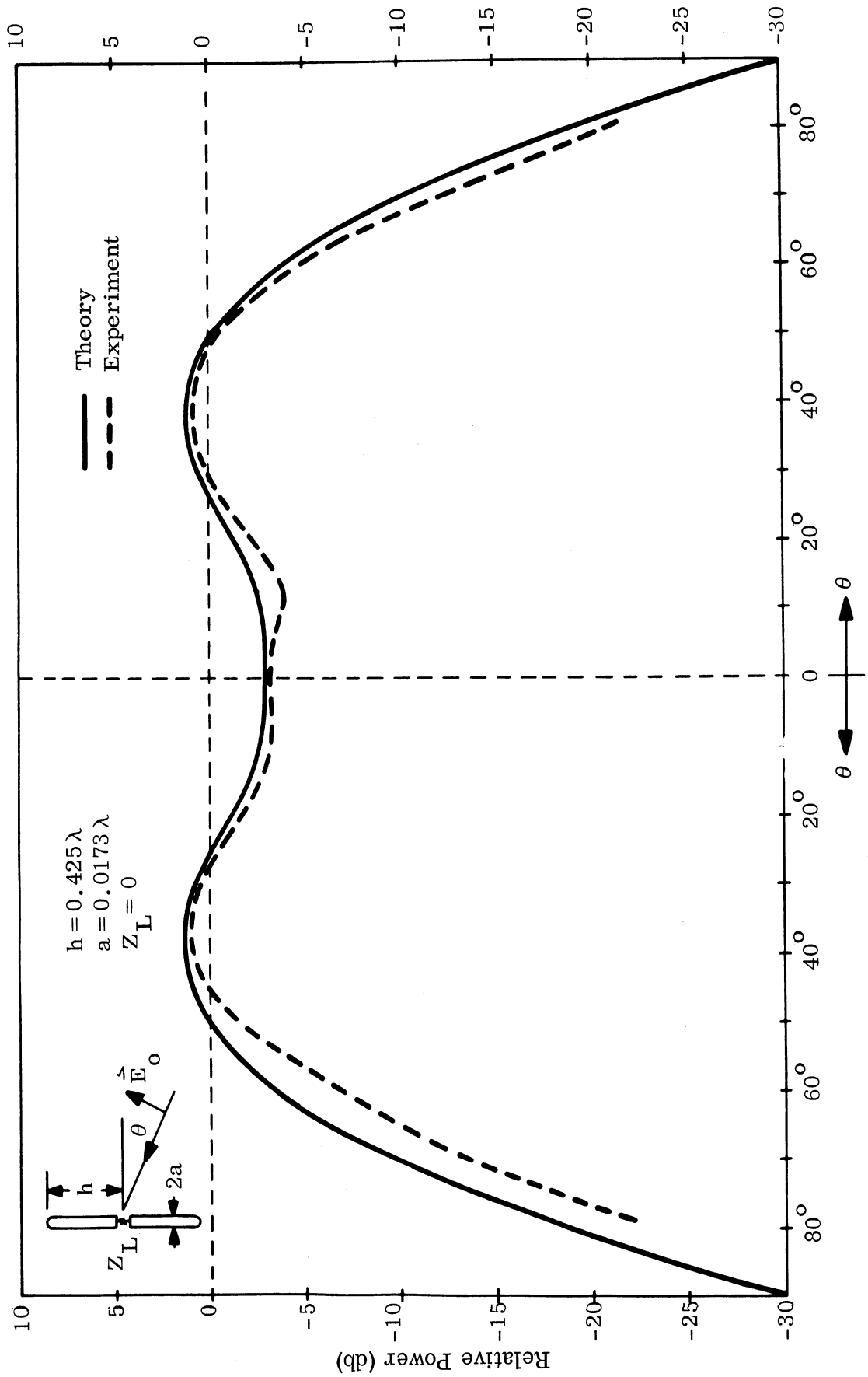

FIG. 2-15: BACK SCATTERING CROSS SECTION OF LOADED CYLINDER VS ASPECT ANGLE (θ)

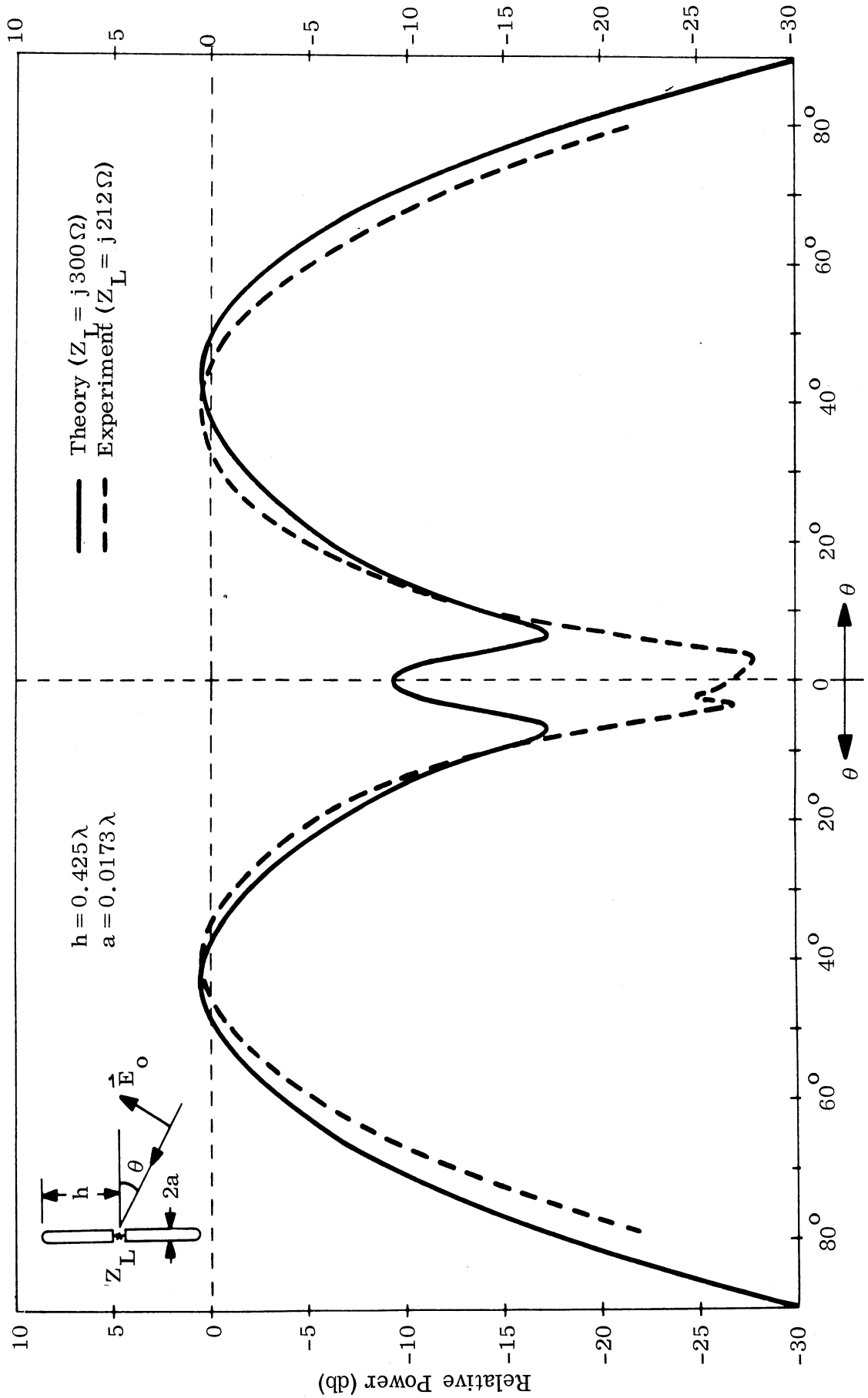

FIG. 2-16: BACK SCATTERING CROSS SECTION OF LOADED CYLINDER VS ASPECT ANGLE (θ)

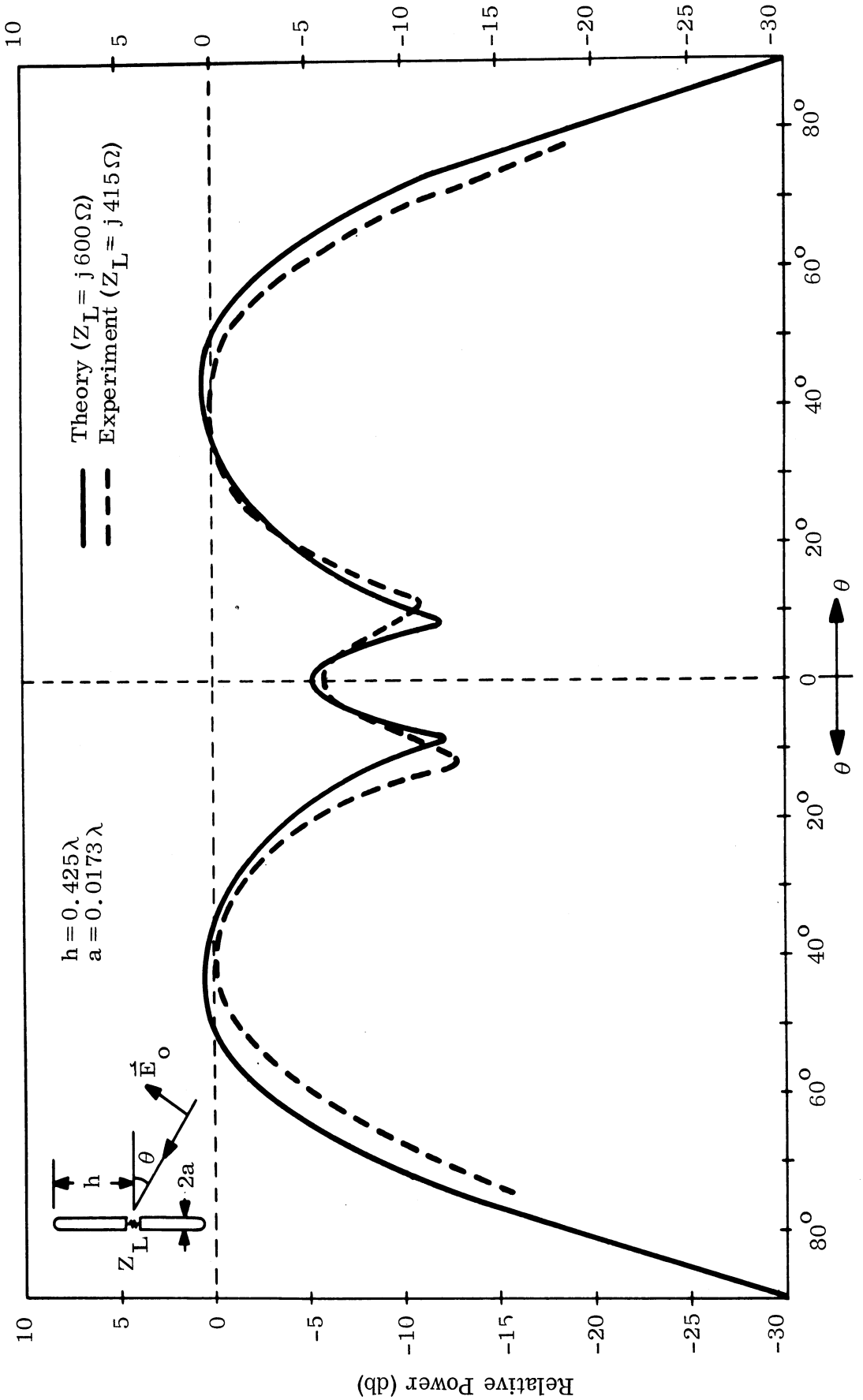

FIG. 2-17: BACK SCATTERING CROSS SECTION OF LOADED CYLINDER VS ASPECT ANGLE (θ)

The agreement between theory and experiment is found to be excellent. This confirms the accuracy of the theory and the experiment and also the feasibility of the reactive loading technique for the reduction of the radar cross section of a metallic body.

2-3. SUMMARY

The induced current on a center-loaded cylinder illuminated by a plane wave at an arbitrary angle is obtained in Section 2-1. This is essentially the generalized version of the case studied in Section 1-1.

It has been found that when a cylinder is illuminated by an obliquely incident plane wave the induced current has a symmetrical and an antisymmetrical component. The symmetrical component can be modified greatly by central loading but the antisymmetrical component is not affected.

In a resonant cylinder the symmetrical component of the induced current dominates the antisymmetrical component. In an antiresonant cylinder the antisymmetrical component is dominant. Therefore, the scattering cross section of a resonant cylinder can be greatly reduced by central loading while the cross section of an antiresonant cylinder can be modified only slightly.

The back scattered field of a center-loaded cylinder illuminated by a plane wave at an arbitrary angle is obtained in Section 2-2. The effect of central loading on the cross section of a resonant and an antiresonant cylinder is carefully studied theoretically and experimentally.

The scattering cross section of a resonant cylinder can be reduced more than 30 db by an optimum loading. The scattering cross section of an antiresonant cylinder can be reduced only in the broadside direction but the large cross section in the off-broadside direction can not be reduced by central loading.

To reduce the overall cross section of an antiresonant cylinder or to increase the bandwidth of the reactive loading technique a double or a multiple loading may prove to be more effective.

ACKNOWLEDGMENT

The authors are grateful to Mr. R.E. Hiatt and Dr. T.B.A. Senior for many helpful discussions and acknowledge the assistance of Mr. L. Zukowski in the preparation of this report. The authors also wish to thank Mr. H. Hunter and Mr. J.A. Ducmanis for their numerical calculations and Mr. E.F. Knott and Mr. V.M. Powers for their contributions on the experimental side.

REFERENCES

Ås, B.O., and H.J. Schmitt (1958) "Backscattering Cross Section of Reactively Loaded Cylindrical Antennas", Harvard University Cruft Laboratory, Scientific Report No. 18.

Hu, Yueh-Ying (1958) "Backscattering Cross Section of a Center-Loaded Cylinder", IRE Trans. AP-6, pp. 140-148.

Iams, H.A. (1950) "Radio Wave Conducting Device", U.S. Patent No. 2,528,367.

King, R.W.P. (1956) The Theory of Linear Antennas, Harvard University Press, Cambridge. pp. 506-511.

Sletten, C.J. (1962) Air Force Cambridge Research Laboratories, private communication.

UNIVERSITY OF MICHIGAN
3 9015 02829 6211